An mTORC1/AKT1/Cathepsin H axis controls filaggrin expression and processing in skin, a novel mechanism for skin barrier disruption in Atopic Dermatitis

Naeem AS, PhD(1,2), Tommasi C, MRes (1,2), Cole C, PhD (3), Brown, Stuart J, PhD(1,2), Zhu Y PhD, (1,2), Way B, MA BMBCh MSc MRCS(1,2), Willis Owen SAG, DPhil(4), Moffatt M, DPhil(4), Cookson WO, DPhil(4), Harper JI, MBBS MD FRCP FRCPCH (1,2), Di WL, PhD(1,2), Brown, Sara J, MD FRCPE (5), Reinheckel T, PhD(6), O'Shaughnessy RFL, PhD (1,2,7).

1. Immunobiology and Dermatology, UCL Institute of Child Health

2. Livingstone Skin Research Centre, UCL Institute of Child Health

3. Computational Biology, School of Life Sciences, University of Dundee, Dundee, UK.

4. National Heart and Lung Institute, Imperial College, London SW3 6LY, UK

5. Centre for Dermatology and Genetic Medicine, Medical Research Institute, University of Dundee, Dundee, United Kingdom

6. Institute of Molecular Medicine and Cell Research, BIOSS Centre of Biological Signalling Studies, Albert-Ludwigs-University, Freiburg, Germany

7. To whom correspondence should be addressed:

Ryan O'Shaughnessy, Immunobiology, UCL Institute of Child Health, 30 Guilford Street, London WC1N 1EH, Phone +44 207 905 2182, Fax Number: +44 207 905 2882 e-mail r.oshaughnessy@ucl.ac.uk

Keywords. Atopic dermatitis, Skin Barrier, filaggrin, RAPTOR, Protease

Abbreviations

AD Atopic Dermatitis

AKT1 V-Akt Murine Thymoma Viral Oncogene Homolog 1

ATRA All trans retinoic acid

CTSH Cathepsin H

ECL Enhanced chemiluminesence

ENCODE The Encyclopedia of DNA Elements

FLG Filaggrin Gene

HMGCR 3-Hydroxy-3-Methylglutaryl-CoA Reductase

HMGCS1 3-Hydroxy-3-Methylglutaryl-CoA Synthase 1

HRP Horseradish peroxidase

IDI1 Isopentenyl-Diphosphate Delta Isomerase 1

IL-13 Interleukin 13

IL-4 Interleukin 4

mTORC1/2 Mechanistic Target Of Rapamycin Complex 1/2

OCT Optimal Cutting Temperature compound

pAKT phosphorylated AKT

PBS Phosphate buffered saline

PCR Polymerase Chain Reaction

RAPTOR Regulatory Associated Protein Of MTOR Complex 1

REK Rat epidermal keratinocytes

SASPase Aspartic Peptidase, Retroviral-Like 1

SDS Sodium Dodecyl Sulphase

SNP Single nucleotide polymorphism

SPF Specific pathogen free

TBST Tris buffered saline with 0.1% Tween 20

Th2 T-helper 2

TSLP Thymic stromal lymphopoietin

Abstract

Background: Filaggrin, encoded by the *FLG* gene, is an important component of the skin's barrier to the external environment and genetic defects in *FLG* strongly associate with Atopic Dermatitis (AD). However, not all AD patients have *FLG* mutations.

Objective: We hypothesised that these patients may possess other defects in filaggrin expression and processing, contributing to barrier disruption and AD, and therefore present novel therapeutic targets for this disease.

Results: We describe the relationship between the mTORC1 protein subunit RAPTOR, the serine/threonine kinase AKT1 and the protease cathepsin H, for which we establish a role in filaggrin expression and processing. Increased RAPTOR levels correlated with decreased filaggrin expression in AD. In keratinocyte cell culture, RAPTOR up-regulation or AKT1 shRNA knockdown reduced the expression of the protease cathepsin H. Skin of cathepsin H-deficient mice and CTSH shRNA knockdown keratinocytes showed reduced filaggrin processing and the mouse showed both impaired skin barrier function and a mild proinflammatory phenotype.

Conclusion: Our findings highlight a novel, potentially treatable, signalling axis controlling filaggrin expression and processing which is defective in AD.

Key messages:

- RAPTOR levels are increased in atopic dermatitis and are inversely proportional to filaggrin expression

-The up-regulation of RAPTOR leads to AKT1 activity down-regulation and downregulation of the protease cathepsin H, which is involved in filaggrin processing, epidermal barrier function and modulates skin immunity.

Capsule: *FLG* mutations strongly associate with Atopic Dermatitis (AD). However, not all AD patients have *FLG* mutations. An mTORC/AKT1 signalling axis controls both filaggrin expression and processing by controlling expression of the protease Cathepsin H.

Introduction

Atopic dermatitis (AD) is a common disease in which the skin is sensitive to allergens and irritants resulting in an immune response characterised by redness and scaling. Current evidence suggests that the primary cause for disease development in the majority of AD cases is a defective skin barrier [12,31] . There is a strong genetic component to AD associated with skin barrier dysfunction[15]. One important protein is the epidermal structural protein filaggrin. Null mutations in the gene encoding filaggrin (*FLG)* are responsible for the common inherited dry skin condition ichthyosis vulgaris, and are a major predisposing factor for AD[48,54]. However only approximately 40% of AD patients in the UK, and around 10% of AD patients in the rest of the world have filaggrin mutations[7,57] and conversely, not all individuals with filaggrin mutations have AD[45], suggesting that other mechanisms might contribute to filaggrin expression and processing defects and hence to the barrier defect observed in AD patients.

Profilaggrin to filaggrin processing is complex, requiring dephosphorylation and numerous proteolytic events; several proteases have been identified that cleave profilaggrin at specific sites releasing the filaggrin monomers and both the N and the C termini[17] . Proteases such as elastase 2 , SASPase and matriptase are reported to be involved in profilaggrin to filaggrin processing [5,18,43,44]. There are also reports of aspartic- and cysteine- type cathepsin proteases playing a role in this process [20,34,35] . AKT1 is required for the correct formation of the cornified envelope[47]. AKT1 activity in the epidermis is increased by treatment with the mTORC1 (RAPTOR containing mammalian target of rapamycin complex) inhibitor rapamycin[59] , suggesting a role of RAPTOR in modulating AKT1 activity. We therefore hypothesised that

AKT1 activity may be reduced in atopic dermatitis skin leading to alteration in protease expression, reduced filaggrin expression and processing and skin barrier disruption.

Using a combination of keratinocyte shRNA knockdown models, human clinical samples and mouse knockouts, we show increased RAPTOR expression correlates with reduced filaggrin expression in the skin of atopic individuals, this being most apparent in those with *FLG* compound heterozygous mutations. RAPTOR overexpression in keratinocytes reduced filaggrin expression, loss of AKT1 activity and filaggrin and loss of cathepsin H. Cathepsin H deficient mice have reduced filaggrin processing, subtle barrier defects, and an elevation in pro-inflammatory molecules, associated with increased macrophage infiltration of the skin and increased mast cell degranulation. Taken together this provides strong evidence that RAPTOR levels and AKT1 signalling are important in modulating filaggrin levels and the immune environment in AD.

Results

Increased RAPTOR expression correlated with reduced filaggrin expression in rat epidermal keratinocytes and in non-lesional AD skin

As inhibition of the mTORC1 complex by rapamycin increases AKT1 phosphorylation in keratinocytes[59], we hypothesised that the inverse could occur; that increased expression of the key mTORC1 protein RAPTOR in AD resulted in a reduction of AKT1 phosphorylation and therefore activity. To test this we examined the expression of RAPTOR, pAKT and filaggrin in the unaffected, non-lesional, non-flexural epidermis of 5 AD early-onset severe patients and of 3 individuals without AD (Figure 1a and b; Supplementary table E1). Non-lesional, non-flexural skin from AD patients have been previously demonstrated to be barrier deficient and represented a way of investigating the disease prior to acute immune involvement [14,26] .pAKT was significantly downregulated on the protein level in unaffected AD skin sections. However in both AD patients and controls there were individuals with RAPTOR present in the spinous and granular layers which corresponded to lower filaggrin levels in these individuals

(Supplementary Figure E1a). To investigate this finding in a larger number of individuals with known *FLG* genotype, we extended our analysis of RAPTOR and filaggrin to a gene expression analysis of non-lesional, non-flexural skin biopsies from 26 AD patients and 10 non-atopic controls of known *FLG* genotype as previously described[14]. All cases of AD had early onset persistent and severe disease. There was no significant change in mRNA levels of RAPTOR in non-lesional atopic skin according to *FLG* genotype (Figure 1c). However, changes in RAPTOR expression correlated with a number of the highly differentially expressed genes in *FLG* compound heterozygotes and filaggrin heterozygotes, including FLG itself (Figure 1d and e and Supplementary table E2). Although Th2 cytokines such as IL-13 and IL-4 are known to be able to modulate expression of filaggrin and alter epidermal barrier function [30,37], rapamycin treated cells did not reduce IL-4 expression and AKT1 knockdown keratinocytes did not have increased levels of IL-4 (Supplementary figure E1b and c). IL-4 or IL-13 were not correlated with RAPTOR levels in the data from Cole et al[14]. Taken together this suggests that the mechanism by which RAPTOR controls filaggrin is not due to increase in IL-4 or IL-13 cytokine expression.

These genes and RAPTOR itself comprised a network centred on the insulin-mediated control of AKT1 which we have described previously and is important in both epidermal skin barrier function and UV protection (Supplementary figure E2a; [59]). A large proportion (17/22=77%) of the correlated and anti-correlated, highly expressed genes with mean normalised read count of 100 or more were also genes whose expression correlated with filaggrin expression[14] (Supplementary figure E2b, Supplementary Table E3) These data demonstrate that in AD, RAPTOR mRNA levels strongly anti-correlated with filaggrin mRNA expression. To directly test the effect of increased RAPTOR, we over-expressed human RAPTOR in rat epidermal keratinocytes. RAPTOR over-expression led to a decrease in AKT phosphorylation. Filaggrin is produced as a long pro-protein which is proteolytically processed to a monomeric mature form. We observed reduction in total and processed monomeric filaggrin, (Figure 1f and g).

A single nucleotide polymorphism in RAPTOR in a retinoid x receptor binding site correlated with increased RAPTOR and decreased filaggrin and cathepsin H levels.

To determine whether there were genetic changes that could lead to a change in RAPTOR expression levels in keratinocytes, we evaluated data from a previously published genome-wide association study[63] for any of the 649 single nucleotide polymorphisms (SNPs) in the *RAPTOR* gene that were over-represented in AD. We were not expecting gene-wide significance ($p<1x10^{-8}$) as RAPTOR overexpression also occurred in normal non-AD skin (Supplementary figure E3a). No SNPs were significantly over-represented, but we found an increased frequency in AD of one commonly observed (>1%) SNP. rs8078605 (C>T) is in an intronic region of RAPTOR in a region of DNA which according to ENCODE data[4] includes a region of acetylated histones in keratinocytes only, suggestive of a keratinocyte-specific enhancer (Supplementary figure E3a), and a binding site for RXRalpha. The variant SNP abolished a key nucleotide of a putative Retinoid-X receptor alpha binding site. In 18 DNA samples examined, 3 heterozygotes and a single homozygote were found (representing a minor allele frequency of 13.9, and 5.6% homozygotes, Supplementary figure E3b). The frequency of this variant allele in Europeans populations was 14% compared to 79% in sub-Saharan populations. This was of particular interest as other SNPs in non-coding parts of RAPTOR, with high prevalence in sub-Saharan populations compared to European populations, associated with putative retinoid binding sites that controlled the level of RAPTOR[60]. We therefore tested if RAPTOR itself was a retinoid responsive gene in human keratinocytes. Treatment of human keratinocytes with all-trans retinoic acid reduced RAPTOR expression levels (Supplementary figure E3c), suggesting that retinoids could control RAPTOR levels in keratinocytes. We therefore hypothesised that RXRalpha binding in the RAPTOR gene reduced RAPTOR expression, and that the rs8078605 C>T variant would lead to increased RAPTOR expression. High RAPTOR, low filaggrin protein levels and low Ctsh levels correlated with the presence of the T/T variant of rs8078605 (Supplementary figure E3d,e and f)

Loss of AKT1 activity or expression leads to reduced filaggrin processing in keratinocytes

We assessed the effect of the PI3Kinase inhibitor wortmannin, which inhibits AKT1 phosphorylation on filaggrin expression and processing in human keratinocytes [46].Wortmannin treatment reduced the levels of

the mature processed filaggrin monomer (Figure 2a). These observations suggest that PI3 kinase signalling through AKT1 was required for the proteolytic processing of filaggrin during late epidermal terminal differentiation. To test whether AKT1 loss was responsible for the observed changes in filaggrin expression after wortmannin treatment in keratinocytes, we transfected a rat epidermal keratinocyte line (REK), known to represent the end stages of terminal differentiation in confluent submerged culture[47], with shRNA to rat Akt1 (Figure 2b and c). We could demonstrate a significant reduction in the levels of processed filaggrin monomer in four separate knockdown lines by Western blot, while levels of total filaggrin and filaggrin mRNA remained unchanged (Figure 2c, d and e). Organotypic skin equivalent cultures from these cells were hyperkeratotic compared to controls (Figure 2f). We could also demonstrate a reduction in filaggrin expression in these organotypic cultures (Figure 2f), with an antibody specific to the repeating mature monomeric form .These data suggest that while RAPTOR increase led to reduction in filaggrin expression, loss of the downstream kinase AKT1 or its activity resulted only in reduced filaggin processing.

mTORC signalling-related proteins and proteases, principally Cathepsin H, are differentially expressed in Akt1 knockdown cells

Differential gene expression analysis was performed on the Akt1 knockdown REK lines with the greatest reduction in AKT1 (A1 and A3). 570 genes were significantly differentially expressed in both lines compared to scrambled controls (Figure 3a). Of these 59 genes had differential expression ≥1.5-fold and 17 genes had differential expression ≥2-fold (Figure 3b; Supplementary table E4). Gene set enrichment analysis (GSEA; Supplementary figure E4a) identified 3 gene ontology groups over-represented in the analysis, Cholesterol homeostasis, Androgen response and consistent with a role downstream of RAPTOR, MTORC signalling (Figure 3c; Supplementary Figure E3b and c), Leading edge analysis identified 3 genes, IDI1, HMGCR and HMGCS1 in all three ontology groups. HMGCS1 was down-regulated in our AKT1 knockdown cells and in AD skin (Supplementary figure E4d and e; [14]). We identified 3 down-regulated proteases or proteolysis-associated proteins in our Akt1 kd cell lines (Figure

3d). We confirmed down-regulation of the most highly downregulated of these, the lysosomal protease cathepsin H (Ctsh, 3-4 fold) by real-time PCR (Figure 3e) and Western blot (Figure 3f). Ctsh was of particular interest as other members of the cathepsin proteases have been implicated in filaggrin processing[20,34,35]. Ctsh was downregulated in human keratinocytes treated with wortmannin (Figure 3g), and was expressed in post-confluent cultured REKs coincident with terminal differentiation and AKT activity (Figure 3h). Reinforcing a potential role in the control of filaggrin processing, Ctsh was expressed co-incident with filaggrin in the granular layer of the epidermis and organotypic cultures, with a reduction of both filaggrin and Ctsh in the Akt1 shRNA expressing organotypic cultures (Figure 3i)

Loss of cathepsin H inhibits filaggrin processing, not expression, and impairs epidermal barrier function. Evidence of compensation in the cathepsin H knockout

Cathepsin H expression was decreased in non-lesional AD epidermis (Figure 4 and b), and was reduced in keratinocytes overexpressing RAPTOR (Figure 4c), suggesting that is was a downstream effector of the RAPTOR/AKT1 axis in atopic dermatitis. To investigate a potential role for Cathepsin H in filaggrin processing, Ctsh expression was knocked down by shRNA in our rat epidermal keratinocyte model. In all 4 shRNA knockdown lines examined there was a reduction of filaggrin processing without reduction in filaggrin mRNA levels (Supplementary figure E5a,b and c), consistent with our Akt1 knockdown data in REKs. There was a trend of reduction of median CTSH levels in the atopic dermatitis RNAseq analysis (Supplementary figure E5d;[14]) , however consistent with the lack of change in Filaggrin mRNA levels, there was no correlation between filaggrin levels and CTSH in AD (Supplementary figure E5e)

Knockdown of both AKT1 and CTSH in human keratinocytes revealed the same reduction in filaggrin processing but no reduction in total filaggin protein levels (Figure 4d and e), strongly implying that the phenomenon we observed in the rat epidermal keratinocyte model was recapitulated in human keratinocytes too, further reinforcing our finding that increase in RAPTOR decreased filaggrin expression, and knockdown of either AKT1 or CTSH resulted in impaired filaggrin processing only.

Transient transfection of Ctsh into the Akt1 kd rat cell line rescued filaggrin processing (Figure 4f and g), suggesting that the loss of Ctsh was directly responsible for the reduction in filaggrin processing.

To investigate the effect of Ctsh reduction *in vivo,* we examined newborn mouse skin from *Ctsh* -/- and +/- mice[9] (Figure 5a and b) by histology. Although there was no change in epidermal thickness, the cornified layer was significantly thinner in both the *Ctsh* +/- and -/- mice. We observed no change in total filaggrin levels (Figure 5c and d) but increased loricrin levels in the *Ctsh* +/- and -/- mice by immunofluorescence (Figure 5e and f). Granular filaggrin expression was lost in the *Ctsh* +/- mice but was partially restored in the *Ctsh* -/- mice (Figure 5d). This was confirmed by western blot, where filaggrin processing was normal while loricrin and keratin 10 expression were increased (Supplementary figure 7c). In adult mice, in contrast, filaggrin and loricrin were most reduced in the Ctsh +/- mice and mostly restored in the Ctsh -/- mouse (Supplementary figure E7a)

Dye penetration assays[11] showed no significant gross barrier defects, but closer examination revealed penetration of dye into the cornified layers of the *Ctsh* +/- mice (Figure 5g) consistent with defective barrier function. Electron microscopy revealed smaller keratohyalin granules specifically in both the *Ctsh* +/- and -/- mice (Figure 5h and i), but the granule size in the -/- mice was partially rescued. This was reflected in a strengthening of cornified envelope integrity in Ctsh -/- mice compared to the weaker cornified envelopes in the *Ctsh* +/- mice (Figure 5j).

We examined the expression of other cathepsins known to process filaggrin[20,34,35], to determine if the rescue in the phenotype seen in the *Ctsh* -/- mouse was due to some kind of compensation by another cathepsin. We were unable to detect cathepins D and L in neonate skin, however the expression of cathepsin B was increased in both the knockout and heterozygous mouse (Supplementary figure E6a), suggesting that the rescue of physical barrier function was possibly due to the up-regulation of this filaggrin-processing protease.

Ctsh-deficient mice show increase in dermal macrophages, mast cell degranulation and pro-inflammatory molecule expression

Defects in the physical barrier in AD result in an immune response[38] which typically includes an increase in mast cell numbers and macrophages and lymphocyte infiltration[27,33] .We saw no change in CD45 positive cells (lymphocytes) in the dermis or epidermis of either the *Ctsh* +/- or *Ctsh* -/- mice (Figure 6a; Supplementary figure E6b). Increased macrophage numbers in the skin are associated with filaggrin-defective and barrier defective epidermis[23,56]. Consistent with this, macrophage (F4/80 positive cell) counts were increased in the skin of the *Ctsh* +/- and *Ctsh* -/- mice (Figure 6a and c). Mast cell degranulation, the release of histamine, proteases and other immune mediators, is a common phenomenon linked to the atopic phenotype[28], and although overall mast cell number was unchanged, degranulation was increased in the skin of the *Ctsh* +/- and *Ctsh* -/- mice (Figure 6b and c).

To determine whether the skin was more pro-inflammatory we investigated cytokine and related protein expression by antibody array dot blot in pooled lysates from whole skin from wild type, and polled *Ctsh* -/- and +/- newborn mouse skin (Figure 6d). There was increase in the expression in a number of cytokines and soluble immune mediators, including interleukin 1-alpha (IL-1a), a protein known to be increased in barrier defective and eczema skin[36] which was subsequently confirmed by immunofluorescence (Figure 6d,e and f). Thymic stromal lymphopoietin (Tslp) expression induces atopic dermatitis in mouse models and is present in lesional atopic dermatitis skin[58] . It also plays a key role in mast cell degranulation. however we saw no significant change in Tslp expression in the epidermis of *Ctsh* -/- and +/- newborn and adult mouse skin, (Figure 6e and f). Taken together these data suggested that loss of Ctsh mediated by RAPTOR increase and AKT1 activity loss in AD leads to mild epidermal barrier disruption and the epidermis subsequently becomes more pro-inflammatory, and although some aspects of the physical barrier are rescued in the knockout mouse, potentially due to compensation by cathepsin B and increased loricrin expression, the immune phenotype is not rescued (Figure 7).

Discussion

Although there has been a great deal of study of *FLG* mutations and their association with barrier disruption and AD, there are surprisingly few reports on variation of filaggrin protein levels and filaggrin processing[41,49,55] . Here we show that increase in RAPTOR correlates with decrease in filaggrin expression and processing not only in AD but also in normal "unaffected" individuals. This is consistent with other work on filaggrin proteases in AD[44] . Taken together these data strongly suggest that there would be value in assessing genetic variants in the normal population as a whole that correlate to barrier disruption and filaggrin expression and processing, and disregarding AD, as this may be a downstream consequence of the silent barrier disruption, that is potentially mediated by its own set of genetic associations[21,29,63].

Our analysis suggested that retinoids could be used as a treatment to reduce RAPTOR expression in AD and hence increase filaggrin expression and processing. Retinoids have been used to successfully treat eczema in a number of studies[19,25,52]. Typically around 50% of individuals respond to retinoid treatment[19]. Although the immunosuppressive properties of retinoids are cited as the cause of recovery, another reason could be the reduction of RAPTOR levels and subsequent increase in filaggrin expression and processing. Both cathepsin H and filaggrin have been reported previously as being up-regulated by retinoids, consistent with this hypothesis[24,51]. It would be interesting to investigate epidermal RAPTOR, cathepsin H and filaggrin levels and processing before and after treatment with retinoids and to determine if there is a different response in patients with different FLG phenotypes. A potential complication would be that treatment with all trans-retinoic acid or retinoic acid metabolism inhibitors can both inhibit and enhance epidermal terminal differentiation[1,2,13,50], so the potential overall effect on epidermal barrier function would be hard to predict.

Interestingly, in the context of the skin barrier and RAPTOR, mTORC1 is a pH sensor, and at acidic pH, such as those encountered in the granular layer of the epidermis, mTORC1 is inhibited [3]. This should

lower filaggrin expression, and would be balanced against filaggrin-derived urocanic acid and pyrrolidone carboxylic acid levels [62]. Coupled with the fact that Cathepsin H is a lysosomal protease, and therefore active at acidic pHs, it is likely that pH is one of the factors that determine overall levels of processed filaggrin.

The skin of Akt1 null mice models and Akt1 knockdown organotypic cultures display hyperkeratosis with reduced cornified envelope strength and reduced filaggrin expression and processing[47,61]. Activation of Akt1 also results in hyperkeratosis and altered filaggrin expression[32,47] demonstrating that normal Akt activity levels are required for correct filaggrin processing and hence epidermal barrier function. The new findings presented here reveal cathepsin H to be required for filaggrin processing and epidermal barrier formation, and that in the skin, RAPTOR regulates cathepsin H expression and filaggrin processing via reduced Akt signalling.

Cathepsin H is expressed ubiquitously and as well as being involved in bulk protein degradation, it does display cell-specific functions such as its role in the processing and secretion of surfactant protein C in type II pneumocytes[6,9]. Ctsh deficient mice have reduced lung surfactant which may interfere with breathing mechanisms causing respiratory complications[9] . Furthermore reduced Ctsh mRNA in airway smooth muscle cells has been reported in asthmatic individuals[22] , suggesting the possibility that low levels of Akt signalling may, in a range of epithelia, contribute to progression of AD to other atopic disease, the so called "atopic march"[10]. The finding that Ctsh is either directly involved or indirectly involved through the activation of other proteases such as granzymes[16], in the processing of key barrier proteins in the epidermis and in the lung leads to the possibility that the atopic march may not only be an immunological phenomenon, but could also be the result of altered barrier function in multiple epithelia.

Cathepsin H deficiency *in vivo* led to an increase in macrophage number and mast cell degranulation, and increased Il1a in the skin of Ctsh +/- and -/- mice. Cathepsin H overexpression typically correlates to macrophage infiltration and a proinflammatory environment in a number of tissues [39,42]. Therefore it is

likely that the loss of Ctsh leads to an increase in other cathepsins, such as with our observation of increased cathepsin B, which may have a proinflammatory role, and is known to play an important role in processing of mast cell proteases[16,40] . It is therefore possible that the immune changes are driven by the increased cathepsin B in both Ctsh +/- and -/- mice. The interplay between these proteases and inhibitors and how this relates to the levels of filaggrin and other related (fused-S100 group) proteins and their processing and subsequently the pro-inflammatory status of the skin in AD is difficult to dissect. This was apparent by the lack of correlation between filaggrin levels and a cathepsin H in AD patients. However understanding how overall filaggrin protease activity levels are altered in atopic skin would provide targets to treat both the barrier and immune aspects of AD.

Individuals with two loss-of-function mutations in *FLG* (compound heterozygotes) show the greatest increase in risk of AD[8,53], and gene expression differences in these individuals is greater than in *FLG* heterozygote and wild type individuals[14], which allowed for the detection of statistically significant differentially expressed genes correlated with RAPTOR expression. Consistent with our work *in vitro*, high levels of RAPTOR correlated with low levels of filaggrin expression, and AKT signalling components. Taken together our findings make a convincing case for the role of RAPTOR in regulating genes, including *FLG*, that are important in the AD phenotype. Also this work suggests that rapamycin or retinoid treatment could be of benefit in these individuals with filaggrin haploinsufficiency and severe AD.

Materials and Methods

Animals: Cathepsin H (Ctsh) knock-out and heterozygote mice were generated as previously described[9] and backcrossed onto the C57BL/6J background for eight generations. *Ctsh*$^{-/-}$,*Ctsh*$^{+/-}$ mice and wild-type littermate controls were bred under SPF conditions in accordance with the German law for Animal Protection (Tierschutzgesetz) as published on 25 May 1998. 3 day old (neonate) mice were obtained from 5 litters and 6 month old (adult) mice were obtained from two separate litters. A maximum of 5 wild-type, 8 *Ctsh*$^{+/-}$ and 10 *Ctsh*$^{-/-}$ neonate mice and 3 of each phenotype of adult mice were used in all analyses, blinding was not used in the assessment of the mouse skin

siRNA knockdown, Cell and Organotypic culture, mouse tissue

Four shRNA plasmids (Qiagen) were used to knockdown Akt1 expression (shRNA1-GCACCGCTTCTTTGCCAACAT, shRNA2-AAGGCACAGGTCGCTACTAT, shRNA3-GAGGCCCAACACCTTCATCAT, shRNA4-GCTGTTCGAGCTCATCCTAAT), and of these 1 and 3 were used for further experiments. Ctsh knockdown was successfully achieved by transient transfection with two shRNA plasmids (shRNA1-CAAGAATGGTCAGTGCAAATT ; shRNA3-CTAGAGTCAGCTGTGGCTATT). The following scrambled control was used GGAATCTCATTCGATGCATAC. Akt1 and Ctsh shRNA knockdown plasmids were transfected into rat epidermal keratinocyte (REK) cells[47] using lipofectamine (Invitrogen) according to manufacturer's instructions. Mycoplasma-testing was performed prior to the experiments. Cells were cultured and G418 (Gibco) selection was performed as previously described[47]. The organotypic cultures were either embedded in OCT for frozen sections, or paraffin embedded. Drug treatments with ATRA (10μM. Fisher Scientific) or Wortmannin (2μM, Sigma), were for 24 hours. Dorsal skin was removed from neonatal (Postnatal day 3) Ctsh +/+, +/- and -/- mice for subsequent analyses

Lentiviral shRNA knockdown in human keratinocytes

$2x10^5$ lentiviral particles (scrambled control, AKT1shRNA and CTSHshRNA, Santa Cruz Biotechnology) were incubated for 24 hours with 50-70% confluent mycoplasma-free keratinocytes grown in Gibco serum-free keratinocyte culture medium (Invitrogen) in a 12 well plate. Cells were trypsinised and selected by puromycin selection for 2 weeks as per manufacturer's instructions. Cells were subsequently calcium switched at 2.4mM $CaCl_2$ for 4 days prior to investigation by western blotting of AKT1, CTSH and Filaggrin.

Western blot and antibodies

Keratinocyte protein lysates and skin protein lysates from commercially available skin samples (Caltagmedsystems) were prepared by boiling in a denaturing SDS buffer (2% 2-mercaptoethanol, 2% SDS, 10mM Tris pH 7.5) for 10 minutes. For the cytokine arrays, Suspensions of T25 Ultra-Turrax (IKA) homogenised neonatal mouse skin was spun down and the suspensions from 2 Ctsh +/+, +/- and -/- mouse skin samples were pooled and used on the cytokine array panel A (RandD Systems) according to manufacturers' instructions. Densitometry of ECL exposures of cytokine arrays and western blots where appropriate were performed using the ImageJ software. Briefly, this was achieved by inverting the monochrome image, removing the background, thresholding the image and then measuring the thresholded bands, then the integrated density (pixel value x band area) was used as a measure of band intensity, which is subsequently normalized by a loading control (Gapdh). Antibodies used were rabbit anti-RAPTOR (24C12) (Cell Signalling Technologies, 1/500),Rabbit anti- filaggrin (M-290) (Santa Cruz Biotechnologies #sc-30230, 1/500), Mouse anti-c-Myc (9E10) (1/500, Sigma), Mouse anti-FLAG (1/100, F1804 Sigma), Rabbit anti-Rictor (Cell Signalling Technologies #2140, 1/500), Rabbit anti pSerine473 Akt (Cell Signalling Technologies #9271, 1/500), Mouse anti Akt-1 (2H10) (Cell Signalling Technologies #2967, 1/500), Mouse anti Gapdh (1/2000, AB2303 Millipore) Rabbit anti-Loricrin (Covance PRB-145P, 1/1000), Rabbit anti-Keratin 10 (Covance PRB-140C, 1/1000), Rabbit anti-Interleukin 4 (Abcam ab9622 ,1/500) and cathepsin H (H-130) (1/500, sc-13988 Santa Cruz Biotechnologies). Primary antibody incubations were in PBS+0.1% Tween-20 or in TBST (100mM Tris

HCl, 0.2M NaCl, 0.1% Tween-20 (v/v) containing either 5% bovine serum albumin (Sigma, Gillingham, UK) or 5% skimmed milk powder either overnight at 4^{o}C or for 1-2 h at room temperature, while secondary antibody incubations were in 5% skimmed milk powder for 1 h at room temperature. The following concentrations were used; swine anti rabbit-HRP (DakoCytomation) 1:3000; rabbit anti mouse HRP (DakoCytomation) 1:2000. Protein was visualized using the ECL plus kit (Amersham).

Immunofluoresence, Immunohistochemistry and eczema and unaffected samples

Clinical material was obtained with informed written consent from patients attending dermatology clinics at Great Ormond Street Hospital, Ethical approval was granted by the local research ethics committee. Normal paraffin embedded skin samples were obtained from a commercially available tissue microarray (BioMax), all tissue samples were from non-flexural areas. Immunohistochemistry and Immunofluorescence on paraffin and frozen sections were by standard techniques. Antibodies used were RAPTOR (24C12) (Cell Signalling Technologies, 1/50), Mouse anti-filaggrin (Genetex GTX23137, 1/50), Cathepsin H (H-130) (Santa Cruz Biotechnologies sc-13988, 1/50), Rabbit anti F4/80 (Bio-Rad AbD SeroTec CL:A3:1), Rabbit anti-Loricrin (Covance PRB-145P 1/200), Rabbit anti-Il1a (H-159) (Santa Cruz Biotechnology sc-7929, 1/50), Rabbit anti-cathepsin B (Biovision 3190-100, 1/25), Rabbit anti-Tslp (Thermo PA5-20321, 1/25), Rabbit anti-CD45 [EP322Y] (Abcam ab40763, 1/25). Primary antibodies were detected using Alexa 488 and 594-conjugated goat anti mouse and anti-rabbit (Invitrogen, 1/500). Cells and Sections were counterstained with 4',6-diamidino-2-phenylindole (DAPI, Sigma). Images were taken with a Leica Upright Microscope with either x20 (NA 0.4) or x40 (NA 1.40) objectives, using a Coolsnap digital camera (MediaCybernetics, Bethesda, Maryland), with the ImagePro 6.0 software (MediaCybernetics, Bethesda, Maryland). Immunofluoresence intensity was measured using imageJ (https://imagej.nih.gov/ij/) to determine the integrated density on a thresholded image after processing to remove background.

RNA extraction and microarray analysis

0.1 mg RNA was extracted from two scrambled REK lines, and 2 biological replicates of each Akt1 shRNA knockdown , and poly-A+ RNA was selected using the Oligotex system (Qiagen). RNA was extracted from the two Ctsh knockdown REK lines using the same approach. Second-strand cDNA was synthesized using the Superscript II kit (Invitrogen, Carlsbad, New Mexico) after the RNA was annealed with a T7 promoter-poly-T primer (Genset, Evry, France). Biotin-labelled cRNA was made from this cDNA (Enzo Diagnostics, Farmingdale, New York). The whole probe was hybridized to the exon array rat genome chip (Affymetrix, Santa Clara, California) according to the manufacturers' specifications. The scrambled controls cells were the base line in all analyses. Genes that were tagged as present and increased in all six analyses with a p-value of less than or equal to 0.05 by Mann–Whitney analysis, a p-value less than 0.05 after Benjamini-Hochberg False Discovery Rate correction and 1.5 fold or more altered in expression, were regarded as differentially expressed. Supervised analysis of over-represented genes was performed by inputting lists of differentially expressed genes into the Gene Set Enrichment Analysis program (http://software.broadinstitute.org/gsea/index.jsp)

Electron Microscopy

Transmission electron microscopy (EM) was performed on wt littermates and Ctsh heterozygous and null mouse tissue (n=2 each genotype). Normal EM protocols were used. Briefly tissues were fixed overnight in glutaraldehyde, with post fixation in 1% Osmium tetroxide in 100mM phosphate buffer for 2 hours at 4^{o}C. En bloc staining with 2% aqueous uranyl acetate was performed for 2 hours, prior to embedding and the cutting of semi thin sections and sections for EM grids.

Realtime PCR

Rat cathepsin H and filaggrin message levels were measured using gene-specific Quantitect primers (Qiagen) and SYBR green (Qiagen) and $\Delta\Delta^{CT}$ relative quantification

Sonication Assay for cornified envelopes and Haemotoxilin Dye Penetration Assays

Cornified envelopes were extracted from the neonatal mouse skin by boiling for 10 min in (50 mm Tris-HCl, pH 7.5, 2% SDS, 5 mm EDTA). Cornified envelopes were pelleted by centrifugation and washed in cornified envelope washing buffer (10 mm Tris-HCl in 0.1% SDS). After resuspension, envelopes were counted by haemocytometer. After sonication with a probe sonicator for 5x1 second pulses, the intact envelopes were counted and expressed as a % of the unsonicated total. The haemotoxlin penetration assay on neonate mouse skin and subsequent sectioning has been described previously [11].

Correlation Analysis of RAPTOR in Human Expression Data and code availability

Skin biopsies from non-lesional, non-flexural skin biopsies from 26 AD patients and 10 non-atopic controls of known *FLG* genotype, (*FLG* wildtype (n=7), *FLG* heterozygous (n=12), and *FLG* compound heterozygous (n=7)) were taken, the RNA extracted and the direct RNA sequencing reads were processed as described previously[14]. The mean expression for each gene was determined across the three *FLG* genotypes in the samples (wild type, heterozygous and compound heterozygous) and correlated to *RAPTOR*'s expression using Pearson's method. Any genes which have an *r* close to 1 or -1 are the most likely candidates to be co-regulated with *RAPTOR* under the *FLG* genotype background. In order to avoid genes with low counts having spurious correlations, only genes with a total mean expression across the three genotypes >25 reads were considered (n=9708).

A significance value for the correlations can be calculated. Firstly the *t* statistic can be determined for gene *i* as:

$$t_i = r_i . \sqrt{\frac{n-2}{1-{r_i}^2}}$$

where r_i is the Pearson's correlation and *n* is the number of genotypes per gene (here, *n*=3) which determines the degrees of freedom (*n* – 2). Given t_i and the degrees of freedom, a p-value can be calculated from the standard *t*-distribution using the 'pt' function in R (v3.1.3). p-values are quoted

unadjusted. The code for this analysis is available from Github (https://github.com/drchriscole/eczemaDRS). All genes with a correlation p-value <0.05 and a log2 fold-change >0.5 or <-0.5 in the wild-type versus compound heterozygote comparison were considered for further investigation using STRING (http://string-db.org/)

Restriction fragment length polymorphism analysis

RFLP analysis was performed on 18 skin samples. DNA was extracted by DNA mini spin kit (Qiagen) according to manufacturers' instructions. The rs8078605 polymorphism introduced a BsmAI site into the locus. F- CACCGCATTTGCTCTTACAA and R- CCTACACATGGTCCTTCATCC (Tm 60^{o}C) primers produced a 454bp amplicon. The T variant after BsmAI digestion gives a 203bp and 251bp product.

Statistical analysis

For qPCR and the analysis of normalised data from western blots, t-test or one way ANOVA were used. For all other analyses non-parametric tests were performed, Kruskal-Wallis with Dunnett post-hoc testing. Specific analyses are also identified in the figure legends

Acknowledgements

We acknowledge UCL genomics for the gene array hybridisation and subsequent analysis. We thank the Electron Microscopy units of Queen Mary University of London and UCL for the transmission electron microscopy analyses. RO is funded by the Great Ormond Street Hospital Children's Charity, AN is funded by a British Skin Foundation studentship (2018s). CC is funded as part of the Centre for Dermatology and Genetic Medicine, University of Dundee Wellcome Trust Strategic Award (098439/Z/12/Z). Sara B is supported by a Wellcome Trust Intermediate Clinical fellowship (086398/Z/08/Z) and a research grant from the Manknell Charitable Trust.

Author Contributions

RO, W-L D, AN and TR conceived and designed the experiments. RO, AN, CT, BW, Stuart B and YZ performed experiments. WOC, MFM, SAGW-O provided the complete GWAS data for the RAPTOR gene. Sara B and CC provided data from gene expression analysis of AD, and performed gene expression correlation analysis. TR bred the *Ctsh* -/+ and -/- mice and prepared tissues. The manuscript was written by RO, JH, AN, CC, TR and Sara B. All authors have read and approved the final version of this manuscript.

Competing Financial Interests Statement

There are no competing financial interests associated with this manuscript.

Figure Legends

Figure 1: Increased RAPTOR expression correlated with reduced filaggrin expression in keratinocytes and AD skin (a) filaggrin, pSerAKT and Raptor Immunofluoresence of in normal (n=3) and unaffected AD skin (n=5). **(b)** Image analysis of filaggrin, pSerAKT in normal and unaffected AD skin. Error bars are s.d. **(c)** RAPTOR expression from RNAseq analysis in Cole et al., 2014[14]. Box shows median and interquartile ranges for wildtype controls atopic dermatitis (AD) of the 3 *FLG* genotypes, wildtype, heterozygous, and compound heterozygous. **(d)** Scatterplots showing correlation of gene expression with RAPTOR expression. The fold-change of all significantly differentially expressed genes (FDR $p< 0.05$) are represented, with Filaggrin (FLG) in orange. **(e)** Graph of fold change of highly correlated and anti-correlated genes in the *FLG* compound heterozygotes (FC Cmpd) and heterozygotes (FC Het). The most highly differentially expressed genes, including FLG are indicated. **(f)** RAPTOR overexpression in rat epidermal keratinocytes model. Western blot of pAkt, Total AKT and filaggrin. Boxes indicate the areas that comprise total filaggrin and filaggrin monomer for densitometry **(g)** Graph of densitometry of total filaggrin, filaggrin monomer, pSerAkt and total AKT in RAPTOR overexpressing REKs in two separate experiments. Gapdh is loading control. *$p<0.05$, Kruskal-Wallis with post-hoc testing (b). Bars 50μm (a)

Figure 2: Loss of Akt1 leads to loss of filaggrin expression and hyperkeratosis in skin-equivalent organotypic cultures. (a) Western blot of lysates from human keratinocytes treated with 2μM Wortmannin or vehicle (DMSO) for 24 hours for Akt, pSerAKT, Filaggrin. n=2 **(b)** Western blot of pAKT and AKT1 in AKT1 knockdown keratinocytes. **(c)** Western blots of Akt1, Filaggrin, Keratin 10 and Loricrin in all Akt1 shRNA expressing lines, Gapdh is loading control. **(d)** Real time PCR analysis of filaggrin expression in AKT1 shRNA expressing lines. **(e)** Graph of mean densitometry of Akt1, total filaggrin and filaggrin monomer, loricrin and keratin 10 in Western blots of Akt1 shRNA knockdown cells (red bars) compared with scrambled (blue bars). Dots indicate separate experimental values **(f)**. Histology and immunofluorescence of Akt1, and filaggrin in Akt1 shRNA expressing organotypic cultures (n=4). Bars 50μm (f). *$p<0.05$, **$p<0.005$, Unpaired T-Test. Error bars are s.d..

Figure 3: Cathepsin H, is a differentiation-dependent protease co-expressed with filaggrin. (a) Heat map of differential gene expression between two Akt1 kd and scrambled control keratinocytes. Blue, down regulated, Yellow, up-regulated. **(b)** Graph of differentially expressed genes. Genes with the highest up and down-regulation, including Cathepsin H (Ctsh) indicated on the graph **(c** and **d)** Heat maps of differentially expressed genes involved in mTORC signalling **(c)** and proteases **(d). (e)** Real time PCR analysis of cathepsin H (Ctsh) expression in Akt1 kd cell lines. Bars show s.d. ** $p < 0.01$ (2-Way ANOVA). **(f)** Western blot of Ctsh expression in Akt1 kd cells and control (scram) cells. **(g)** Western blot of Ctsh, pAKT and total AKT in normal human epidermal keratinocytes treated with wortmannin (WORT) or vehicle (DMSO) **(h)** Western blot of pre and post-confluent REKs for pSerAKT, Ctsh and keratin 1. **(i)** Co-immunofluoresence of Ctsh and filaggrin. Gapdh is loading control in all western blots, bar 50µm (i)

Figure 4: Cathepsin H is a filaggrin processing protease controlled by Raptor and AKT1. (a) Ctsh Immunofluoresence in normal and unaffected AD skin (n=5) **(b)** Graph of Ctsh expression in normal and unaffected AD skin. Error bars are s.d. **(c)** Western blot of Cathepsin H in RAPTOR overexpressing rat keratinocytes. **(d)** Western blot of human epidermal keratinocytes (NHEKs) expressing AKT1 and CTSH shRNA **(e)** Graph of mean densitometry of Akt1, total filaggrin and filaggrin monomer and Ctsh. **(f)** Western blot of Filaggin and Ctsh in Akt1 kd cells transiently transfected with Ctsh or empty vector. **(g)** Graph of mean densitometry for total filaggrin and filaggrin monomer. 2 separate experiments are shown*$p<0.05$, **$p<0.005$, Unpaired T-Test (e,g). Gapdh is loading control for all western blots, bar 50µm (a)

Figure 5: Reduced filaggrin processing and impaired epidermal barrier in Cathepsin H deficient mouse skin. (a). Histology of Ctsh -/-, Ctsh +/- , and wt mouse neonatal skin (n=5,8 and 10 respectively) **(b)** Graph of stratum corneum thickness in Ctsh -/-, Ctsh +/- , and wt neonatal epidermis. **(c)** Filaggrin immunofluoresence in Ctsh -/-, Ctsh +/- , and wt neonatal epidermis. Inset shows granular layer detail in the filaggrin immunofluorescence **(d)** Graph of immunofluorescence of total filaggrin (upper) and for occurrence (counts) of granular filaggrin expression (lower) **(e)** loricrin immunofluoresence in Ctsh -/-, Ctsh +/- , and littermate control mouse neonatal epidermis **(f)** Graph of loricrin immunofluorescence intensity **(g)** Representative haemotoxylin dye penetration experiment on neonatal mouse skin. **(h)** Representative electron microscopy showing the reduced size and number of keratohyalin granules in the Ctsh +/- mice. 'k' ,keratohyalin granules **(i)** Keratohyalin granules size in Ctsh -/-, Ctsh +/- , wt mouse neonatal epidermis. **(j)** Sonication analysis of cornified envelopes from skin from Ctsh -/-, Ctsh +/- and wildtype neonate skin. Bars and boxes shows median and interquartile range (i,j) *$p<0.05$, **$p<0.05$ #$p<0.05$ Fishers exact test (d). Bars 50µm (a,c and g), 2µm (h)

Figure 6: Loss of Cathepsin H increases skin macrophages, mast cell degranulation and proinflammatory molecule expression. (a) Immunofluorescence of macrophages (F4/80 +ve) in wt, Ctsh -/- (ko) and Ctsh +/- (het) mouse neonatal skin **(b)** toluidine blue staining for dermal mast cells. **(c)** Graph of average F4/80 +ve cell, mast cell counts and % degranulating mast cells per field of view in wt, Ctsh -/- (ko) and Ctsh +/- (het) mouse neonatal skin **(d)** Densitometry of the cytokine arrays incubated with pooled lysates from 2 Wt (WT), and 2 Heterozygous or knockout mice (Het/Ko). **(e)** Il1a, and Tslp immunofluorescence in Ctsh -/-, Ctsh +/- , and wt neonatal skin. **(f)** Graph of immunofluorescence intensity of Tslp and Il1a. Bars 50µm (a,b and e). *$p<0.05$, **$p<0.005$ (c and f)

Figure 7: The mTORC/AKT1/Cathepsin H axis in the control of the physical and immune skin barrier. The variant SNP rs 8078605 prevents RXR binding to the putative intragenic enhancer in RAPTOR, potentially increasing RAPTOR expression which itself reduces filaggrin expression. This increases the ratio of mTORC1 to mTORC2, reducing Akt1 phosphorylation. This leads to reduced Cathepsin H expression and decreases filaggrin processing. Up-regulation of other filaggrin processing proteases such as Cathepsin B in response not only leads to rescue of barrier function but also causes macrophage infiltration, mast cell activity and pro-inflammatory cytokine expression

Reference List

[1] B. J. Aneskievich and E. Fuchs, "Terminal differentiation in keratinocytes involves positive as well as negative regulation by retinoic acid receptors and retinoid X receptors at retinoid response elements," Mol. Cell Biol. **12(11)**, 4862 (1992).
Ref Type: Journal

[2] D. Asselineau and M. Darmon, "Retinoic acid provokes metaplasia of epithelium formed in vitro by adult human epidermal keratinocytes," Differentiation. **58(4)**, 297 (1995).
Ref Type: Journal

[3] A. D. Balgi*, et al.*, "Regulation of mTORC1 signaling by pH," PLoS. One. **6(6)**, e21549 (2011).
Ref Type: Journal

[4] B. E. Bernstein*, et al.*, "An integrated encyclopedia of DNA elements in the human genome," Nature. **489**(7414), 57 (2012).
Ref Type: Journal

[5] C. Bonnart*, et al.*, "Elastase 2 is expressed in human and mouse epidermis and impairs skin barrier function in Netherton syndrome through filaggrin and lipid misprocessing," J. Clin. Invest. **120**(3), 871 (2010).
Ref Type: Journal

[6] F. Brasch*, et al.*, "Involvement of cathepsin H in the processing of the hydrophobic surfactant-associated protein C in type II pneumocytes," Am. J. Respir. Cell Mol. Biol. **26**(6), 659 (2002).
Ref Type: Journal

[7] S. J. Brown and W. H. McLean, "One remarkable molecule: filaggrin," J. Invest Dermatol. **132(3 Pt 2)**, 751 (2012).
Ref Type: Journal

[8] S. J. Brown*, et al.*, "Prevalent and low-frequency null mutations in the filaggrin gene are associated with early-onset and persistent atopic eczema," J. Invest Dermatol. **128(6)**, 1591 (2008).
Ref Type: Journal

[9] F. Buhling*, et al.*, "Gene targeting of the cysteine peptidase cathepsin H impairs lung surfactant in mice," PLoS. One. **6**(10), e26247 (2011).
Ref Type: Journal

[10] J. A. Burgess*, et al.*, "Does eczema lead to asthma?," J. Asthma. **46**(5), 429 (2009).
Ref Type: Journal

[11] C. Byrne*, et al.*, "Whole-mount assays for gene induction and barrier formation in the developing epidermis," Methods Mol. Biol. **585:271-86. doi: 10.1007/978-1-60761-380-0_19.**, 271 (2010).
Ref Type: Journal

[12] R. E. Callard and J. I. Harper, "The skin barrier, atopic dermatitis and allergy: a role for Langerhans cells?," Trends Immunol. **28**(7), 294 (2007).
Ref Type: Journal

[13] A. Chawla*, et al.*, "Nuclear receptors and lipid physiology: opening the X-files," Science. **294**(5548), 1866 (2001).
Ref Type: Journal

[14] C. Cole*, et al.*, "Filaggrin-stratified transcriptomic analysis of pediatric skin identifies mechanistic pathways in patients with atopic dermatitis," J. Allergy Clin. Immunol. **134(1)**, 82 (2014).
Ref Type: Journal

[15] M. J. Cork*, et al.*, "New perspectives on epidermal barrier dysfunction in atopic dermatitis: gene-environment interactions," J. Allergy Clin. Immunol. **118**(1), 3 (2006).
Ref Type: Journal

[16] M. E. D'Angelo*, et al.*, "Cathepsin H is an additional convertase of pro-granzyme B," J. Biol. Chem. **285(27)**, 20514 (2010).
Ref Type: Journal

[17] S. J. de Veer*, et al.*, "Proteases: common culprits in human skin disorders," Trends Mol. Med. (13), 10 (2013).
Ref Type: Journal

[18] G. Denecker*, et al.*, "Caspase-14 protects against epidermal UVB photodamage and water loss," Nat. Cell Biol. **9(6)**, 666 (2007).
Ref Type: Journal

[19] T. L. Diepgen, E. Pfarr, and T. Zimmermann, "Efficacy and tolerability of alitretinoin for chronic hand eczema under daily practice conditions: results of the TOCCATA open study comprising 680 patients," Acta Derm. Venereol. **92**(3), 251 (2012).
Ref Type: Journal

[20] F. Egberts*, et al.*, "Cathepsin D is involved in the regulation of transglutaminase 1 and epidermal differentiation," J. Cell Sci. **117(Pt 11)**, 2295 (2004).
Ref Type: Journal

[21] D. Ellinghaus*, et al.*, "High-density genotyping study identifies four new susceptibility loci for atopic dermatitis," Nat. Genet. **45**(7), 808 (2013).
Ref Type: Journal

[22] A. Faiz*, et al.*, "The expression and activity of cathepsins D, H and K in asthmatic airways," PLoS. One. **8**(3), e57245 (2013).
Ref Type: Journal

[23] P. G. Fallon*, et al.*, "A homozygous frameshift mutation in the mouse Flg gene facilitates enhanced percutaneous allergen priming," Nat. Genet. **41**(5), 602 (2009).
Ref Type: Journal

[24] G. R. Flentke*, et al.*, "Microarray analysis of retinoid-dependent gene activity during rat embryogenesis: increased collagen fibril production in a model of retinoid insufficiency," Dev. Dyn. **229**(4), 886 (2004).
Ref Type: Journal

[25] M. Grahovac*, et al.*, "Treatment of atopic eczema with oral alitretinoin," Br. J. Dermatol. **162**(1), 217 (2010).
Ref Type: Journal

[26] R. Gruber*, et al.*, "Diverse regulation of claudin-1 and claudin-4 in atopic dermatitis," Am. J. Pathol. **185(10)**, 2777 (2015).
Ref Type: Journal

[27] E. Guttman-Yassky, K. E. Nograles, and J. G. Krueger, "Contrasting pathogenesis of atopic dermatitis and psoriasis--part II: immune cell subsets and therapeutic concepts," J. Allergy Clin. Immunol. **127(6)**, 1420 (2011).
Ref Type: Journal

[28] E. Guttman-Yassky, K. E. Nograles, and J. G. Krueger, "Contrasting pathogenesis of atopic dermatitis and psoriasis--part II: immune cell subsets and therapeutic concepts," J. Allergy Clin. Immunol. **127(6)**, 1420 (2011).
Ref Type: Journal

[29] T. Hirota*, et al.*, "Genome-wide association study identifies eight new susceptibility loci for atopic dermatitis in the Japanese population," Nat. Genet. **44**(11), 1222 (2012).
Ref Type: Journal

[30] M. D. Howell*, et al.*, " Th2 cytokines act on S100/A11 to downregulate keratinocyte differentiation," J Invest Dermatol. **128(9)**, 2248 (2008).
Ref Type: Journal

[31] I. Jakasa*, et al.*, "Percutaneous penetration of sodium lauryl sulphate is increased in uninvolved skin of patients with atopic dermatitis compared with control subjects," Br. J. Dermatol. **155**(1), 104 (2006).
Ref Type: Journal

[32] S. M. Janes*, et al.*, "Transient activation of FOXN1 in keratinocytes induces a transcriptional programme that promotes terminal differentiation: contrasting roles of FOXN1 and Akt," J. Cell Sci. **117**(Pt 18), 4157 (2004).
Ref Type: Journal

[33] S. Kasraie and T. Werfel, "Role of macrophages in the pathogenesis of atopic dermatitis," Mediators. Inflamm. **2013**, 942375 (2013).
Ref Type: Journal

[34] A. Kawada*, et al.*, "Rat epidermal cathepsin L-like proteinase: purification and some hydrolytic properties toward filaggrin and synthetic substrates," J. Biochem. **118(2)**, 332 (1995).
Ref Type: Journal

[35] A. Kawada*, et al.*, "Rat epidermal cathepsin B: purification and characterization of proteolytic properties toward filaggrin and synthetic substrates," Int. J. Biochem. Cell Biol. **27(2)**, 175 (1995).
Ref Type: Journal

[36] S. Kezic*, et al.*, "Filaggrin loss-of-function mutations are associated with enhanced expression of IL-1 cytokines in the stratum corneum of patients with atopic dermatitis and in a murine model of filaggrin deficiency," J. Allergy Clin. Immunol. **129**(4), 1031 (2012).
Ref Type: Journal

[37] B. E. Kim*, et al.*, "Loricrin and involucrin expression is down-regulated by Th2 cytokines through STAT-6," Clin. Immunol. **126(3)**, 332 (2008).
Ref Type: Journal

[38] I. H. Kuo*, et al.*, "The cutaneous innate immune response in patients with atopic dermatitis," J. Allergy Clin. Immunol. **131(2)**, 266 (2013).
Ref Type: Journal

[39] C. Lambert*, et al.*, "Gene expression pattern of synovial cells from inflammatory and normal areas of osteoarthritis synovial membrane," Arthritis Rheum. 10 (2013).
Ref Type: Journal

[40] Q. T. Le*, et al.*, "Processing of human protryptase in mast cells involves cathepsins L, B, and C," J. Immunol. **187(4)**, 1912 (2011).
Ref Type: Journal

[41] M. Li*, et al.*, "Analyses of FLG mutation frequency and filaggrin expression in isolated ichthyosis vulgaris (IV) and atopic dermatitis-associated IV," Br. J. Dermatol. **168**(6), 1335 (2013).
Ref Type: Journal

[42] X. Li*, et al.*, "Increased expression of cathepsins and obesity-induced proinflammatory cytokines in lacrimal glands of male NOD mouse," Invest Ophthalmol. Vis. Sci. **51(10)**, 5019 (2010).
Ref Type: Journal

[43] K. List*, et al.*, "Loss of proteolytically processed filaggrin caused by epidermal deletion of Matriptase/MT-SP1," J. Cell Biol. **163**(4), 901 (2003).
Ref Type: Journal

[44] T. Matsui*, et al.*, "SASPase regulates stratum corneum hydration through profilaggrin-to-filaggrin processing," EMBO Mol. Med. **3**(6), 320 (2011).
Ref Type: Journal

[45] G. M. O'Regan*, et al.*, "Filaggrin in atopic dermatitis," J. Allergy Clin. Immunol. **122**(4), 689 (2008).
Ref Type: Journal

[46] R. F. O'Shaughnessy*, et al.*, "Cutaneous human papillomaviruses down-regulate AKT1, whereas AKT2 up-regulation and activation associates with tumors," Cancer Res. **67(17)**, 8207 (2007).
Ref Type: Journal

[47] R. F. O'Shaughnessy, *et al.*, "AKT-dependent HspB1 (Hsp27) activity in epidermal differentiation," J. Biol. Chem. **282**(23), 17297 (2007).
Ref Type: Journal

[48] C. N. Palmer, *et al.*, "Common loss-of-function variants of the epidermal barrier protein filaggrin are a major predisposing factor for atopic dermatitis," Nat. Genet. **38**(4), 441 (2006).
Ref Type: Journal

[49] L. Pellerin, *et al.*, "Defects of filaggrin-like proteins in both lesional and nonlesional atopic skin," J. Allergy Clin. Immunol. **131**(4), 1094 (2013).
Ref Type: Journal

[50] M. Rendl, *et al.*, "Caspase-14 expression by epidermal keratinocytes is regulated by retinoids in a differentiation-associated manner," J. Invest Dermatol. **119(5)**, 1150 (2002).
Ref Type: Journal

[51] D. S. Rosenthal, *et al.*, "Acute or chronic topical retinoic acid treatment of human skin in vivo alters the expression of epidermal transglutaminase, loricrin, involucrin, filaggrin, and keratins 6 and 13 but not keratins 1, 10, and 14," J. Invest Dermatol. **98**(3), 343 (1992).
Ref Type: Journal

[52] T. Ruzicka, *et al.*, "Efficacy and safety of oral alitretinoin (9-cis retinoic acid) in patients with severe chronic hand eczema refractory to topical corticosteroids: results of a randomized, double-blind, placebo-controlled, multicentre trial," Br. J. Dermatol. **158**(4), 808 (2008).
Ref Type: Journal

[53] A. Sandilands, *et al.*, "Prevalent and rare mutations in the gene encoding filaggrin cause ichthyosis vulgaris and predispose individuals to atopic dermatitis," J. Invest Dermatol. **126(8)**, 1770 (2006).
Ref Type: Journal

[54] A. Sandilands, *et al.*, "Comprehensive analysis of the gene encoding filaggrin uncovers prevalent and rare mutations in ichthyosis vulgaris and atopic eczema," Nat. Genet. **39**(5), 650 (2007).
Ref Type: Journal

[55] T. Seguchi, *et al.*, "Decreased expression of filaggrin in atopic skin," Arch. Dermatol. Res. **288**(8), 442 (1996).
Ref Type: Journal

[56] L. M. Sevilla, *et al.*, "Epidermal inactivation of the glucocorticoid receptor triggers skin barrier defects and cutaneous inflammation," J. Invest Dermatol. **133**(2), 361 (2013).
Ref Type: Journal

[57] F. J. Smith, *et al.*, "Loss-of-function mutations in the gene encoding filaggrin cause ichthyosis vulgaris," Nat. Genet. **38**(3), 337 (2006).
Ref Type: Journal

[58] V. Soumelis*, et al.*, "Human epithelial cells trigger dendritic cell mediated allergic inflammation by producing TSLP," Nat. Immunol. **3(7)**, 673 (2002).
Ref Type: Journal

[59] K. Sully*, et al.*, "The mTOR inhibitor rapamycin opposes carcinogenic changes to epidermal Akt1/PKBalpha isoform signaling," Oncogene. **32**(27), 3254 (2013).
Ref Type: Journal

[60] C. Sun*, et al.*, "Allele-specific down-regulation of RPTOR expression induced by retinoids contributes to climate adaptations," PLoS. Genet. **6**(10), e1001178 (2010).
Ref Type: Journal

[61] B. R. Thrash*, et al.*, "AKT1 provides an essential survival signal required for differentiation and stratification of primary human keratinocytes," J. Biol. Chem. **281**(17), 12155 (2006).
Ref Type: Journal

[62] K. Vavrova*, et al.*, "Filaggrin deficiency leads to impaired lipid profile and altered acidification pathways in a 3D skin construct," J. Invest Dermatol. **134(3)**, 746 (2014).
Ref Type: Journal

[63] S. Weidinger*, et al.*, "A genome-wide association study of atopic dermatitis identifies loci with overlapping effects on asthma and psoriasis," Hum. Mol. Genet. **22**(23), 4841 (2013).
Ref Type: Journal

Supplementary table E1

Patient information for the 5 AD patients from Great Ormond Street Hospital. Location of biopsy for the non-lesional samples. Previous treatment, AZA, azathioprine; CSA cyclosporine

Patient	Sex	Age	Location of Biopsy	Previous Treatment
1	F	13	R Waist	oral steroid and AZA
2	M	13	L Arm	AZA
3	M	13	L Thigh	AZA
4	F	12	R Upper leg	AZA and CSA
5	M	11	Lower Back	No systemic treatment

Patient information for the Cole et al, cohort[14]: biopsies were taken from the non-lesional skin (the upper buttock with no clinical signs of active inflammation) of children aged 6 to 16 years who had early onset, persistent and severe atopic eczema. The 10 controls were non-atopic individuals ie no eczema, asthma or hay fever. Severity measurement is by physician global assessment

	severity at time of biopsy				
	mild	moderate	severe	not recorded	total
FLG wt	1	4	2	0	7
FLG het	3	4	4	1	12
FLG compound het	1	2	3	1	7
Total	5	10	9	2	26

Supplementary table E2: List of the 84 genes strongly correlated or anti-correlated with RAPTOR expression levels in unaffected compound heterozygote AD patient skin that are significantly differentially expressed in Cole et al 2014[14], GeneName, official HUGO nomenclature, WT, Het and Cmpd, are mean normalised expression levels of WT, Heterozygote and Compound Heterozygote respectively, s.d are the standard deviations of each cohort. Cor, Pearson correlation coefficient. FC fold change, pval is the p value after correction for multiple testing

Gene	Description	WT	Het	Cmpd	WT.sd	Het.sd	Cmpd.sd	cor	FC	logFC	pval
PTPRC	protein tyrosine phosphatase, receptor type, C	6.6	11	16	3	14	21	1	2.5	1.3	0.0079
IRF1	interferon regulatory factor 1	18	30	43	6.9	44	73	1	2.4	1.3	0.012
ISG15	ISG15 ubiquitin-like modifier	12	19	27	5.1	35	45	1	2.3	1.2	0.023
HAPLN3	hyaluronan and proteoglycan link protein 3	7.2	11	14	2	12	19	1	1.9	0.91	0.023
TIMM22	translocase of inner mitochondrial membrane 22 homolog (yeast)	9.6	13	17	3.6	6.5	11	1	1.8	0.84	0.0074
CKAP2	cytoskeleton associated protein 2	15	20	26	2.9	7.3	6.5	1	1.7	0.78	0.0013
CARD10	caspase recruitment domain family, member 10	12	16	21	5.6	5.6	8.1	1	1.7	0.78	0.014
TAP2	transporter 2, ATP-binding cassette, sub-family B (MDR/TAP)	38	47	62	7.9	33	61	1	1.7	0.73	0.031
TRIM22	tripartite motif containing 22	28	39	47	4.7	52	63	0.99	1.7	0.76	0.049
DBF4	DBF4 zinc finger	8	10	13	3.3	2.7	2.4	1	1.6	0.7	0.0071

UBE2L6	ubiquitin-conjugating enzyme E2L 6	25	32	38	8.6	24	37	1	1.5	0.59	0.0085
SNX11	sorting nexin 11	8.3	10	12	1.5	2.5	2.9	1	1.5	0.55	0.009
GXYLT1	glucoside xylosyltransferase 1	7.2	8.6	10	2	2.2	3.2	1	1.5	0.54	0.0096
IFI27	interferon, alpha-inducible protein 27	190	230	280	140	340	450	1	1.5	0.54	0.011
PSMB10	proteasome (prosome, macropain) subunit, beta type, 10	13	16	19	4.2	12	17	1	1.5	0.57	0.015
LCP2	lymphocyte cytosolic protein 2 (SH2 domain containing leukocyte protein of 76kDa)	8.2	9.8	12	2.1	8.1	8.3	1	1.5	0.56	0.023
PARP9	poly (ADP-ribose) polymerase family, member 9	31	40	48	12	46	54	1	1.5	0.62	0.024
NUAK2	NUAK family, SNF1-like kinase, 2	18	23	27	11	12	13	1	1.5	0.55	0.026
KCNK1	potassium channel, two pore domain subfamily K, member 1	30	37	44	7	9.2	6.7	0.99	1.5	0.55	0.035
HLA-DOA	major histocompatibility complex, class II, DO alpha	13	15	18	3.4	6.9	13	1	1.4	0.51	0.012
PRAF2	PRA1 domain family, member 2	19	16	14	4.3	3.4	4.4	-1	0.71	-0.5	0.025
NOV	nephroblastoma overexpressed	53	46	37	16	14	8.9	-1	0.7	-0.51	0.0049
ZBTB14	zinc finger and BTB domain containing 14	13	11	9	3.6	2.8	2.2	-1	0.7	-0.52	0.017
ENTPD4	ectonucleoside triphosphate diphosphohydrolase 4	18	15	12	3.6	3	2.9	-1	0.7	-0.52	0.022
SLC9B2	solute carrier family 9, subfamily B (NHA2,	17	15	12	5.2	3.7	3.1	-1	0.7	-0.51	0.026

	cation proton antiporter 2), member 2										
TPM2	tropomyosin 2 (beta)	110	90	75	66	40	21	-1	0.7	-0.52	0.028
LAMA3	laminin, alpha 3	19	16	13	9.2	3.8	5.1	-1	0.7	-0.52	0.041
RHOU	ras homolog family member U	17	14	12	7.4	5.8	3.5	-1	0.7	-0.51	0.046
ABHD4	abhydrolase domain containing 4	11	9.8	7.9	1.7	2.3	1.7	-1	0.69	-0.54	0.0028
MXRA8	matrix-remodelling associated 8	21	18	15	8.3	5.4	4.7	-1	0.69	-0.54	0.01
CD1A	CD1a molecule	31	26	21	12	8.7	9.5	-1	0.69	-0.53	0.021
RNF152	ring finger protein 152	43	36	30	7.6	8.9	6.8	-1	0.69	-0.53	0.024
CLDN10	claudin 10	13	11	8.7	9.5	5.7	5.5	-1	0.68	-0.56	0.032
GPR137	G protein-coupled receptor 137	11	8.9	7.4	3.6	2.3	3	-1	0.68	-0.55	0.04
ZDHHC11	zinc finger, DHHC-type containing 11	29	24	20	16	12	12	-1	0.68	-0.56	0.041
RP11-613D13.4	none	28	25	19	17	8	6.6	-1	0.68	-0.56	0.045
LPCAT1	lysophosphatidylcholine acyltransferase 1	15	12	10	4.2	3.8	3.2	-1	0.68	-0.56	0.046
DCLK1	doublecortin-like kinase 1	18	16	12	9.7	7.1	7	-1	0.68	-0.55	0.049
MT-ND1	mitochondrially encoded NADH dehydrogenase 1	360	310	240	92	91	40	-1	0.67	-0.57	0.0023
NCALD	neurocalcin delta	38	33	25	16	12	10	-1	0.67	-0.58	0.017
NNMT	nicotinamide N-methyltransferase	30	26	20	13	14	6.6	-1	0.67	-0.57	0.017
WNK2	WNK lysine deficient protein kinase 2	12	11	8.4	3.8	4	4	-1	0.67	-0.57	0.019
PIGV	phosphatidylinositol glycan anchor biosynthesis, class V	11	9.6	7.4	1.7	3.5	2.9	-1	0.67	-0.58	0.022

CCNG2	cyclin G2	27	24	18	11	8.1	11	-1	0.67	-0.58	0.036
PRELP	proline/arginine-rich end leucine-rich repeat protein	60	49	40	23	8.1	11	-1	0.67	-0.57	0.041
C11orf96	chromosome 11 open reading frame 96	28	25	19	17	8	6	-1	0.67	-0.58	0.049
FLNC	filamin C, gamma	13	11	8.3	5.9	3.8	4	-1	0.66	-0.59	0.0016
SNED1	sushi, nidogen and EGF-like domains 1	11	9.8	7.6	5.5	4.2	3.9	-1	0.66	-0.59	0.0072
FMOD	fibromodulin	32	28	21	13	9.1	6.7	-1	0.66	-0.6	0.028
MT-ND5	mitochondrially encoded NADH dehydrogenase 5	630	550	410	300	240	180	-1	0.66	-0.61	0.035
TLE2	transducin-like enhancer of split 2	13	12	8.6	4.3	3	3.5	-1	0.66	-0.6	0.049
UTY	ubiquitously transcribed tetratricopeptide repeat containing, Y-linked	13	11	8.6	5.2	6.9	5.4	-1	0.65	-0.62	0.015
CYBA	cytochrome b-245, alpha polypeptide	11	9.3	7.3	3.3	4.8	7.1	-1	0.65	-0.63	0.021
KLF9	Kruppel-like factor 9	60	49	39	36	18	12	-1	0.64	-0.65	0.023
ZDHHC11B	zinc finger, DHHC-type containing 11B	26	23	17	17	12	8.3	-1	0.64	-0.64	0.032
THBS1	thrombospondin 1	32	25	20	19	9	6.6	-1	0.64	-0.65	0.039
CRELD1	cysteine-rich with EGF-like domains 1	22	17	14	6.7	3	4.7	-1	0.64	-0.65	0.046
RAI2	retinoic acid induced 2	15	13	9.6	3.9	4.7	4.6	-1	0.63	-0.68	0.021
NOVA1	neuro-oncological ventral antigen 1	20	17	12	5	5.6	6.2	-1	0.63	-0.67	0.046
EBF1	early B-cell factor 1	19	16	12	8.8	6	3.3	-1	0.62	-0.68	0.014
FAM13A	family with sequence similarity 13, member A	39	31	24	33	11	5.1	-1	0.62	-0.7	0.014
HNMT	histamine N-	19	15	12	4.3	5	5.2	-1	0.62	-0.68	0.036

	methyltransferase										
ZG16B	zymogen granule protein 16B	49	38	30	32	15	12	-1	0.62	-0.69	0.043
IGF2	insulin-like growth factor 2	21	17	13	12	6.7	3.8	-1	0.61	-0.7	0.0099
MT-CO1	mitochondrially encoded cytochrome c oxidase I	460	370	280	120	140	59	-1	0.61	-0.71	0.016
HOTAIR	HOX transcript antisense RNA	13	11	7.8	7.4	3.3	5.4	-1	0.6	-0.73	0.0056
MXRA7	matrix-remodelling associated 7	15	12	9.1	5.4	3.2	2.7	-1	0.6	-0.74	0.013
INSR	insulin receptor	14	12	8.7	7.8	3.4	5.3	-1	0.6	-0.73	0.024
LIG1	ligase I, DNA, ATP-dependent	15	12	8.7	3.1	5.3	3.5	-1	0.6	-0.75	0.031
SPRN	shadow of prion protein homolog (zebrafish)	14	11	8.2	5.3	6.1	4.6	-1	0.58	-0.79	0.027
HRH1	histamine receptor H1	11	9.4	6.3	5.6	4.7	3.4	-1	0.58	-0.78	0.047
RGCC	regulator of cell cycle	74	58	42	29	25	11	-1	0.57	-0.8	0.012
PRR4	proline rich 4 (lacrimal)	54	40	30	60	69	24	-1	0.56	-0.83	0.05
S100P	S100 calcium binding protein P	62	47	34	18	17	24	-1	0.54	-0.89	0.026
IGFBP6	insulin-like growth factor binding protein 6	84	65	45	40	21	8.3	-1	0.53	-0.91	0.0075
MUCL1	mucin-like 1	460	350	240	290	190	200	-1	0.53	-0.92	0.028
KIAA1841	KIAA1841	21	17	11	8.3	4.9	3.6	-1	0.5	-1	0.017
MT-CO2	mitochondrially encoded cytochrome c oxidase II	110	89	54	36	53	19	-1	0.5	-0.99	0.043
C2orf74	chromosome 2 open reading frame 74	19	15	8.5	8.2	5.2	3.1	-1	0.46	-1.1	0.044
HSPB6	heat shock protein, alpha-crystallin-related, B6	24	19	10	14	7.6	6.8	-1	0.43	-1.2	0.04

CYP4B1	cytochrome P450, family 4, subfamily B, polypeptide 1	22	14	8.6	13	6.8	4.2	-1	0.4	-1.3	0.042
CILP	cartilage intermediate layer protein, nucleotide pyrophosphohydrolase	33	25	11	18	19	7.9	-1	0.32	-1.6	0.032
FLG	filaggrin	3300	1900	920	680	460	270	-1	0.28	-1.8	0.044
SCGB1D2	secretoglobin, family 1D, member 2	110	61	30	63	65	17	-1	0.28	-1.8	0.049

Supplementary Table E3 Concordance of the top 22 highly expressed and differentially expressed genes strongly correlated or anti-correlated with RAPTOR expression with gene whose expression level correlated with FLG expression levels[14] in unaffected compound heterozygote AD patient skin that are significantly differentially expressed, Gray denote either positive or negative correlation in both analyses. GeneName, official HUGO nomenclature, WT, Het and Cmpd, are mean normalised expression levels of WT, Heterozygote and Compound Heterozygote respectively, s.d are the standard deviations of each cohort. Cor, pearson correlation coefficient. FC fold change, pval is the p value after correction for multiple testing

Gene	Description	WT	Cmpd	FC	logFC	pval
TAP2	**transporter 2, ATP-binding cassette, sub-family B (MDR/TAP)**	38	62	1.7	0.73	**0.031**
TRIM22	**tripartite motif containing 22**	28	47	1.7	0.76	**0.049**
IFI27	**interferon, alpha-inducible protein 27**	190	280	1.5	0.54	**0.011**
KCNK1	**potassium channel, two pore domain subfamily K, member 1**	30	44	1.5	0.55	**0.035**
PARP9	**poly (ADP-ribose) polymerase family, member 9**	31	48	1.5	0.62	**0.024**
NOV	**nephroblastoma overexpressed**	53	37	0.7	-0.51	**0.005**
TPM2	**tropomyosin 2 (beta)**	110	75	0.7	-0.52	**0.028**
RNF152	**ring finger protein 152**	43	30	0.7	-0.53	**0.024**
MT-ND1	**mitochondrially encoded NADH dehydrogenase 1**	360	240	0.7	-0.57	**0.002**
PRELP	**proline/arginine-rich end leucine-rich repeat protein**	60	40	0.7	-0.57	**0.041**
MT-ND5	**mitochondrially encoded NADH dehydrogenase 5**	630	410	0.7	-0.61	**0.035**
KLF9	**Kruppel-like factor 9**	60	39	0.6	-0.65	**0.023**
ZG16B	**zymogen granule protein 16B**	49	30	0.6	-0.69	**0.043**
MT-CO1	**mitochondrially encoded cytochrome c oxidase I**	460	280	0.6	-0.71	**0.016**
RGCC	**regulator of cell cycle**	74	42	0.6	-0.8	**0.012**
PRR4	**proline rich 4 (lacrimal)**	54	30	0.6	-0.83	**0.05**
S100P	**S100 calcium binding protein P**	62	34	0.5	-0.89	**0.026**
IGFBP6	**insulin-like growth factor binding protein 6**	84	45	0.5	-0.91	**0.008**
MUCL1	**mucin-like 1**	460	240	0.5	-0.92	**0.028**
MT-CO2	**mitochondrially encoded cytochrome c oxidase II**	110	54	0.5	-0.99	**0.043**
FLG	**filaggrin**	3300	920	0.3	-1.8	**0.044**
SCGB1D2	**secretoglobin, family 1D, member 2**	110	30	0.3	-1.8	**0.049**

Supplementary Table E4

A table showing the average fold change in expression in both Akt1 kd lines in expression of all genes 2-fold and above differentially expressed; The 1.5 –fold or more down-regulated genes related to MTORC signalling and Proteases in the GSEA analysis are also shown in this table.

2-fold up- and down-regulated genes		
Symbol	**Entrez Gene Name**	**Fold Change**
Khdrbs3	KH domain containing, RNA binding, signal transduction associated 3	7.4
Pdlim2	PDZ and LIM domain 2	7.2
Ckmt1	creatine kinase, mitochondrial 1	5.2
Tmbim4	transmembrane BAX inhibitor motif containing 4	5.1
Bin3	bridging integrator 3	5.1
Sema3a	sema domain, immunoglobulin domain (Ig), short basic domain, secreted, (semaphorin) 3A	4.8
Ppp3cc	protein phosphatase 3, catalytic subunit, gamma isoform	4.7
Cldn3	claudin 3	3.7
Asrgl1	asparaginase like 1	3.6
Ccbl1	cysteine conjugate-beta lyase, cytoplasmic	3.6
Expi	extracellular proteinase inhibitor	3.5
Sepp1	selenoprotein P, plasma, 1	-2.1
Fads1	fatty acid desaturase 1	-2.1
Pkib	protein kinase (cAMP-dependent, catalytic) inhibitor beta	-2.1
Il33	interleukin 33	-2.1
Nt5e	5' nucleotidase, ecto	-2.4
Calml3	calmodulin-like 3	-2.7
S100g	S100 calcium binding protein G	-2.7
Slfn3	schlafen 3	-2.9
Ctsh	cathepsin H	-3.9
1.5-fold or more down-regulated genes involved in mTORC signalling		
Fads2	Fatty Acid Desaturase 2	-1.6
Cth	Cystathionine Gamma-Lyase	-1.8
Hmgcs1	3-Hydroxy-3-Methylglutaryl-CoA Synthase 1 (Soluble)	-1.9
Elovl6	ELOVL Fatty Acid Elongase 6	-1.9
Idi1	Isopentenyl-Diphosphate Delta Isomerase 1	-2.0
Fads1	Fatty Acid Desaturase 1	-2.1
1.5-fold or more down-regulated proteases		
Ace2	Angiotensin I Converting Enzyme 2	-1.6
Pcsk6	Proprotein Convertase Subtilisin/Kexin Type 6	-1.6
C1s	Complement Component 1, S Subcomponent	-1.6
Ctsh	Cathepsin H	-3.9

Supplementary Figure E1: Raptor and Filaggrin in normal skin and non lesional AD skin; IL-4 expression (a) Left, densitometry of filaggrin in Normal and AD non-lesional skin. Middle, Filaggrin levels in high and low RAPTOR expressing non-lesional AD patient skin. Right, Filaggrin levels in high and low RAPTOR expressing normal skin. *$p<0.05$, ** $p<0.005$ Mann-Whitney U-test. Bars, left and middle are the interquartile range. **(b)** IL-4 Western blot in rat epidermal keratinocytes treated with rapamycin (Rapa) for 24 hours (10nM). **(c)** IL-4 Western blot in AKT1 kd human keratinocytes. (b and c). Gapdh is loading control in (b,c).

Supplementary Figure E2: Analysis of the highly differentially expressed genes in AD which anti-correlate and correlate with RAPTOR expression. (a) STRING (http://string-db.org/) network of functionally interacting genes, with RAPTOR and AKT1 and the anti-correlated genes in green and red for anti-correlated and correlated genes respectively. Highly expressed genes that also correlated with FLG expression are indicated with an asterisk **(b)** Venn diagram showing the large overlap betweenhighly expressed genes correlating with RAPTOR expression and genes previously determined[14] to be correlated with the loss of filaggrin expression.

Supplementary figure E3: a SNP variant correlates with increased RAPTOR expression, reduced filaggrin expression and processing and reduced Cathepsin H expression. (a) Genomic context and of SNP rs8078605 and a graph of the GWAS data[63] from the RAPTOR region, y-axis, LOD score, the p-value for rs8078605 was 0.067. **(b)** Piechart showing prevalence of each genotype of the SNP rs8078605 in European and sub-Saharan African populations, Normal and AD individuals **(c)** RAPTOR expression in human keratinocytes in response to ATRA. Gapdh is loading control. Bar chart shows RAPTOR densitometry in 2 separate experiments **(d)** RAPTOR densitometry of western blots of 9 human skin samples with the C/ C (n=6), T/C (n=2) or T/T (n=1) variants in rs8078605. **(e)** Plot of RAPTOR densitometry against normalised western blot densitometry of a corresponding filaggrin western blot. T/T and C/T rs8078705 variants are marked on the graph, as is the correlation coefficient (R^2). **(f)** filaggrin and Ctsh Western blots from human samples, keratin 5 is an epidermal loading control.

Supplementary figure E4: Analysis of genes differentially expressed in Akt1kd keratinocytes. (a) Graph of enrichment scores for all significantly differentially expressed genes, including Ctsh **(b)** Graph of enrichment scores of genes involved in MTORC signalling **(c)**. Graph of 1/p values (uncorrected) of the three most over-represented functional groups in scrambled control cells by GSEA analysis. **(d)**. Leading edge analysis of the most differentially expressed genes in these three ontology groups, with several genes including HMGCS1 present in all gene ontology groups. **(e)** HMGCS1 expression in AD according to the RNAseq data in Cole et al., 2013.

Supplementary figure E5: Cathepsin H is required for Filaggrin processing but expression does not correlate with Filaggrin in atopic dermatitis. (a) Western blot of filaggrin and Cathepsin H in 4 Ctsh kd lines. **(b)** Graph of mean densitometry of total filaggrin, filaggrin monomer and Ctsh, n=4 **(c)** Real time PCR analysis of filaggrin expression in two Ctsh shRNA lines. **(d)** cathepsin H expression represented from RNAseq analysis in Cole et al., 2014. Box shows median and interquartile ranges in

wildtype controls and the three eczema *FLG* phenotypes **(e)** Scatterplots showing Pearson correlation (x-axis) of gene expression levels with cathepsin H expression. The fold-change of all significantly differentially expressed genes (FDR p< 0.05) are represented on the y axis, with Filaggrin (FLG) in orange. Correlations are between FLG wildtype, FLG heterozygous and FLG compound heterozygous (n=7).

Supplementary figure E6: Cathepsin B expression increases in Cathepsin H deficient mouse epidermis. (a) Ctsh and Cathepsin B (Ctsb) immunofluoresence in Ctsh -/-, Ctsh +/- and wt mouse epidermis. Graph shows Ctsb intensity in the neonate epidermis, bars are median **(b)** CD45 Immunofluorescence and in the dermis of Ctsh -/-, Ctsh +/- , and wt mouse skin. *p<0.05, **p<0.005 Bar 50µm.

Supplementary Figure E7 – Barrier proteins and immune mediators in adult Ctsh +/- and -/- mouse epidermis(a) histology, filaggrin and loricrin immunofluoresence of adult mouse Ctsh +/-, -/- and wt epidermis. **(b)** Il1a and Tslp immunofluorescence of Il1a and Tslp adult mouse Ctsh +/-, -/- and wt epidermis **(c)** Western blot of filaggrin, keratin 10 and loricrin **(d)** Graphs of densitometry of total filaggrin and filaggrin monomer. p values are shown on the graph. bars 50 µm (a,b)

Supplementary Methods

Restriction fragment length polymorphism analysis

RFLP analysis was performed on 18 skin samples. DNA was extracted by DNA mini spin kit (Qiagen) according to manufacturers' instructions. The rs8078605 polymorphism introduced a BsmAI site into the locus. F- CACCGCATTTGCTCTTACAA and R- CCTACACATGGTCCTTCATCC (Tm 60^{o}C) primers produced a 454bp amplicon. The T variant after BsmAI digestion gives a 203bp and 251bp product.

An mTORC1/AKT1/Cathepsin H axis controls filaggrin expression and processing in skin, a novel mechanism for skin barrier disruption in Atopic Dermatitis

Aishath S .Naeem, PhD(1,2), Cristina Tommasi , MRes (1,2), Christian Cole , PhD (3), Stuart J Brown, PhD(1,2), Yanan Zhu, PhD, (1,2), Benjamin Way , MA BMBCh MSc MRCS(1,2), Saffron AG Willis Owen, DPhil(4), Miriam Moffatt, DPhil(4), William O. Cookson, DPhil(4), John I. Harper, MBBS MD FRCP FRCPCH (1,2), Di WL, PhD(1,2), Sara J. Brown, MD FRCPE (5), Thomas Reinheckel, PhD(6), Ryan F.L. O'Shaughnessy, PhD (1,2,7).

1. Immunobiology and Dermatology, UCL Institute of Child Health

2. Livingstone Skin Research Centre, UCL Institute of Child Health

3. Computational Biology, School of Life Sciences, University of Dundee, Dundee, UK.

4. National Heart and Lung Institute, Imperial College, London SW3 6LY, UK

5. Centre for Dermatology and Genetic Medicine, Medical Research Institute, University of Dundee, Dundee, United Kingdom

6. Institute of Molecular Medicine and Cell Research, BIOSS Centre of Biological Signalling Studies, Albert-Ludwigs-University, Freiburg, Germany

7. To whom correspondence should be addressed:

Ryan O'Shaughnessy, Immunobiology, UCL Institute of Child Health, 30 Guilford Street, London WC1N 1EH, Phone +44 207 905 2182, Fax Number: +44 207 905 2882 e-mail r.oshaughnessy@ucl.ac.uk

Keywords. Atopic dermatitis, Skin Barrier, filaggrin, RAPTOR, Protease

Abbreviations

AD Atopic Dermatitis

AKT1 V-Akt Murine Thymoma Viral Oncogene Homolog 1

ATRA All trans retinoic acid

CTSH Cathepsin H

ECL Enhanced chemiluminesence

ENCODE The Encyclopedia of DNA Elements

FLG Filaggrin Gene

HMGCR 3-Hydroxy-3-Methylglutaryl-CoA Reductase

HMGCS1 3-Hydroxy-3-Methylglutaryl-CoA Synthase 1

HRP Horseradish peroxidase

IDI1 Isopentenyl-Diphosphate Delta Isomerase 1

IL-13 Interleukin 13

IL-4 Interleukin 4

mTORC1/2 Mechanistic Target Of Rapamycin Complex 1/2

OCT Optimal Cutting Temperature compound

pAKT phosphorylated AKT

PBS Phosphate buffered saline

PCR Polymerase Chain Reaction

RAPTOR Regulatory Associated Protein Of MTOR Complex 1

REK Rat epidermal keratinocytes

SASPase Aspartic Peptidase, Retroviral-Like 1

SDS Sodium Dodecyl Sulphase

SNP Single nucleotide polymorphism

SPF Specific pathogen free

TBST Tris buffered saline with 0.1% Tween 20

Th2 T-helper 2

TSLP Thymic stromal lymphopoietin

Abstract

Background: Filaggrin, encoded by the *FLG* gene, is an important component of the skin's barrier to the external environment and genetic defects in *FLG* strongly associate with Atopic Dermatitis (AD). However, not all AD patients have *FLG* mutations.

Objective: We hypothesised that these patients may possess other defects in filaggrin expression and processing, contributing to barrier disruption and AD, and therefore present novel therapeutic targets for this disease.

Results: We describe the relationship between the mTORC1 protein subunit RAPTOR, the serine/threonine kinase AKT1 and the protease cathepsin H, for which we establish a role in filaggrin expression and processing. Increased RAPTOR levels correlated with decreased filaggrin expression in AD. In keratinocyte cell culture, RAPTOR up-regulation or AKT1 shRNA knockdown reduced the expression of the protease cathepsin H. Skin of cathepsin H-deficient mice and CTSH shRNA knockdown keratinocytes showed reduced filaggrin processing and the mouse showed both impaired skin barrier function and a mild proinflammatory phenotype.

Conclusion: Our findings highlight a novel, potentially treatable, signalling axis controlling filaggrin expression and processing which is defective in AD.

Key messages:

- RAPTOR levels are increased in atopic dermatitis and are inversely proportional to filaggrin expression

-The up-regulation of RAPTOR leads to AKT1 activity down-regulation and downregulation of the protease cathepsin H, which is involved in filaggrin processing, epidermal barrier function and modulates skin immunity.

Capsule: *FLG* mutations strongly associate with Atopic Dermatitis (AD). However, not all AD patients have *FLG* mutations. An mTORC/AKT1 signalling axis controls both filaggrin expression and processing by controlling expression of the protease Cathepsin H.

Introduction

Atopic dermatitis (AD) is a common disease in which the skin is sensitive to allergens and irritants resulting in an immune response characterised by redness and scaling. Current evidence suggests that the primary cause for disease development in the majority of AD cases is a defective skin barrier [12,31] . There is a strong genetic component to AD associated with skin barrier dysfunction[15]. One important protein is the epidermal structural protein filaggrin. Null mutations in the gene encoding filaggrin (*FLG)* are responsible for the common inherited dry skin condition ichthyosis vulgaris, and are a major predisposing factor for AD[48,54]. However only approximately 40% of AD patients in the UK, and around 10% of AD patients in the rest of the world have filaggrin mutations[7,57] and conversely, not all individuals with filaggrin mutations have AD[45], suggesting that other mechanisms might contribute to filaggrin expression and processing defects and hence to the barrier defect observed in AD patients.

Profilaggrin to filaggrin processing is complex, requiring dephosphorylation and numerous proteolytic events; several proteases have been identified that cleave profilaggrin at specific sites releasing the filaggrin monomers and both the N and the C termini[17] . Proteases such as elastase 2 , SASPase and matriptase are reported to be involved in profilaggrin to filaggrin processing [5,18,43,44]. There are also reports of aspartic- and cysteine- type cathepsin proteases playing a role in this process [20,34,35] . AKT1 is required for the correct formation of the cornified envelope[47]. AKT1 activity in the epidermis is increased by treatment with the mTORC1 (RAPTOR containing mammalian target of rapamycin complex) inhibitor rapamycin[59] , suggesting a role of RAPTOR in modulating AKT1 activity. We therefore hypothesised that

AKT1 activity may be reduced in atopic dermatitis skin leading to alteration in protease expression, reduced filaggrin expression and processing and skin barrier disruption.

Using a combination of keratinocyte shRNA knockdown models, human clinical samples and mouse knockouts, we show increased RAPTOR expression correlates with reduced filaggrin expression in the skin of atopic individuals, this being most apparent in those with *FLG* compound heterozygous mutations. RAPTOR overexpression in keratinocytes reduced filaggrin expression, loss of AKT1 activity and filaggrin and loss of cathepsin H. Cathepsin H deficient mice have reduced filaggrin processing, subtle barrier defects, and an elevation in pro-inflammatory molecules, associated with increased macrophage infiltration of the skin and increased mast cell degranulation. Taken together this provides strong evidence that RAPTOR levels and AKT1 signalling are important in modulating filaggrin levels and the immune environment in AD.

Results

Increased RAPTOR expression correlated with reduced filaggrin expression in rat epidermal keratinocytes and in non-lesional AD skin

As inhibition of the mTORC1 complex by rapamycin increases AKT1 phosphorylation in keratinocytes[59], we hypothesised that the inverse could occur; that increased expression of the key mTORC1 protein RAPTOR in AD resulted in a reduction of AKT1 phosphorylation and therefore activity. To test this we examined the expression of RAPTOR, pAKT and filaggrin in the unaffected, non-lesional, non-flexural epidermis of 5 AD early-onset severe patients and of 3 individuals without AD (Figure 1a and b; Supplementary table E1). Non-lesional, non-flexural skin from AD patients have been previously demonstrated to be barrier deficient and represented a way of investigating the disease prior to acute immune involvement [14,26] .pAKT was significantly downregulated on the protein level in unaffected AD skin sections. However in both AD patients and controls there were individuals with RAPTOR present in the spinous and granular layers which corresponded to lower filaggrin levels in these individuals

(Supplementary Figure E1a). To investigate this finding in a larger number of individuals with known *FLG* genotype, we extended our analysis of RAPTOR and filaggrin to a gene expression analysis of non-lesional, non-flexural skin biopsies from 26 AD patients and 10 non-atopic controls of known *FLG* genotype as previously described[14]. All cases of AD had early onset persistent and severe disease. There was no significant change in mRNA levels of RAPTOR in non-lesional atopic skin according to *FLG* genotype (Figure 1c). However, changes in RAPTOR expression correlated with a number of the highly differentially expressed genes in *FLG* compound heterozygotes and filaggrin heterozygotes, including FLG itself (Figure 1d and e and Supplementary table E2). Although Th2 cytokines such as IL-13 and IL-4 are known to be able to modulate expression of filaggrin and alter epidermal barrier function [30,37], rapamycin treated cells did not reduce IL-4 expression and AKT1 knockdown keratinocytes did not have increased levels of IL-4 (Supplementary figure E1b and c). IL-4 and IL-13 expression levels were not correlated with RAPTOR levels in the data from Cole et al[14]. Taken together this suggests that the mechanism by which RAPTOR controls filaggrin is not due to increase in either IL-4 or IL-13 cytokine expression.

These genes and RAPTOR itself comprised a network centred on the insulin-mediated control of AKT1 which we have described previously and is important in both epidermal skin barrier function and UV protection (Supplementary figure E2a; [59]). A large proportion (17/22=77%) of the correlated and anti-correlated, highly expressed genes with mean normalised read count of 100 or more were also genes whose expression correlated with filaggrin expression[14] (Supplementary figure E2b, Supplementary Table E3) These data demonstrate that in AD, RAPTOR mRNA levels strongly anti-correlated with filaggrin mRNA expression. To directly test the effect of increased RAPTOR, we over-expressed human RAPTOR in rat epidermal keratinocytes. RAPTOR over-expression led to a decrease in AKT phosphorylation. Filaggrin is produced as a long pro-protein which is proteolytically processed to a monomeric mature form. We observed reduction in total and processed monomeric filaggrin, (Figure 1f and g).

A single nucleotide polymorphism in RAPTOR in a retinoid x receptor binding site correlated with increased RAPTOR and decreased filaggrin and cathepsin H levels.

To determine whether there were genetic changes that could lead to a change in RAPTOR expression levels in keratinocytes, we evaluated data from a previously published genome-wide association study[63] for any of the 649 single nucleotide polymorphisms (SNPs) in the *RAPTOR* gene that were over-represented in AD. We were not expecting gene-wide significance ($p<1x10^{-8}$) as RAPTOR overexpression also occurred in normal non-AD skin (Supplementary figure E3a). No SNPs were significantly over-represented, but we found an increased frequency in AD of one commonly observed (>1%) SNP. rs8078605 (C>T) is in an intronic region of RAPTOR in a region of DNA which according to ENCODE data[4] includes a region of acetylated histones in keratinocytes only, suggestive of a keratinocyte-specific enhancer (Supplementary figure E3a), and a binding site for RXRalpha. The variant SNP abolished a key nucleotide of a putative Retinoid-X receptor alpha binding site. In 18 DNA samples examined, 3 heterozygotes and a single homozygote were found (representing a minor allele frequency of 13.9, and 5.6% homozygotes, Supplementary figure E3b). The frequency of this variant allele in Europeans populations was 14% compared to 79% in sub-Saharan populations. This was of particular interest as other SNPs in non-coding parts of RAPTOR, with high prevalence in sub-Saharan populations compared to European populations, associated with putative retinoid binding sites that controlled the level of RAPTOR[60]. We therefore tested if RAPTOR itself was a retinoid responsive gene in human keratinocytes. Treatment of human keratinocytes with all-trans retinoic acid reduced RAPTOR expression levels (Supplementary figure E3c), suggesting that retinoids could control RAPTOR levels in keratinocytes. We therefore hypothesised that RXRalpha binding in the RAPTOR gene reduced RAPTOR expression, and that the rs8078605 C>T variant would lead to increased RAPTOR expression. High RAPTOR, low filaggrin protein levels and low Ctsh levels correlated with the presence of the T/T variant of rs8078605 (Supplementary figure E3d,e and f)

Loss of AKT1 activity or expression leads to reduced filaggrin processing in keratinocytes

We assessed the effect of the PI3Kinase inhibitor wortmannin, which inhibits AKT1 phosphorylation on filaggrin expression and processing in human keratinocytes [46].Wortmannin treatment reduced the levels of the mature processed filaggrin monomer (Figure 2a). These observations suggest that PI3 kinase signalling through AKT1 was required for the proteolytic processing of filaggrin during late epidermal terminal differentiation. To test whether AKT1 loss was responsible for the observed changes in filaggrin expression after wortmannin treatment in keratinocytes, we transfected a rat epidermal keratinocyte line (REK), known to represent the end stages of terminal differentiation in confluent submerged culture[47], with shRNA to rat Akt1 (Figure 2b and c). We could demonstrate a significant reduction in the levels of processed filaggrin monomer in four separate knockdown lines by Western blot, while levels of total filaggrin and filaggrin mRNA remained unchanged (Figure 2c, d and e). Organotypic skin equivalent cultures from these cells were hyperkeratotic compared to controls (Figure 2f). We could also demonstrate a reduction in filaggrin expression in these organotypic cultures (Figure 2f), with an antibody specific to the repeating mature monomeric form .These data suggest that while RAPTOR increase led to reduction in filaggrin expression, loss of the downstream kinase AKT1 or its activity resulted only in reduced filaggin processing.

mTORC signalling-related proteins and proteases, principally Cathepsin H, are differentially expressed in Akt1 knockdown cells

Differential gene expression analysis was performed on the knockdown REK lines with the greatest reduction in Akt1 (A1 and A3). 570 genes were significantly differentially expressed in both lines compared to scrambled controls (Figure 3a). Of these 59 genes had differential expression ≥1.5-fold and 17 genes had differential expression ≥2-fold (Figure 3b; Supplementary table E4). Gene set enrichment analysis (GSEA; Supplementary figure E4a) identified 3 gene ontology groups over-represented in the analysis, Cholesterol homeostasis, Androgen response and consistent with a role downstream of RAPTOR, MTORC signalling (Figure 3c; Supplementary Figure E3b and c), Leading edge analysis identified 3 genes, IDI1, HMGCR and HMGCS1 in all three ontology groups. HMGCS1 was down-

regulated in our AKT1 knockdown cells and in AD skin (Supplementary figure E4d and e; [14]). We identified 3 down-regulated proteases or proteolysis-associated proteins in our Akt1 kd cell lines (Figure 3d). We confirmed down-regulation of the most highly downregulated of these, the lysosomal protease cathepsin H (Ctsh, 3-4 fold) by real-time PCR (Figure 3e) and Western blot (Figure 3f). Ctsh was of particular interest as other members of the cathepsin proteases have been implicated in filaggrin processing[20,34,35]. Ctsh was downregulated in human keratinocytes treated with wortmannin (Figure 3g), and was expressed in post-confluent cultured REKs coincident with terminal differentiation and AKT activity (Figure 3h). Reinforcing a potential role in the control of filaggrin processing, Ctsh was expressed co-incident with filaggrin in the granular layer of the epidermis and organotypic cultures, with a reduction of both filaggrin and Ctsh in the Akt1 shRNA expressing organotypic cultures (Figure 3i)

Loss of cathepsin H inhibits filaggrin processing, not expression, and impairs epidermal barrier function. Evidence of compensation in the cathepsin H knockout

Cathepsin H expression was decreased in non-lesional AD epidermis (Figure 4 and b), and was reduced in keratinocytes overexpressing RAPTOR (Figure 4c), suggesting that is was a downstream effector of the RAPTOR/AKT1 axis in atopic dermatitis. To investigate a potential role for cathepsin H in filaggrin processing, Ctsh expression was knocked down by shRNA in our rat epidermal keratinocyte model. In all 4 shRNA knockdown lines examined there was a reduction of filaggrin processing without reduction in filaggrin mRNA levels (Supplementary figure E5a,b and c), consistent with our Akt1 knockdown data in REKs. There was a trend of reduction of median CTSH levels in the atopic dermatitis RNAseq analysis (Supplementary figure E5d;[14]) , however consistent with the lack of change in Filaggrin mRNA levels, there was no correlation between filaggrin levels and CTSH in AD (Supplementary figure E5e)

Knockdown of both AKT1 and CTSH in human keratinocytes revealed the same reduction in filaggrin processing but no reduction in total filaggin protein levels (Figure 4d and e), strongly implying that the phenomenon we observed in the rat epidermal keratinocyte model was recapitulated in human

keratinocytes too, further reinforcing our finding that increase in RAPTOR decreased filaggrin expression, and knockdown of either AKT1 or CTSH resulted in impaired filaggrin processing only. Transient transfection of Ctsh into the Akt1 kd rat cell line rescued filaggrin processing (Figure 4f and g), suggesting that the loss of Ctsh was directly responsible for the reduction in filaggrin processing.

To investigate the effect of Ctsh reduction *in vivo,* we examined newborn mouse skin from *Ctsh* -/- and +/- mice[9] (Figure 5a and b) by histology. Although there was no change in epidermal thickness, the cornified layer was significantly thinner in both the *Ctsh* +/- and -/- mice. We observed no change in total filaggrin levels (Figure 5c and d) but increased loricrin levels in the *Ctsh* +/- and -/- mice by immunofluorescence (Figure 5e and f). Granular filaggrin expression was lost in the *Ctsh* +/- mice but was partially restored in the *Ctsh* -/- mice (Figure 5d). This was confirmed by western blot, where filaggrin processing was normal while expression of loricrin and keratin 10 was increased (Supplementary figure 7c). In adult mice, in contrast, filaggrin and loricrin were reduced in expression in the Ctsh +/- mice and mostly restored in the Ctsh -/- mouse (Supplementary figure E7a)

Dye penetration assays[11] showed no significant gross barrier defects, but closer examination revealed penetration of dye into the cornified layers of the *Ctsh* +/- mice (Figure 5g) consistent with defective barrier function. Electron microscopy revealed smaller keratohyalin granules specifically in both the *Ctsh* +/- and -/- mice (Figure 5h and i), but the granule size in the -/- mice was partially rescued. This was reflected in a strengthening of cornified envelope integrity in Ctsh -/- mice compared to the weaker cornified envelopes in the *Ctsh* +/- mice (Figure 5j).

We examined the expression of other cathepsins known to process filaggrin[20,34,35], to determine if the rescue in the phenotype seen in the *Ctsh* -/- mouse was due to some kind of compensation by another cathepsin. We were unable to detect cathepins D and L in neonate skin, however the expression of cathepsin B was increased in both the knockout and heterozygous mouse (Supplementary figure E6a),

suggesting that the rescue of physical barrier function was possibly due to the up-regulation of this filaggrin-processing protease.

Ctsh-deficient mice show increase in dermal macrophages, mast cell degranulation and pro-inflammatory molecule expression

Defects in the physical barrier in AD result in an immune response[38] which typically includes an increase in mast cell numbers and macrophages and lymphocyte infiltration[27,33] .We saw no change in CD45 positive cells (lymphocytes) in the dermis or epidermis of either the *Ctsh* +/- or *Ctsh* -/- mice (Figure 6a; Supplementary figure E6b). Increased macrophage numbers in the skin are associated with filaggrin-defective and barrier defective epidermis[23,56]. Consistent with this, macrophage (F4/80 positive cell) counts were increased in the skin of the *Ctsh* +/- and *Ctsh* -/- mice (Figure 6a and c). Mast cell degranulation, the release of histamine, proteases and other immune mediators, is a common phenomenon linked to the atopic phenotype[28], and although overall mast cell number was unchanged, degranulation was increased in the skin of the *Ctsh* +/- and *Ctsh* -/- mice (Figure 6b and c).

To determine whether the skin was more pro-inflammatory we investigated cytokine and related protein expression by antibody array dot blot in pooled lysates from whole skin from wild type, and polled *Ctsh* -/- and +/- newborn mouse skin (Figure 6d). There was increase in the expression in a number of cytokines and soluble immune mediators, including interleukin 1-alpha (IL-1a), a protein known to be increased in barrier defective and eczema skin[36] which was subsequently confirmed by immunofluorescence (Figure 6d,e and f). Thymic stromal lymphopoietin (Tslp) expression induces atopic dermatitis in mouse models and is present in lesional atopic dermatitis skin[58] . It also plays a key role in mast cell degranulation. however we saw no significant change in Tslp expression in the epidermis of *Ctsh* -/- and +/- newborn and adult mouse skin, (Figure 6e and f). Taken together these data suggested that loss of Ctsh mediated by RAPTOR increase and AKT1 activity loss in AD leads to mild epidermal barrier disruption and the epidermis subsequently becomes more pro-inflammatory, and although some aspects of the physical

barrier are rescued in the knockout mouse, potentially due to compensation by cathepsin B and increased loricrin expression, the immune phenotype is not rescued (Figure 7).

Discussion

Although there has been a great deal of study of *FLG* mutations and their association with barrier disruption and AD, there are surprisingly few reports on variation of filaggrin protein levels and filaggrin processing[41,49,55] . Here we show that increase in RAPTOR correlates with decrease in filaggrin expression and processing not only in AD but also in normal "unaffected" individuals. This is consistent with other work on filaggrin proteases in AD[44] . Taken together these data strongly suggest that there would be value in assessing genetic variants in the normal population as a whole that correlate to barrier disruption and filaggrin expression and processing, and disregarding AD, as this may be a downstream consequence of the silent barrier disruption, that is potentially mediated by its own set of genetic associations[21,29,63].

Our analysis suggested that retinoids could be used as a treatment to reduce RAPTOR expression in AD and hence increase filaggrin expression and processing. Retinoids have been used to successfully treat eczema in a number of studies[19,25,52]. Typically around 50% of individuals respond to retinoid treatment[19]. Although the immunosuppressive properties of retinoids are cited as the cause of recovery, another reason could be the reduction of RAPTOR levels and subsequent increase in filaggrin expression and processing. Both cathepsin H and filaggrin have been reported previously as being up-regulated by retinoids, consistent with this hypothesis[24,51]. It would be interesting to investigate epidermal RAPTOR, cathepsin H and filaggrin levels and processing before and after treatment with retinoids and to determine if there is a different response in patients with different FLG phenotypes. A potential complication would be that treatment with all trans-retinoic acid or retinoic acid metabolism inhibitors can both inhibit and enhance epidermal terminal differentiation[1,2,13,50], so the potential overall effect on epidermal barrier function would be hard to predict.

Interestingly, in the context of the skin barrier and RAPTOR, mTORC1 is a pH sensor, and at acidic pH, such as those encountered in the granular layer of the epidermis, mTORC1 is inhibited [3]. This should lower filaggrin expression, and would be balanced against filaggrin-derived urocanic acid and pyrrolidone carboxylic acid levels [62]. Coupled with the fact that cathepsin H is a lysosomal protease, and therefore active at acidic pHs, it is likely that pH is one of the factors that determine overall levels of processed filaggrin.

The skin of Akt1 null mice models and Akt1 knockdown organotypic cultures display hyperkeratosis with reduced cornified envelope strength and reduced filaggrin expression and processing[47,61]. Activation of Akt1 also results in hyperkeratosis and altered filaggrin expression[32,47] demonstrating that normal Akt activity levels are required for correct filaggrin processing and hence epidermal barrier function. The new findings presented here reveal cathepsin H to be required for filaggrin processing and epidermal barrier formation, and that in the skin, RAPTOR regulates cathepsin H expression and filaggrin processing via reduced Akt signalling.

Cathepsin H is expressed ubiquitously and as well as being involved in bulk protein degradation, it does display cell-specific functions such as its role in the processing and secretion of surfactant protein C in type II pneumocytes[6,9]. Ctsh deficient mice have reduced lung surfactant which may interfere with breathing mechanisms causing respiratory complications[9] . Furthermore reduced Ctsh mRNA in airway smooth muscle cells has been reported in asthmatic individuals[22] , suggesting the possibility that low levels of Akt signalling may, in a range of epithelia, contribute to progression of AD to other atopic disease, the so called “atopic march”[10]. The finding that Ctsh is either directly involved or indirectly involved, through the activation of other proteases such as granzymes[16], in the processing of key barrier proteins in the epidermis and in the lung leads to the possibility that the atopic march may not only be an immunological phenomenon, but could also be the result of altered barrier function in multiple epithelia.

Cathepsin H deficiency *in vivo* led to an increase in macrophage number and mast cell degranulation, and increased Il1a in the skin of Ctsh +/- and -/- mice. Cathepsin H overexpression typically correlates to macrophage infiltration and a proinflammatory environment in a number of tissues [39,42]. Therefore it is likely that the loss of Ctsh leads to an increase in other cathepsins, such as with our observation of increased cathepsin B, which may have a proinflammatory role, and is known to play an important role in processing of mast cell proteases[16,40] . It is therefore possible that the immune changes are driven by the increased cathepsin B in both Ctsh +/- and -/- mice. The interplay between these proteases and inhibitors and how this relates to the levels of filaggrin and other related (fused-S100 group) proteins and their processing and subsequently the pro-inflammatory status of the skin in AD is difficult to dissect. This was apparent by the lack of correlation between filaggrin levels and a cathepsin H in AD patients. However understanding how overall filaggrin protease activity levels are altered in atopic skin would provide targets to treat both the barrier and immune aspects of AD.

Individuals with two loss-of-function mutations in *FLG* (compound heterozygotes) show the greatest increase in risk of AD[8,53], and gene expression differences in these individuals is greater than in *FLG* heterozygote and wild type individuals[14], which allowed for the detection of statistically significant differentially expressed genes correlated with RAPTOR expression. Consistent with our work *in vitro*, high levels of RAPTOR correlated with low levels of filaggrin expression, and AKT signalling components. Taken together our findings make a convincing case for the role of RAPTOR in regulating genes, including *FLG*, that are important in the AD phenotype. Also this work suggests that rapamycin or retinoid treatment could be of benefit in these individuals with filaggrin haploinsufficiency and severe AD.

Materials and Methods

Animals: Cathepsin H (Ctsh) knock-out and heterozygote mice were generated as previously described[9] and backcrossed onto the C57BL/6J background for eight generations. *Ctsh*$^{-/-}$,*Ctsh*$^{+/-}$ mice and wild-type littermate controls were bred under SPF conditions in accordance with the German law for Animal Protection (Tierschutzgesetz) as published on 25 May 1998. 3 day old (neonate) mice were obtained from 5 litters and 6 month old (adult) mice were obtained from two separate litters. A maximum of 5 wild-type, 8 *Ctsh*$^{+/-}$ and 10 *Ctsh*$^{-/-}$ neonate mice and 3 of each phenotype of adult mice were used in all analyses, blinding was not used in the assessment of the mouse skin

siRNA knockdown, Cell and Organotypic culture, mouse tissue

Four shRNA plasmids (Qiagen) were used to knockdown Akt1 expression (shRNA1-GCACCGCTTCTTTGCCAACAT, shRNA2-AAGGCACAGGTCGCTACTAT, shRNA3-GAGGCCCAACACCTTCATCAT, shRNA4-GCTGTTCGAGCTCATCCTAAT), and of these 1 and 3 were used for further experiments. Ctsh knockdown was successfully achieved by transient transfection with two shRNA plasmids (shRNA1-CAAGAATGGTCAGTGCAAATT ; shRNA3-CTAGAGTCAGCTGTGGCTATT). The following scrambled control was used GGAATCTCATTCGATGCATAC. Akt1 and Ctsh shRNA knockdown plasmids were transfected into rat epidermal keratinocyte (REK) cells[47] using lipofectamine (Invitrogen) according to manufacturer's instructions. Mycoplasma-testing was performed prior to the experiments. Cells were cultured and G418 (Gibco) selection was performed as previously described[47]. The organotypic cultures were either embedded in OCT for frozen sections, or paraffin embedded. Drug treatments with ATRA (10μM. Fisher Scientific) or Wortmannin (2μM, Sigma), were for 24 hours. Dorsal skin was removed from neonatal (Postnatal day 3) Ctsh +/+, +/- and -/- mice for subsequent analyses

Lentiviral shRNA knockdown in human keratinocytes

$2x10^5$ lentiviral particles (scrambled control, AKT1shRNA and CTSHshRNA, Santa Cruz Biotechnology) were incubated for 24 hours with 50-70% confluent mycoplasma-free keratinocytes grown in Gibco serum-free keratinocyte culture medium (Invitrogen) in a 12 well plate. Cells were trypsinised and selected by puromycin selection for 2 weeks as per manufacturer's instructions. Cells were subsequently calcium switched at 2.4mM $CaCl_2$ for 4 days prior to investigation by western blotting of AKT1, CTSH and Filaggrin.

Western blot and antibodies

Keratinocyte protein lysates and skin protein lysates from commercially available skin samples (Caltagmedsystems) were prepared by boiling in a denaturing SDS buffer (2% 2-mercaptoethanol, 2% SDS, 10mM Tris pH 7.5) for 10 minutes. For the cytokine arrays, Suspensions of T25 Ultra-Turrax (IKA) homogenised neonatal mouse skin was spun down and the suspensions from 2 Ctsh +/+, +/- and -/- mouse skin samples were pooled and used on the cytokine array panel A (RandD Systems) according to manufacturers' instructions. Densitometry of ECL exposures of cytokine arrays and western blots where appropriate were performed using the ImageJ software. Briefly, this was achieved by inverting the monochrome image, removing the background, thresholding the image and then measuring the thresholded bands, then the integrated density (pixel value x band area) was used as a measure of band intensity, which is subsequently normalized by a loading control (Gapdh). Antibodies used were rabbit anti-RAPTOR (24C12) (Cell Signalling Technologies, 1/500),Rabbit anti- filaggrin (M-290) (Santa Cruz Biotechnologies #sc-30230, 1/500), Mouse anti-c-Myc (9E10) (1/500, Sigma), Mouse anti-FLAG (1/100, F1804 Sigma), Rabbit anti-Rictor (Cell Signalling Technologies #2140, 1/500), Rabbit anti pSerine473 Akt (Cell Signalling Technologies #9271, 1/500), Mouse anti Akt-1 (2H10) (Cell Signalling Technologies #2967, 1/500), Mouse anti Gapdh (1/2000, AB2303 Millipore) Rabbit anti-Loricrin (Covance PRB-145P, 1/1000), Rabbit anti-Keratin 10 (Covance PRB-140C, 1/1000), Rabbit anti-Interleukin 4 (Abcam ab9622 ,1/500) and cathepsin H (H-130) (1/500, sc-13988 Santa Cruz Biotechnologies). Primary antibody incubations were in PBS+0.1% Tween-20 or in TBST (100mM Tris

HCl, 0.2M NaCl, 0.1% Tween-20 (v/v) containing either 5% bovine serum albumin (Sigma, Gillingham, UK) or 5% skimmed milk powder either overnight at 4^{o}C or for 1-2 h at room temperature, while secondary antibody incubations were in 5% skimmed milk powder for 1 h at room temperature. The following concentrations were used; swine anti rabbit-HRP (DakoCytomation) 1:3000; rabbit anti mouse HRP (DakoCytomation) 1:2000. Protein was visualized using the ECL plus kit (Amersham).

Immunofluoresence, Immunohistochemistry and eczema and unaffected samples

Clinical material was obtained with informed written consent from patients attending dermatology clinics at Great Ormond Street Hospital, Ethical approval was granted by the local research ethics committee. Normal paraffin embedded skin samples were obtained from a commercially available tissue microarray (BioMax), all tissue samples were from non-flexural areas. Immunohistochemistry and Immunofluorescence on paraffin and frozen sections were by standard techniques. Antibodies used were RAPTOR (24C12) (Cell Signalling Technologies, 1/50), Mouse anti-filaggrin (Genetex GTX23137, 1/50), Cathepsin H (H-130) (Santa Cruz Biotechnologies sc-13988, 1/50), Rabbit anti F4/80 (Bio-Rad AbD SeroTec CL:A3:1), Rabbit anti-Loricrin (Covance PRB-145P 1/200), Rabbit anti-Il1a (H-159) (Santa Cruz Biotechnology sc-7929, 1/50), Rabbit anti-cathepsin B (Biovision 3190-100, 1/25), Rabbit anti-Tslp (Thermo PA5-20321, 1/25), Rabbit anti-CD45 [EP322Y] (Abcam ab40763, 1/25). Primary antibodies were detected using Alexa 488 and 594-conjugated goat anti mouse and anti-rabbit (Invitrogen, 1/500). Cells and Sections were counterstained with 4',6-diamidino-2-phenylindole (DAPI, Sigma). Images were taken with a Leica Upright Microscope with either x20 (NA 0.4) or x40 (NA 1.40) objectives, using a Coolsnap digital camera (MediaCybernetics, Bethesda, Maryland), with the ImagePro 6.0 software (MediaCybernetics, Bethesda, Maryland). Immunofluoresence intensity was measured using imageJ (https://imagej.nih.gov/ij/) to determine the integrated density on a thresholded image after processing to remove background.

RNA extraction and microarray analysis

0.1 mg RNA was extracted from two scrambled REK lines, and 2 biological replicates of each Akt1 shRNA knockdown , and poly-A+ RNA was selected using the Oligotex system (Qiagen). RNA was extracted from the two Ctsh knockdown REK lines using the same approach. Second-strand cDNA was synthesized using the Superscript II kit (Invitrogen, Carlsbad, New Mexico) after the RNA was annealed with a T7 promoter-poly-T primer (Genset, Evry, France). Biotin-labelled cRNA was made from this cDNA (Enzo Diagnostics, Farmingdale, New York). The whole probe was hybridized to the exon array rat genome chip (Affymetrix, Santa Clara, California) according to the manufacturers' specifications. The scrambled controls cells were the base line in all analyses. Genes that were tagged as present and increased in all six analyses with a p-value of less than or equal to 0.05 by Mann–Whitney analysis, a p-value less than 0.05 after Benjamini-Hochberg False Discovery Rate correction and 1.5 fold or more altered in expression, were regarded as differentially expressed. Supervised analysis of over-represented genes was performed by inputting lists of differentially expressed genes into the Gene Set Enrichment Analysis program (http://software.broadinstitute.org/gsea/index.jsp)

Electron Microscopy

Transmission electron microscopy (EM) was performed on wt littermates and Ctsh heterozygous and null mouse tissue (n=2 each genotype). Normal EM protocols were used. Briefly tissues were fixed overnight in glutaraldehyde, with post fixation in 1% Osmium tetroxide in 100mM phosphate buffer for 2 hours at 4^{o}C. En bloc staining with 2% aqueous uranyl acetate was performed for 2 hours, prior to embedding and the cutting of semi thin sections and sections for EM grids.

Realtime PCR

Rat cathepsin H and filaggrin message levels were measured using gene-specific Quantitect primers (Qiagen) and SYBR green (Qiagen) and $\Delta\Delta^{CT}$ relative quantification

Sonication Assay for cornified envelopes and Haemotoxilin Dye Penetration Assays

Cornified envelopes were extracted from the neonatal mouse skin by boiling for 10 min in (50 mm Tris-HCl, pH 7.5, 2% SDS, 5 mm EDTA). Cornified envelopes were pelleted by centrifugation and washed in cornified envelope washing buffer (10 mm Tris-HCl in 0.1% SDS). After resuspension, envelopes were counted by haemocytometer. After sonication with a probe sonicator for 5x1 second pulses, the intact envelopes were counted and expressed as a % of the unsonicated total. The haemotoxlin penetration assay on neonate mouse skin and subsequent sectioning has been described previously [11].

Correlation Analysis of RAPTOR in Human Expression Data and code availability

Skin biopsies from non-lesional, non-flexural skin biopsies from 26 AD patients and 10 non-atopic controls of known *FLG* genotype, (*FLG* wildtype (n=7), *FLG* heterozygous (n=12), and *FLG* compound heterozygous (n=7)) were taken, the RNA extracted and the direct RNA sequencing reads were processed as described previously[14]. The mean expression for each gene was determined across the three *FLG* genotypes in the samples (wild type, heterozygous and compound heterozygous) and correlated to *RAPTOR*'s expression using Pearson's method. Any genes which have an *r* close to 1 or -1 are the most likely candidates to be co-regulated with *RAPTOR* under the *FLG* genotype background. In order to avoid genes with low counts having spurious correlations, only genes with a total mean expression across the three genotypes >25 reads were considered (n=9708).

A significance value for the correlations can be calculated. Firstly the *t* statistic can be determined for gene *i* as:

$$t_i = r_i . \sqrt{\frac{n-2}{1-{r_i}^2}}$$

where r_i is the Pearson's correlation and *n* is the number of genotypes per gene (here, *n*=3) which determines the degrees of freedom (*n* – 2). Given t_i and the degrees of freedom, a p-value can be calculated from the standard *t*-distribution using the 'pt' function in R (v3.1.3). p-values are quoted

unadjusted. The code for this analysis is available from Github (https://github.com/drchriscole/eczemaDRS). All genes with a correlation p-value <0.05 and a log2 fold-change >0.5 or <-0.5 in the wild-type versus compound heterozygote comparison were considered for further investigation using STRING (http://string-db.org/)

Restriction fragment length polymorphism analysis

RFLP analysis was performed on 18 skin samples. DNA was extracted by DNA mini spin kit (Qiagen) according to manufacturers' instructions. The rs8078605 polymorphism introduced a BsmAI site into the locus. F- CACCGCATTTGCTCTTACAA and R- CCTACACATGGTCCTTCATCC (Tm 60^{o}C) primers produced a 454bp amplicon. The T variant after BsmAI digestion gives a 203bp and 251bp product.

Statistical analysis

For qPCR and the analysis of normalised data from western blots, t-test or one way ANOVA were used. For all other analyses non-parametric tests were performed, Kruskal-Wallis with Dunnett post-hoc testing. Specific analyses are also identified in the figure legends

Acknowledgements

We acknowledge UCL genomics for the gene array hybridisation and subsequent analysis. We thank the Electron Microscopy units of Queen Mary University of London and UCL for the transmission electron microscopy analyses. RO is funded by the Great Ormond Street Hospital Children's Charity, AN is funded by a British Skin Foundation studentship (2018s). CC is funded as part of the Centre for Dermatology and Genetic Medicine, University of Dundee Wellcome Trust Strategic Award (098439/Z/12/Z). Sara B is supported by a Wellcome Trust Senior Research Fellowship in Clinical Science (106865/Z/15/Z) and a research grant from the Manknell Charitable Trust.

Author Contributions

RO, W-L D, AN and TR conceived and designed the experiments. RO, AN, CT, BW, Stuart B and YZ performed experiments. WOC, MFM, SAGW-O provided the complete GWAS data for the RAPTOR gene. Sara B and CC provided data from gene expression analysis of AD, and performed gene expression correlation analysis. TR bred the *Ctsh* -/+ and -/- mice and prepared tissues. The manuscript was written by RO, JH, AN, CC, TR and Sara B. All authors have read and approved the final version of this manuscript.

Competing Financial Interests Statement

There are no competing financial interests associated with this manuscript.

Figure Legends

Figure 1: Increased RAPTOR expression correlated with reduced filaggrin expression in keratinocytes and AD skin (a) filaggrin, pSerAKT and Raptor Immunofluoresence in normal (n=3) and unaffected AD skin (n=5). **(b)** Image analysis of filaggrin, pSerAKT in normal and unaffected AD skin. Error bars are s.d. **(c)** RAPTOR expression from RNAseq analysis in Cole et al., 2014[14]. Box shows median and interquartile ranges for wildtype controls and atopic dermatitis (AD) of the 3 *FLG* genotypes, **(d)** Scatterplots showing Fold-change and correlation of differentially expressed genes (FDR $p< 0.05$) with RAPTOR. Filaggrin (FLG) is orange. **(e)** Graph of fold-change of highly correlated and anti-correlated genes in the *FLG* compound heterozygotes (FC Cmpd) and heterozygotes (FC Het). **(f)** Western blot of pAkt, Total AKT and filaggrin in RAPTOR overexpressing keratinocytes. Boxes indicate total filaggrin and filaggrin monomer for densitometry **(g)** Graph of densitometry of (f), n=2. Gapdh is loading control. *$p<0.05$ (b). Bars 50μm (a)

Figure 2: Loss of Akt1 leads to loss of filaggrin expression and hyperkeratosis in skin-equivalent organotypic cultures. (a) Western blot of Akt, pSerAkt, Filaggrin in human keratinocytes treated with 2μM Wortmannin or vehicle (DMSO) for 24 hours n=2 **(b)** Western blot of pSerAkt and Akt1 in Akt1 knockdown keratinocytes. **(c)** Western blots of Akt1, Filaggrin, keratin 10 and Loricrin in all Akt1 shRNA expressing lines, Gapdh is loading control. **(d)** Real time PCR analysis of filaggrin expression in Akt1 shRNA expressing lines. **(e)** Graph of mean densitometry of Akt1, total filaggrin and filaggrin monomer, loricrin and keratin 10 in Western blots of Akt1 shRNA knockdown cells (red bars) compared with scrambled (blue bars) **(f)**. Histology and immunofluorescence of Akt1, and filaggrin in Akt1 shRNA expressing organotypic cultures (n=4). Bars 50μm (f). *$p<0.05$, **$p<0.005$, Unpaired T-Test. Error bars are s.d.

Figure 3: Cathepsin H, is a differentiation-dependent protease co-expressed with filaggrin. (a) Heat map of differential gene expression between two Akt1 kd and scrambled control keratinocytes. Blue, down-regulated, Yellow, up-regulated. **(b)** Graph of highly differentially expressed genes (DEGs) including Cathepsin H (Ctsh). **(c** and **d)** Heat maps of DEGs involved in mTORC signalling **(c)** and proteases **(d). (e)** qPCR analysis of Ctsh in Akt1 kd cell lines. Bars show s.d. ** $p < 0.01$ (2-Way ANOVA). **(f)** Western blot of Ctsh in Akt1 kd cells and control (scram) cells. **(g)** Western blot of CTSH, pAKT and total AKT in human keratinocytes treated with wortmannin (WORT) or vehicle (DMSO) **(h)** Western blot of pre and post-confluent REKs for pSerAKT, Ctsh and keratin 1. **(i)** Co-immunofluoresence of Ctsh and filaggrin. Gapdh is loading control in all western blots, bar 50μm (i)

Figure 4: Cathepsin H is a filaggrin processing protease controlled by Raptor and AKT1. (a) Ctsh Immunofluoresence in normal and unaffected AD skin (n=5) **(b)** Graph of Ctsh fluorescence intensity. Error bars are s.d. **(c)** Western blot of Ctsh in RAPTOR over-expressing REKs. **(d)** Western blot AKT1, filaggrin and Ctsh of AKT1 and CTSH kd human keratinocytes (NHEKs). **(e)** Graph of mean densitometry of Akt1, total filaggrin and filaggrin monomer and Ctsh. **(f)** Western blot of Filaggin and Ctsh in Akt1 kd REKs transiently transfected with Ctsh or empty vector. **(g)** Graph of mean densitometry for total filaggrin and filaggrin monomer. 2 separate experiments are shown*$p<0.05$, **$p<0.005$, Unpaired T-Test (e,g). Gapdh is loading control for western blots, bar 50µm (a)

Figure 5: Reduced filaggrin processing and impaired epidermal barrier in Cathepsin H deficient mouse skin. (a). Histology of Ctsh -/-, Ctsh +/- , and wt mouse neonatal skin (n=5,8 and 10 respectively) **(b)** Graph of stratum corneum thickness. **(c)** Filaggrin immunofluoresence. Inset shows granular layer detail **(d)** Graph of filaggrin immunofluorescence (upper) and for occurrence (counts) of granular filaggrin expression (lower) **(e)** loricrin immunofluorescence. **(f)** Graph of loricrin immunofluorescence intensity **(g)** Haemotoxylin dye penetration. **(h)** Electron microscopy of keratohyalin granules 'k' ,keratohyalin granules **(i)** Graph of Keratohyalin granule size **(j)** Sonication analysis of cornified envelopes. Bars and boxes shows median and interquartile range (i,j) *$p<0.05$, **$p<0.05$ #$p<0.05$ Fishers exact test (d). Bars 50µm (a,c and g), 2µm (h)

Figure 6: Loss of Cathepsin H increases skin macrophages, mast cell degranulation and proinflammatory molecule expression. (a) Immunofluorescence of macrophages (F4/80 +ve) in wt, Ctsh -/- (ko) and Ctsh +/- (het) mouse neonatal skin **(b)** toluidine blue staining. **(c**) Graph of average F4/80 +ve cell, mast cell counts and % degranulating mast cells per field of view. **(d)** Densitometry of the cytokine arrays incubated with pooled lysates from 2 Wt (WT), and 2 Heterozygous or knockout mice (Het/Ko). **(e)** Il1a, and Tslp immunofluorescence. **(f)** Graph of immunofluorescence intensity of Tslp and Il1a. Bars 50μm (a,b and e). *$p<0.05$, **$p<0.005$ (c and f)

Figure 7: The mTORC/AKT1/Cathepsin H axis in the control of the physical and immune skin barrier. The variant SNP rs 8078605 prevents RXR binding to the putative intragenic enhancer in RAPTOR, potentially increasing RAPTOR expression which itself reduces filaggrin expression. This increases the ratio of mTORC1 to mTORC2, reducing Akt1 phosphorylation. This leads to reduced Cathepsin H expression and decreases filaggrin processing. Up-regulation of other filaggrin processing proteases in response, such as Cathepsin B, not only leads to rescue of barrier function but also causes macrophage infiltration, mast cell activity and pro-inflammatory cytokine expression

Reference List

[1] B. J. Aneskievich and E. Fuchs, "Terminal differentiation in keratinocytes involves positive as well as negative regulation by retinoic acid receptors and retinoid X receptors at retinoid response elements," Mol. Cell Biol. **12(11)**, 4862 (1992).
Ref Type: Journal

[2] D. Asselineau and M. Darmon, "Retinoic acid provokes metaplasia of epithelium formed in vitro by adult human epidermal keratinocytes," Differentiation. **58(4)**, 297 (1995).
Ref Type: Journal

[3] A. D. Balgi*, et al.*, "Regulation of mTORC1 signaling by pH," PLoS. One. **6(6)**, e21549 (2011).
Ref Type: Journal

[4] B. E. Bernstein*, et al.*, "An integrated encyclopedia of DNA elements in the human genome," Nature. **489**(7414), 57 (2012).
Ref Type: Journal

[5] C. Bonnart*, et al.*, "Elastase 2 is expressed in human and mouse epidermis and impairs skin barrier function in Netherton syndrome through filaggrin and lipid misprocessing," J. Clin. Invest. **120**(3), 871 (2010).
Ref Type: Journal

[6] F. Brasch*, et al.*, "Involvement of cathepsin H in the processing of the hydrophobic surfactant-associated protein C in type II pneumocytes," Am. J. Respir. Cell Mol. Biol. **26**(6), 659 (2002).
Ref Type: Journal

[7] S. J. Brown and W. H. McLean, "One remarkable molecule: filaggrin," J. Invest Dermatol. **132(3 Pt 2)**, 751 (2012).
Ref Type: Journal

[8] S. J. Brown*, et al.*, "Prevalent and low-frequency null mutations in the filaggrin gene are associated with early-onset and persistent atopic eczema," J. Invest Dermatol. **128(6)**, 1591 (2008).
Ref Type: Journal

[9] F. Buhling*, et al.*, "Gene targeting of the cysteine peptidase cathepsin H impairs lung surfactant in mice," PLoS. One. **6**(10), e26247 (2011).
Ref Type: Journal

[10] J. A. Burgess*, et al.*, "Does eczema lead to asthma?," J. Asthma. **46**(5), 429 (2009).
Ref Type: Journal

[11] C. Byrne*, et al.*, "Whole-mount assays for gene induction and barrier formation in the developing epidermis," Methods Mol. Biol. **585:271-86. doi: 10.1007/978-1-60761-380-0_19.**, 271 (2010).
Ref Type: Journal

[12] R. E. Callard and J. I. Harper, "The skin barrier, atopic dermatitis and allergy: a role for Langerhans cells?," Trends Immunol. **28**(7), 294 (2007).
Ref Type: Journal

[13] A. Chawla*, et al.*, "Nuclear receptors and lipid physiology: opening the X-files," Science. **294**(5548), 1866 (2001).
Ref Type: Journal

[14] C. Cole*, et al.*, "Filaggrin-stratified transcriptomic analysis of pediatric skin identifies mechanistic pathways in patients with atopic dermatitis," J. Allergy Clin. Immunol. **134(1)**, 82 (2014).
Ref Type: Journal

[15] M. J. Cork*, et al.*, "New perspectives on epidermal barrier dysfunction in atopic dermatitis: gene-environment interactions," J. Allergy Clin. Immunol. **118**(1), 3 (2006).
Ref Type: Journal

[16] M. E. D'Angelo*, et al.*, "Cathepsin H is an additional convertase of pro-granzyme B," J. Biol. Chem. **285(27)**, 20514 (2010).
Ref Type: Journal

[17] S. J. de Veer*, et al.*, "Proteases: common culprits in human skin disorders," Trends Mol. Med. (13), 10 (2013).
Ref Type: Journal

[18] G. Denecker*, et al.*, "Caspase-14 protects against epidermal UVB photodamage and water loss," Nat. Cell Biol. **9(6)**, 666 (2007).
Ref Type: Journal

[19] T. L. Diepgen, E. Pfarr, and T. Zimmermann, "Efficacy and tolerability of alitretinoin for chronic hand eczema under daily practice conditions: results of the TOCCATA open study comprising 680 patients," Acta Derm. Venereol. **92**(3), 251 (2012).
Ref Type: Journal

[20] F. Egberts*, et al.*, "Cathepsin D is involved in the regulation of transglutaminase 1 and epidermal differentiation," J. Cell Sci. **117(Pt 11)**, 2295 (2004).
Ref Type: Journal

[21] D. Ellinghaus*, et al.*, "High-density genotyping study identifies four new susceptibility loci for atopic dermatitis," Nat. Genet. **45**(7), 808 (2013).
Ref Type: Journal

[22] A. Faiz*, et al.*, "The expression and activity of cathepsins D, H and K in asthmatic airways," PLoS. One. **8**(3), e57245 (2013).
Ref Type: Journal

[23] P. G. Fallon*, et al.*, "A homozygous frameshift mutation in the mouse Flg gene facilitates enhanced percutaneous allergen priming," Nat. Genet. **41**(5), 602 (2009).
Ref Type: Journal

[24] G. R. Flentke*, et al.*, "Microarray analysis of retinoid-dependent gene activity during rat embryogenesis: increased collagen fibril production in a model of retinoid insufficiency," Dev. Dyn. **229**(4), 886 (2004).
Ref Type: Journal

[25] M. Grahovac*, et al.*, "Treatment of atopic eczema with oral alitretinoin," Br. J. Dermatol. **162**(1), 217 (2010).
Ref Type: Journal

[26] R. Gruber*, et al.*, "Diverse regulation of claudin-1 and claudin-4 in atopic dermatitis," Am. J. Pathol. **185(10)**, 2777 (2015).
Ref Type: Journal

[27] E. Guttman-Yassky, K. E. Nograles, and J. G. Krueger, "Contrasting pathogenesis of atopic dermatitis and psoriasis--part II: immune cell subsets and therapeutic concepts," J. Allergy Clin. Immunol. **127(6)**, 1420 (2011).
Ref Type: Journal

[28] E. Guttman-Yassky, K. E. Nograles, and J. G. Krueger, "Contrasting pathogenesis of atopic dermatitis and psoriasis--part II: immune cell subsets and therapeutic concepts," J. Allergy Clin. Immunol. **127(6)**, 1420 (2011).
Ref Type: Journal

[29] T. Hirota*, et al.*, "Genome-wide association study identifies eight new susceptibility loci for atopic dermatitis in the Japanese population," Nat. Genet. **44**(11), 1222 (2012).
Ref Type: Journal

[30] M. D. Howell*, et al.*, " Th2 cytokines act on S100/A11 to downregulate keratinocyte differentiation," J Invest Dermatol. **128(9)**, 2248 (2008).
Ref Type: Journal

[31] I. Jakasa*, et al.*, "Percutaneous penetration of sodium lauryl sulphate is increased in uninvolved skin of patients with atopic dermatitis compared with control subjects," Br. J. Dermatol. **155**(1), 104 (2006).
Ref Type: Journal

[32] S. M. Janes*, et al.*, "Transient activation of FOXN1 in keratinocytes induces a transcriptional programme that promotes terminal differentiation: contrasting roles of FOXN1 and Akt," J. Cell Sci. **117**(Pt 18), 4157 (2004).
Ref Type: Journal

[33] S. Kasraie and T. Werfel, "Role of macrophages in the pathogenesis of atopic dermatitis," Mediators. Inflamm. **2013**, 942375 (2013).
Ref Type: Journal

[34] A. Kawada*, et al.*, "Rat epidermal cathepsin L-like proteinase: purification and some hydrolytic properties toward filaggrin and synthetic substrates," J. Biochem. **118(2)**, 332 (1995).
Ref Type: Journal

[35] A. Kawada*, et al.*, "Rat epidermal cathepsin B: purification and characterization of proteolytic properties toward filaggrin and synthetic substrates," Int. J. Biochem. Cell Biol. **27(2)**, 175 (1995).
Ref Type: Journal

[36] S. Kezic*, et al.*, "Filaggrin loss-of-function mutations are associated with enhanced expression of IL-1 cytokines in the stratum corneum of patients with atopic dermatitis and in a murine model of filaggrin deficiency," J. Allergy Clin. Immunol. **129**(4), 1031 (2012).
Ref Type: Journal

[37] B. E. Kim*, et al.*, "Loricrin and involucrin expression is down-regulated by Th2 cytokines through STAT-6," Clin. Immunol. **126(3)**, 332 (2008).
Ref Type: Journal

[38] I. H. Kuo*, et al.*, "The cutaneous innate immune response in patients with atopic dermatitis," J. Allergy Clin. Immunol. **131(2)**, 266 (2013).
Ref Type: Journal

[39] C. Lambert*, et al.*, "Gene expression pattern of synovial cells from inflammatory and normal areas of osteoarthritis synovial membrane," Arthritis Rheum. 10 (2013).
Ref Type: Journal

[40] Q. T. Le*, et al.*, "Processing of human protryptase in mast cells involves cathepsins L, B, and C," J. Immunol. **187(4)**, 1912 (2011).
Ref Type: Journal

[41] M. Li*, et al.*, "Analyses of FLG mutation frequency and filaggrin expression in isolated ichthyosis vulgaris (IV) and atopic dermatitis-associated IV," Br. J. Dermatol. **168**(6), 1335 (2013).
Ref Type: Journal

[42] X. Li*, et al.*, "Increased expression of cathepsins and obesity-induced proinflammatory cytokines in lacrimal glands of male NOD mouse," Invest Ophthalmol. Vis. Sci. **51(10)**, 5019 (2010).
Ref Type: Journal

[43] K. List*, et al.*, "Loss of proteolytically processed filaggrin caused by epidermal deletion of Matriptase/MT-SP1," J. Cell Biol. **163**(4), 901 (2003).
Ref Type: Journal

[44] T. Matsui*, et al.*, "SASPase regulates stratum corneum hydration through profilaggrin-to-filaggrin processing," EMBO Mol. Med. **3**(6), 320 (2011).
Ref Type: Journal

[45] G. M. O'Regan*, et al.*, "Filaggrin in atopic dermatitis," J. Allergy Clin. Immunol. **122**(4), 689 (2008).
Ref Type: Journal

[46] R. F. O'Shaughnessy*, et al.*, "Cutaneous human papillomaviruses down-regulate AKT1, whereas AKT2 up-regulation and activation associates with tumors," Cancer Res. **67(17)**, 8207 (2007).
Ref Type: Journal

[47] R. F. O'Shaughnessy, *et al.*, "AKT-dependent HspB1 (Hsp27) activity in epidermal differentiation," J. Biol. Chem. **282**(23), 17297 (2007).
Ref Type: Journal

[48] C. N. Palmer, *et al.*, "Common loss-of-function variants of the epidermal barrier protein filaggrin are a major predisposing factor for atopic dermatitis," Nat. Genet. **38**(4), 441 (2006).
Ref Type: Journal

[49] L. Pellerin, *et al.*, "Defects of filaggrin-like proteins in both lesional and nonlesional atopic skin," J. Allergy Clin. Immunol. **131**(4), 1094 (2013).
Ref Type: Journal

[50] M. Rendl, *et al.*, "Caspase-14 expression by epidermal keratinocytes is regulated by retinoids in a differentiation-associated manner," J. Invest Dermatol. **119(5)**, 1150 (2002).
Ref Type: Journal

[51] D. S. Rosenthal, *et al.*, "Acute or chronic topical retinoic acid treatment of human skin in vivo alters the expression of epidermal transglutaminase, loricrin, involucrin, filaggrin, and keratins 6 and 13 but not keratins 1, 10, and 14," J. Invest Dermatol. **98**(3), 343 (1992).
Ref Type: Journal

[52] T. Ruzicka, *et al.*, "Efficacy and safety of oral alitretinoin (9-cis retinoic acid) in patients with severe chronic hand eczema refractory to topical corticosteroids: results of a randomized, double-blind, placebo-controlled, multicentre trial," Br. J. Dermatol. **158**(4), 808 (2008).
Ref Type: Journal

[53] A. Sandilands, *et al.*, "Prevalent and rare mutations in the gene encoding filaggrin cause ichthyosis vulgaris and predispose individuals to atopic dermatitis," J. Invest Dermatol. **126(8)**, 1770 (2006).
Ref Type: Journal

[54] A. Sandilands, *et al.*, "Comprehensive analysis of the gene encoding filaggrin uncovers prevalent and rare mutations in ichthyosis vulgaris and atopic eczema," Nat. Genet. **39**(5), 650 (2007).
Ref Type: Journal

[55] T. Seguchi, *et al.*, "Decreased expression of filaggrin in atopic skin," Arch. Dermatol. Res. **288**(8), 442 (1996).
Ref Type: Journal

[56] L. M. Sevilla, *et al.*, "Epidermal inactivation of the glucocorticoid receptor triggers skin barrier defects and cutaneous inflammation," J. Invest Dermatol. **133**(2), 361 (2013).
Ref Type: Journal

[57] F. J. Smith, *et al.*, "Loss-of-function mutations in the gene encoding filaggrin cause ichthyosis vulgaris," Nat. Genet. **38**(3), 337 (2006).
Ref Type: Journal

[58] V. Soumelis*, et al.*, "Human epithelial cells trigger dendritic cell mediated allergic inflammation by producing TSLP," Nat. Immunol. **3(7)**, 673 (2002).
Ref Type: Journal

[59] K. Sully*, et al.*, "The mTOR inhibitor rapamycin opposes carcinogenic changes to epidermal Akt1/PKBalpha isoform signaling," Oncogene. **32**(27), 3254 (2013).
Ref Type: Journal

[60] C. Sun*, et al.*, "Allele-specific down-regulation of RPTOR expression induced by retinoids contributes to climate adaptations," PLoS. Genet. **6**(10), e1001178 (2010).
Ref Type: Journal

[61] B. R. Thrash*, et al.*, "AKT1 provides an essential survival signal required for differentiation and stratification of primary human keratinocytes," J. Biol. Chem. **281**(17), 12155 (2006).
Ref Type: Journal

[62] K. Vavrova*, et al.*, "Filaggrin deficiency leads to impaired lipid profile and altered acidification pathways in a 3D skin construct," J. Invest Dermatol. **134(3)**, 746 (2014).
Ref Type: Journal

[63] S. Weidinger*, et al.*, "A genome-wide association study of atopic dermatitis identifies loci with overlapping effects on asthma and psoriasis," Hum. Mol. Genet. **22**(23), 4841 (2013).
Ref Type: Journal

Figure 1
Click here to download high resolution image

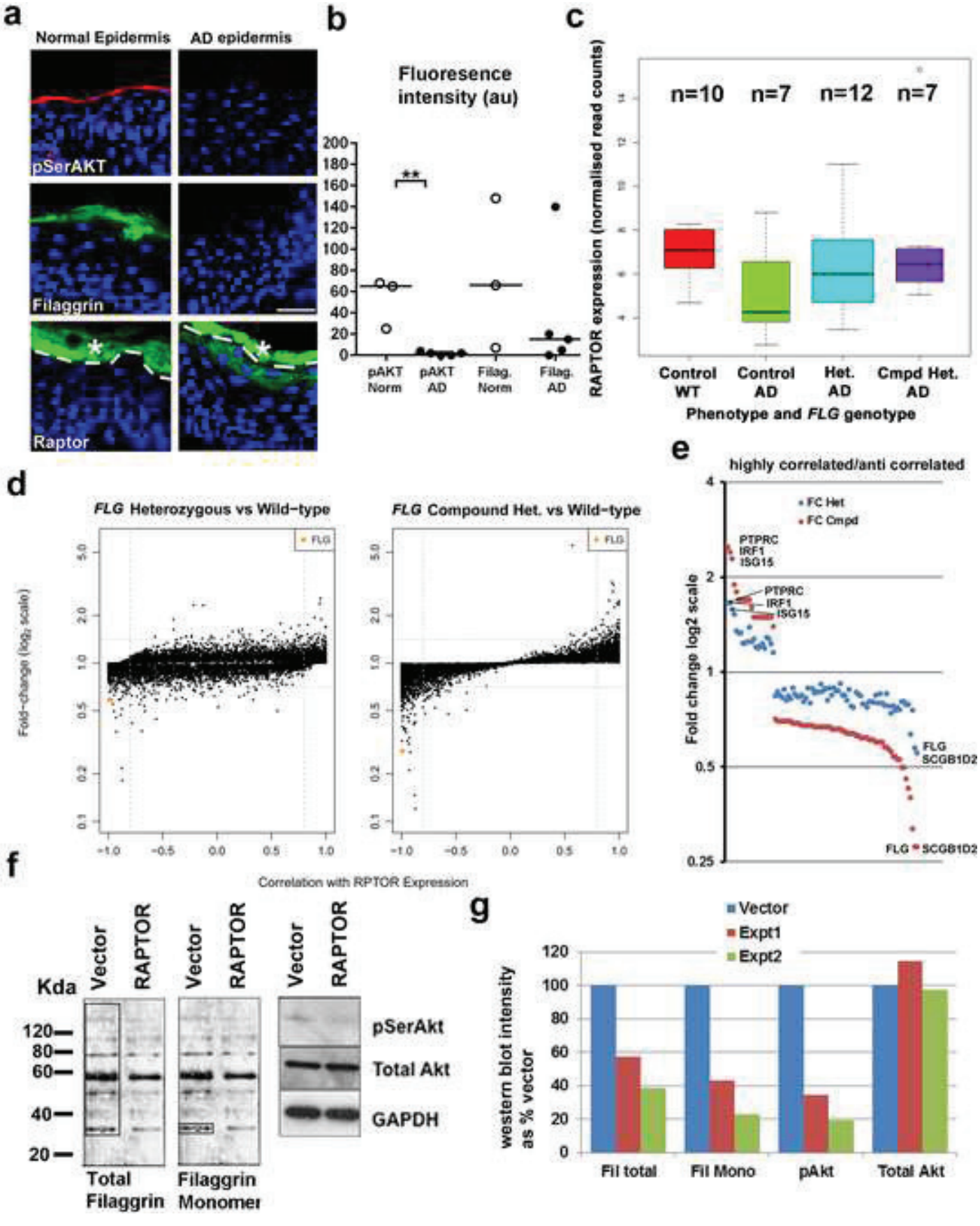

Figure 2

Click here to download high resolution image

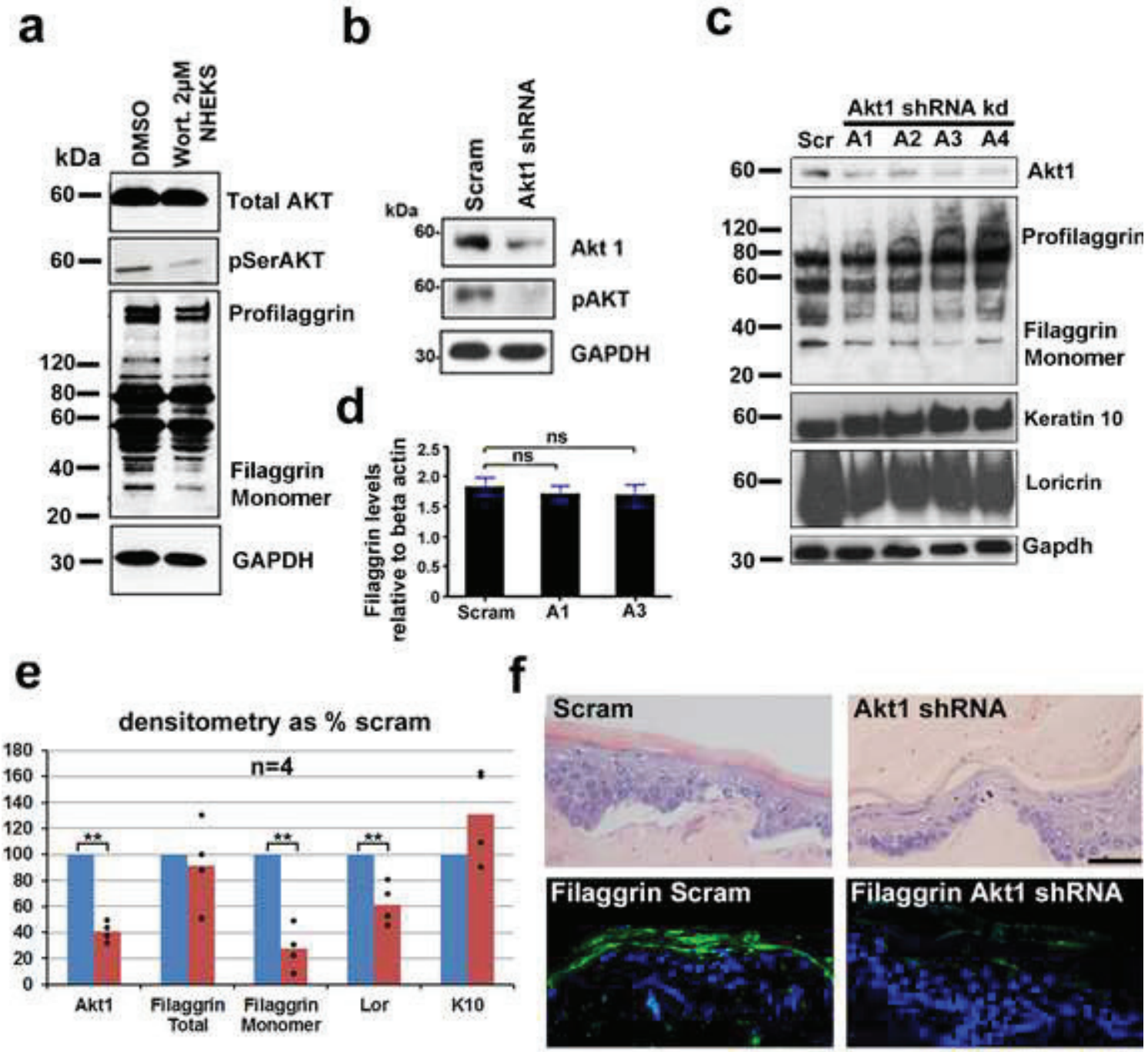

Figure 3

Click here to download high resolution image

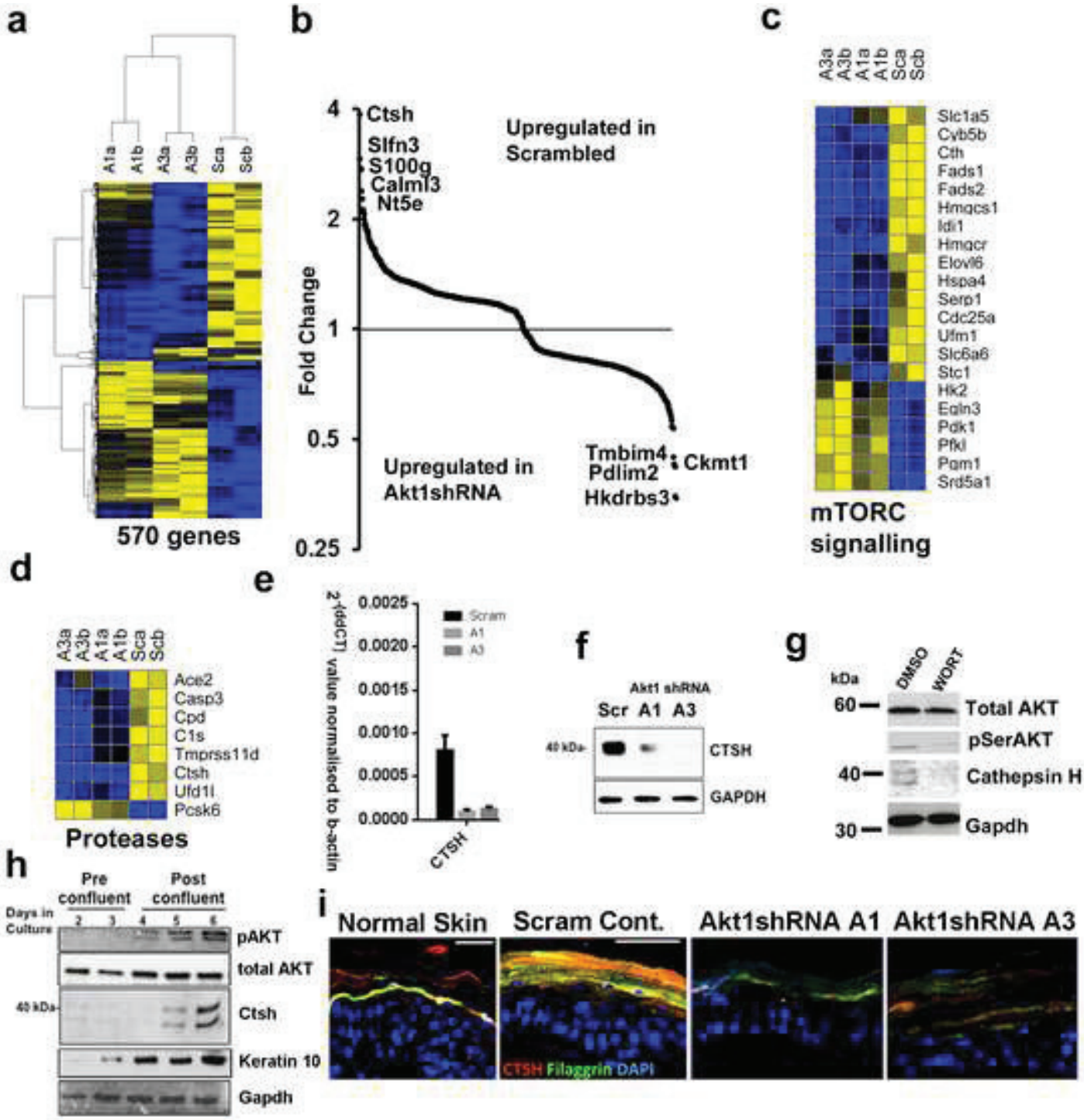

Figure 4

Click here to download high resolution image

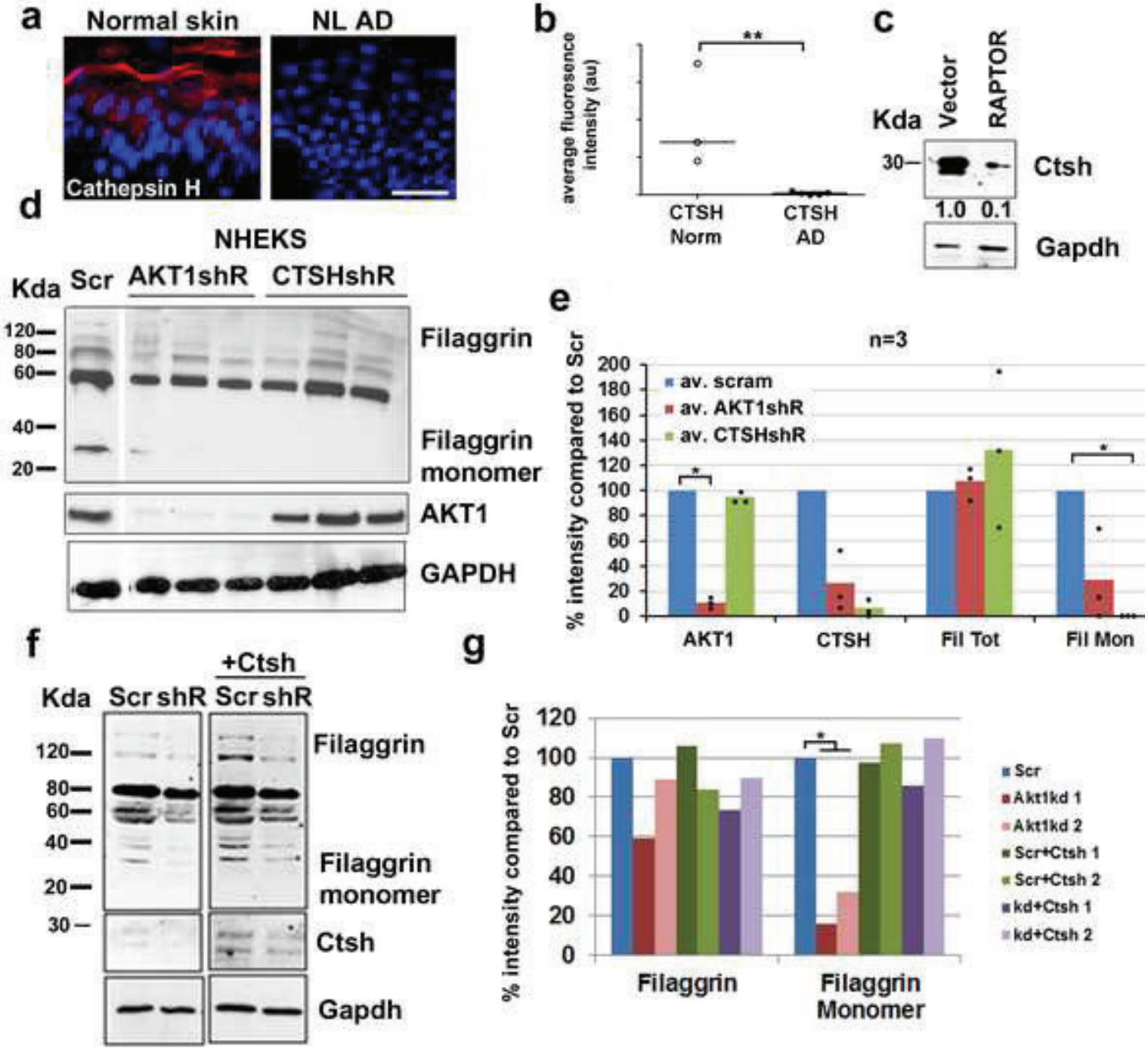

Figure 5

Click here to download high resolution image

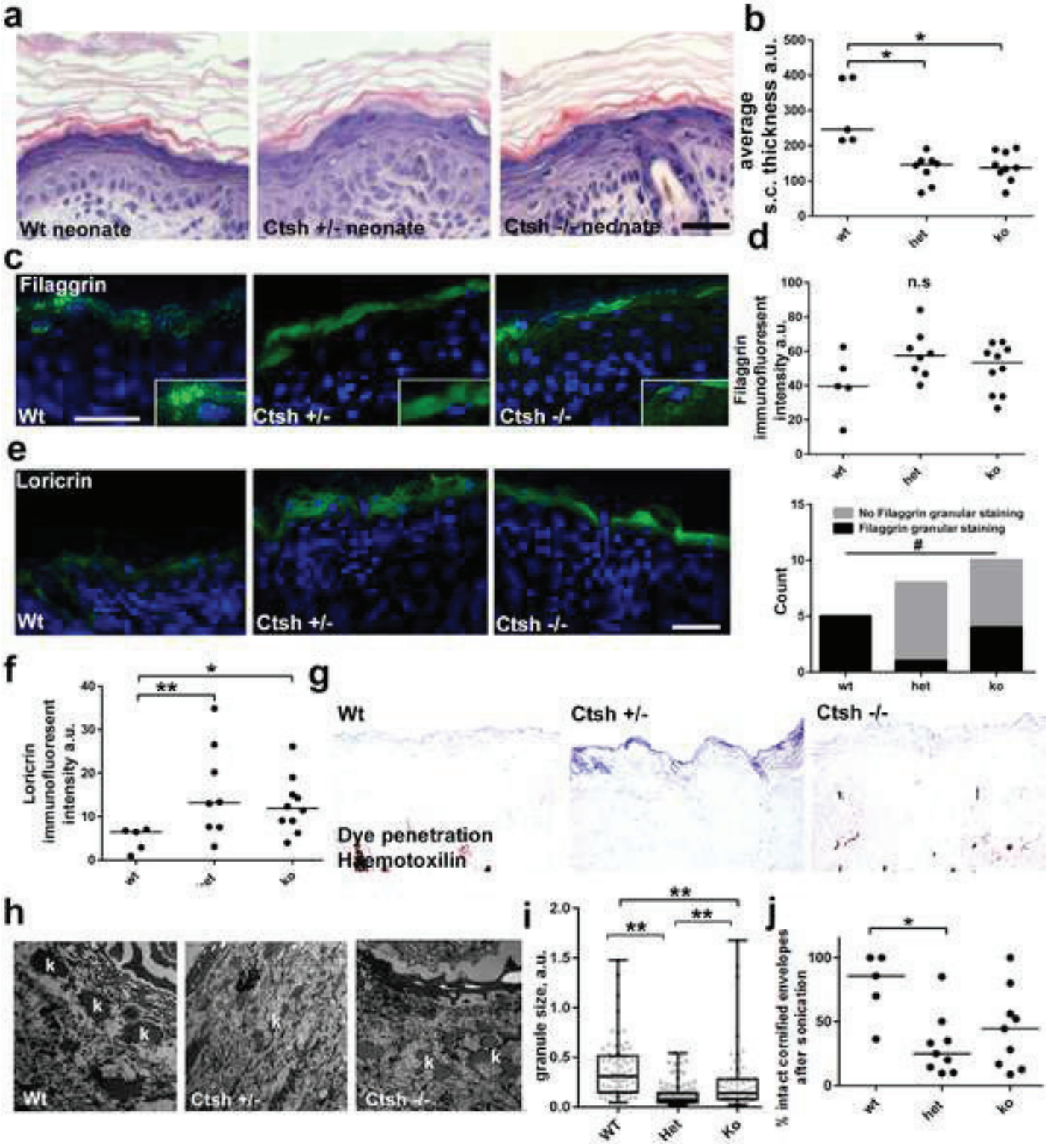

Figure 6

Click here to download high resolution image

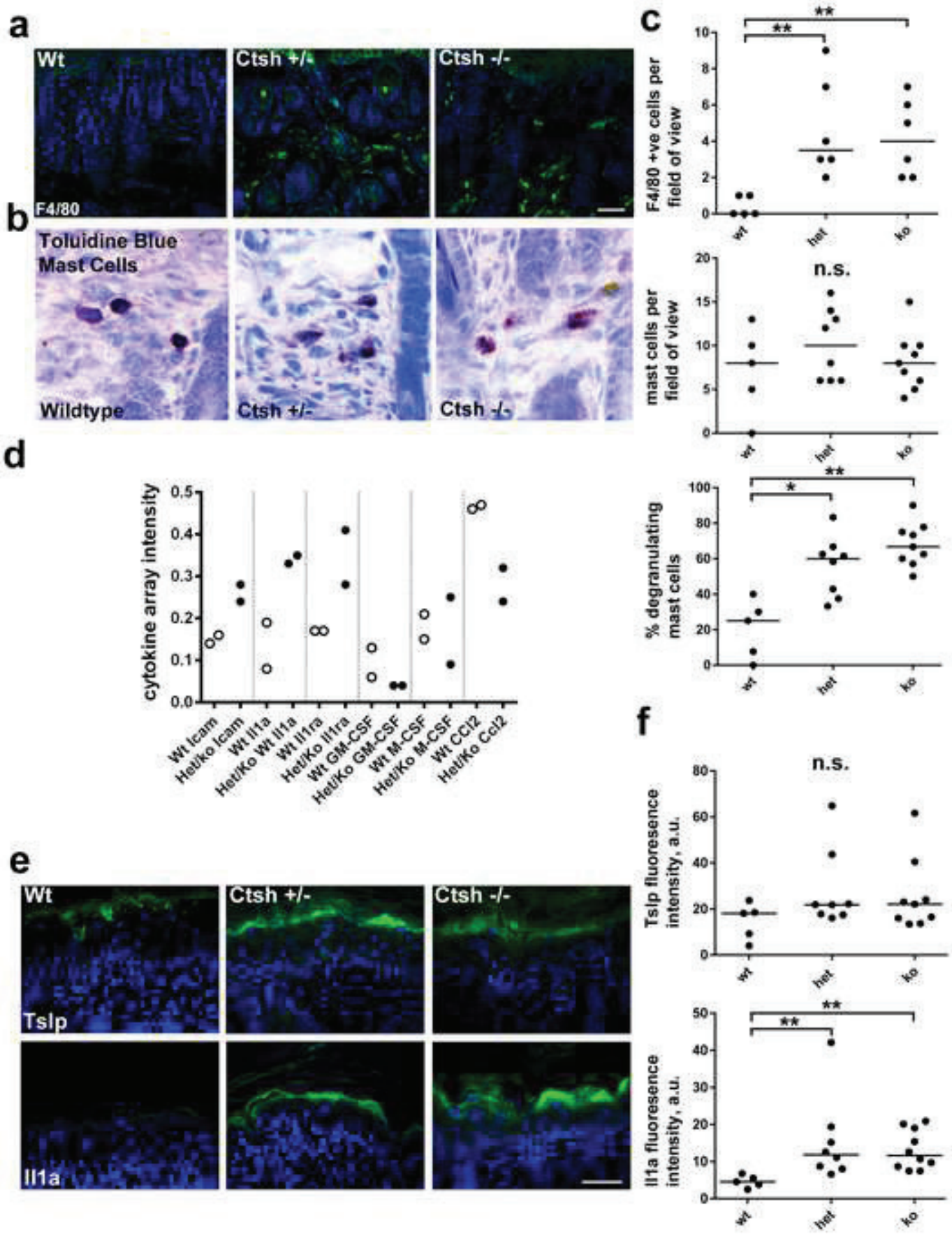

Figure 7

Click here to download high resolution image

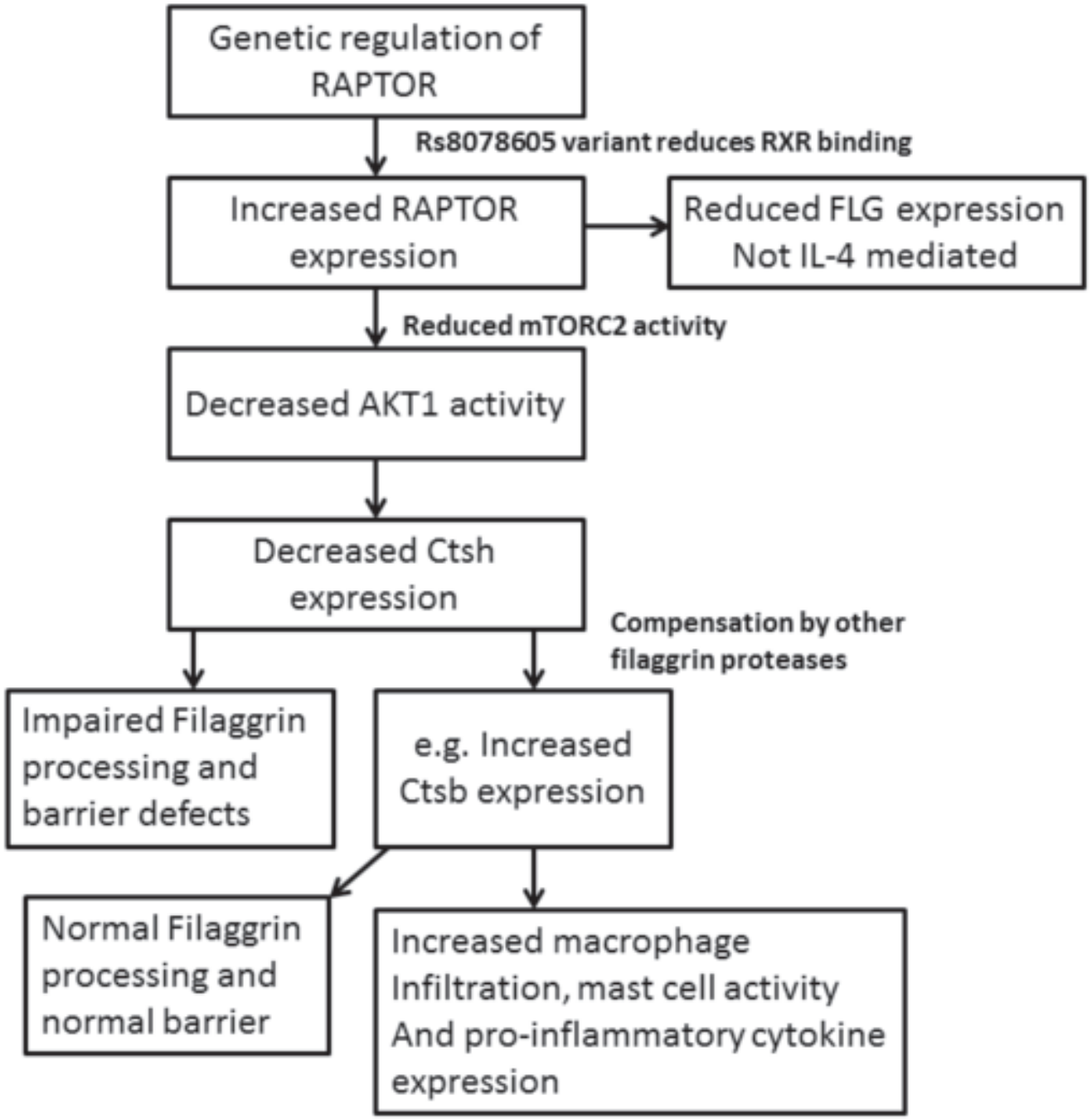

Supplementary Figure E1: Raptor and Filaggrin in normal skin and non lesional AD skin; IL-4 expression (a) Left, densitometry of filaggrin in Normal and AD non-lesional skin. Middle, Filaggrin levels in high and low RAPTOR expressing non-lesional AD patient skin. Right, Filaggrin levels in high and low RAPTOR expressing normal skin. *$p<0.05$, ** $p<0.005$ Mann-Whitney U-test. Bars, left and middle are the interquartile range. **(b)** IL-4 Western blot in rat epidermal keratinocytes treated with rapamycin (Rapa) for 24 hours (10nM). **(c)** IL-4 Western blot in AKT1 kd human keratinocytes. (b and c). Gapdh is loading control in (b,c).

Supplementary Figure E2: Analysis of the highly differentially expressed genes in AD which anti-correlate and correlate with RAPTOR expression. (a) STRING (http://string-db.org/) network of functionally interacting genes, with RAPTOR and AKT1 and the anti-correlated genes in green and red for anti-correlated and correlated genes respectively. Highly expressed genes that also correlated with FLG expression are indicated with an asterisk **(b)** Venn diagram showing the large overlap betweenhighly expressed genes correlating with RAPTOR expression and genes previously determined[14] to be correlated with the loss of filaggrin expression.

Supplementary figure E3: a SNP variant correlates with increased RAPTOR expression, reduced filaggrin expression and processing and reduced Cathepsin H expression. (a) Genomic context and of SNP rs8078605 and a graph of the GWAS data[63] from the RAPTOR region, y-axis, LOD score, the p-value for rs8078605 was 0.067. **(b)** Piechart showing prevalence of each genotype of the SNP rs8078605 in European and sub-Saharan African populations, Normal and AD individuals **(c)** RAPTOR expression in human keratinocytes in response to ATRA. Gapdh is loading control. Bar chart shows RAPTOR densitometry in 2 separate experiments **(d)** RAPTOR densitometry of western blots of 9 human skin samples with the C/ C (n=6), T/C (n=2) or T/T (n=1) variants in rs8078605. **(e)** Plot of RAPTOR densitometry against normalised western blot densitometry of a corresponding filaggrin western blot. T/T and C/T rs8078705 variants are marked on the graph, as is the correlation coefficient (R^2). **(f)** filaggrin and Ctsh Western blots from human samples, keratin 5 is an epidermal loading control.

Supplementary figure E4: Analysis of genes differentially expressed in Akt1kd keratinocytes. (a) Graph of enrichment scores for all significantly differentially expressed genes, including Ctsh **(b)** Graph of enrichment scores of genes involved in MTORC signalling **(c)**. Graph of 1/p values (uncorrected) of the three most over-represented functional groups in scrambled control cells by GSEA analysis. **(d)**. Leading edge analysis of the most differentially expressed genes in these three ontology groups, with several genes including HMGCS1 present in all gene ontology groups. **(e)** HMGCS1 expression in AD according to the RNAseq data in Cole et al., 2013.

Supplementary figure E5: Cathepsin H is required for Filaggrin processing but expression does not correlate with Filaggrin in atopic dermatitis. (a) Western blot of filaggrin and Cathepsin H in 4 Ctsh kd lines. **(b)** Graph of mean densitometry of total filaggrin, filaggrin monomer and Ctsh, n=4 **(c)** Real time PCR analysis of filaggrin expression in two Ctsh shRNA lines. **(d**) cathepsin H expression represented from RNAseq analysis in Cole et al., 2014. Box shows median and interquartile ranges in

wildtype controls and the three eczema *FLG* phenotypes **(e)** Scatterplots showing Pearson correlation (x-axis) of gene expression levels with cathepsin H expression. The fold-change of all significantly differentially expressed genes (FDR p< 0.05) are represented on the y axis, with Filaggrin (FLG) in orange. Correlations are between FLG wildtype, FLG heterozygous and FLG compound heterozygous (n=7).

Supplementary figure E6: Cathepsin B expression increases in Cathepsin H deficient mouse epidermis. (a) Ctsh and Cathepsin B (Ctsb) immunofluoresence in Ctsh -/-, Ctsh +/- and wt mouse epidermis. Graph shows Ctsb intensity in the neonate epidermis, bars are median **(b)** CD45 Immunofluorescence and in the dermis of Ctsh -/-, Ctsh +/- , and wt mouse skin. *p<0.05, **p<0.005 Bar 50μm.

Supplementary Figure E7 – Barrier proteins and immune mediators in adult Ctsh +/- and -/- mouse epidermis(a) histology, filaggrin and loricrin immunofluoresence of adult mouse Ctsh +/-, -/- and wt epidermis. **(b)** Il1a and Tslp immunofluorescence of Il1a and Tslp adult mouse Ctsh +/-, -/- and wt epidermis **(c)** Western blot of filaggrin, keratin 10 and loricrin **(d)** Graphs of densitometry of total filaggrin and filaggrin monomer. p values are shown on the graph. bars 50 μm (a,b)

Supplementary Methods

Restriction fragment length polymorphism analysis

RFLP analysis was performed on 18 skin samples. DNA was extracted by DNA mini spin kit (Qiagen) according to manufacturers' instructions. The rs8078605 polymorphism introduced a BsmAI site into the locus. F- CACCGCATTTGCTCTTACAA and R- CCTACACATGGTCCTTCATCC (Tm 60^{o}C) primers produced a 454bp amplicon. The T variant after BsmAI digestion gives a 203bp and 251bp product.

Repository E Figure 1

Click here to download high resolution image

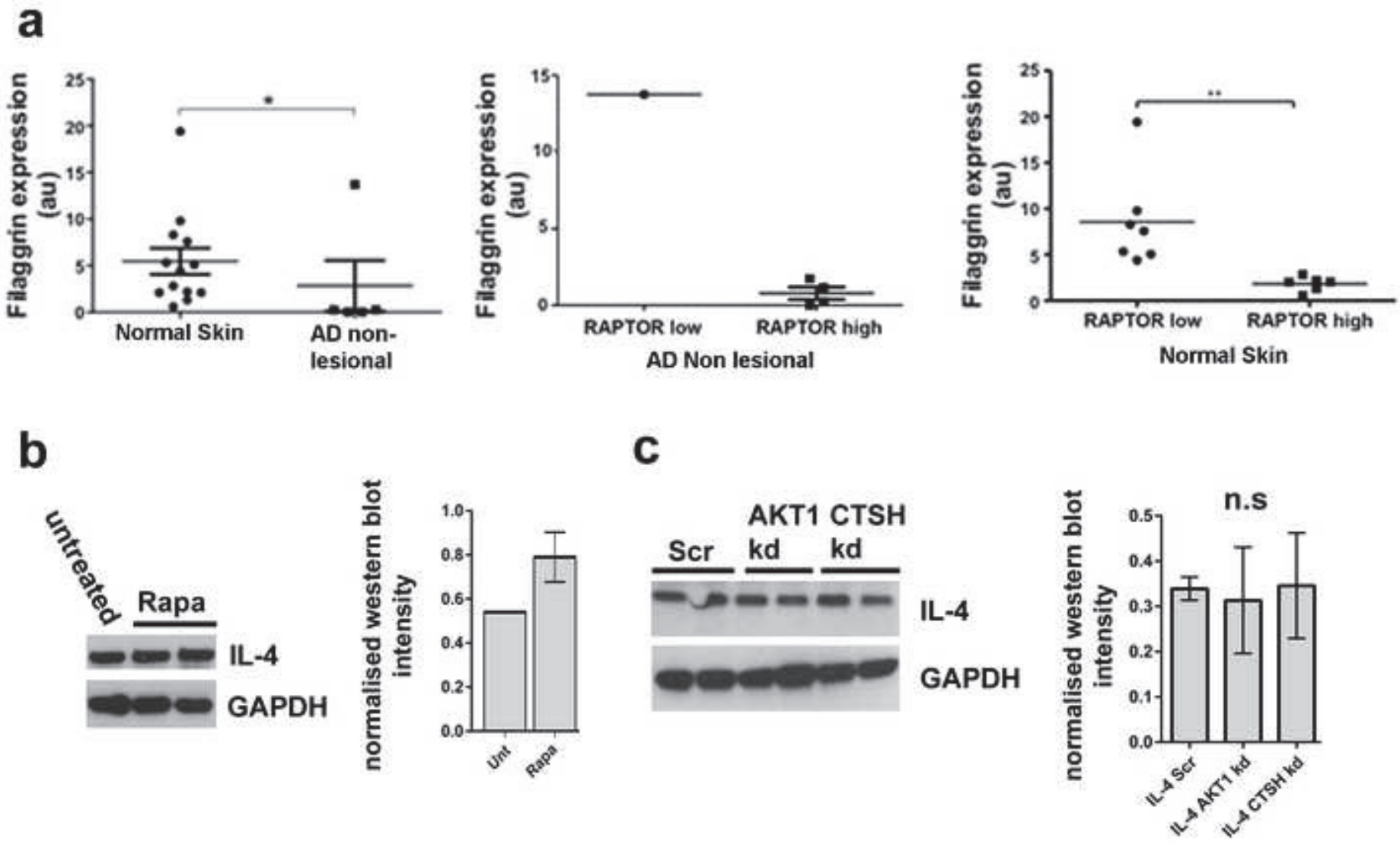

Repository E Figure 2
Click here to download high resolution image

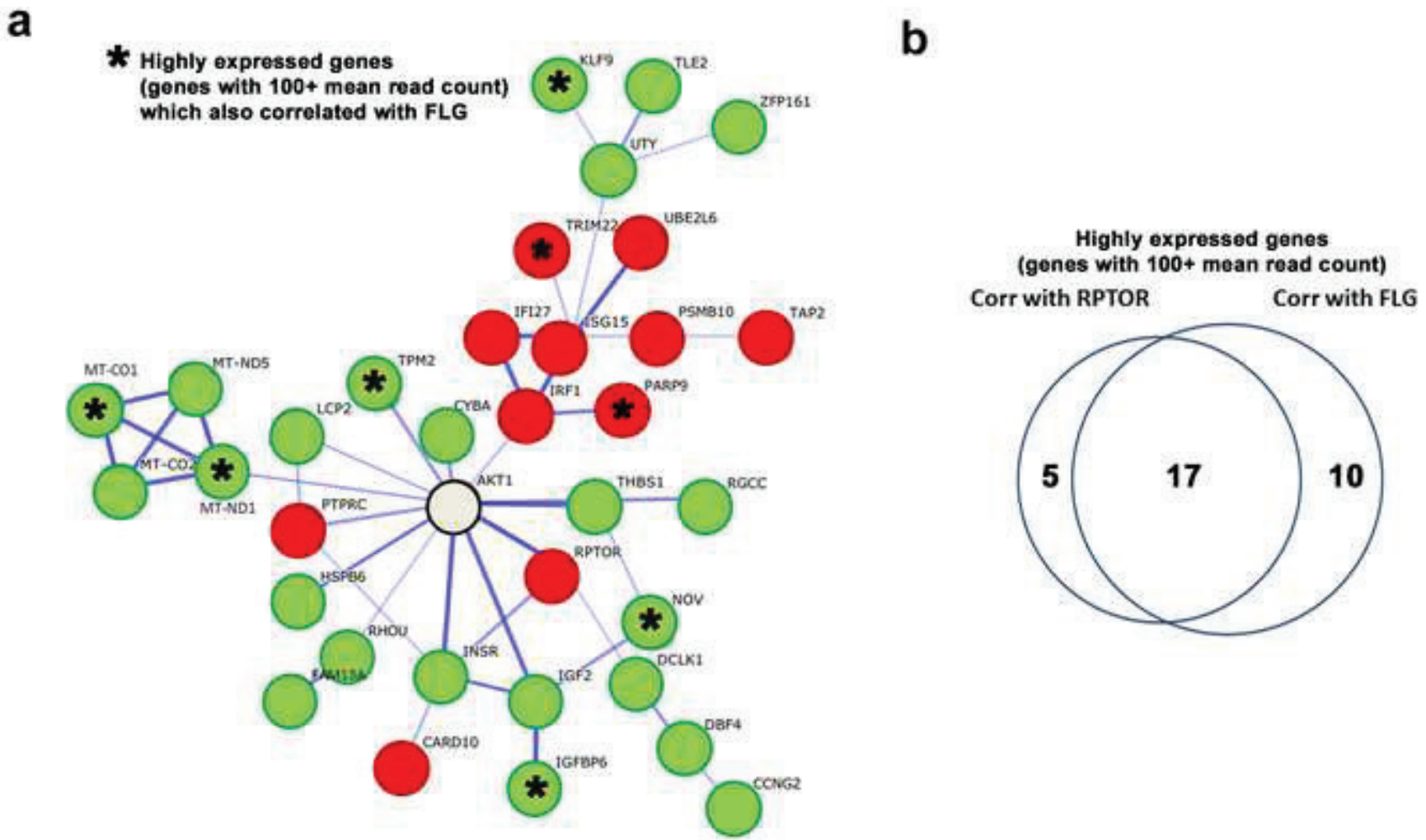

Repository E Figure 3

Click here to download high resolution image

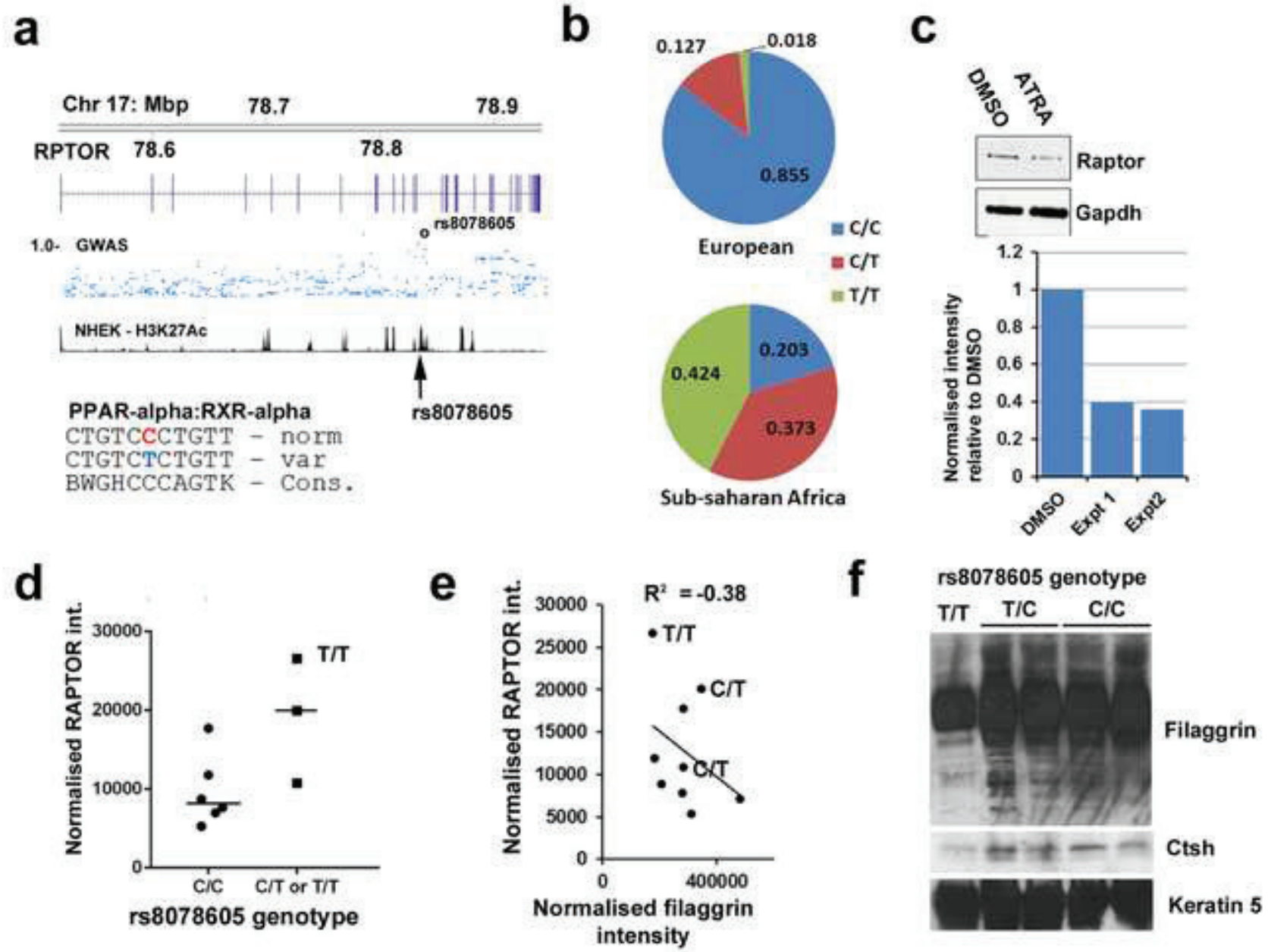

Repository E Figure 4

Click here to download high resolution image

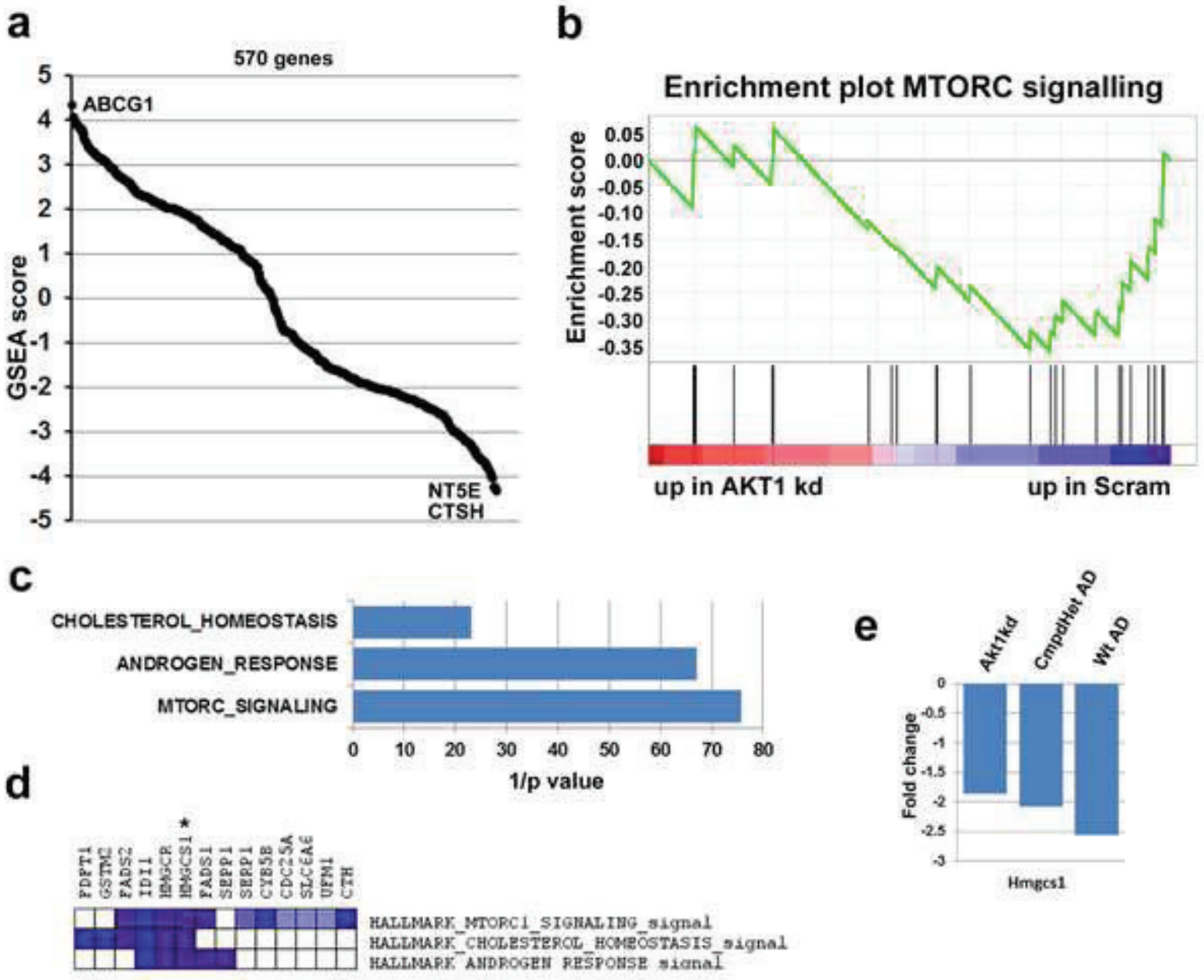

Repository E Figure 5

Click here to download high resolution image

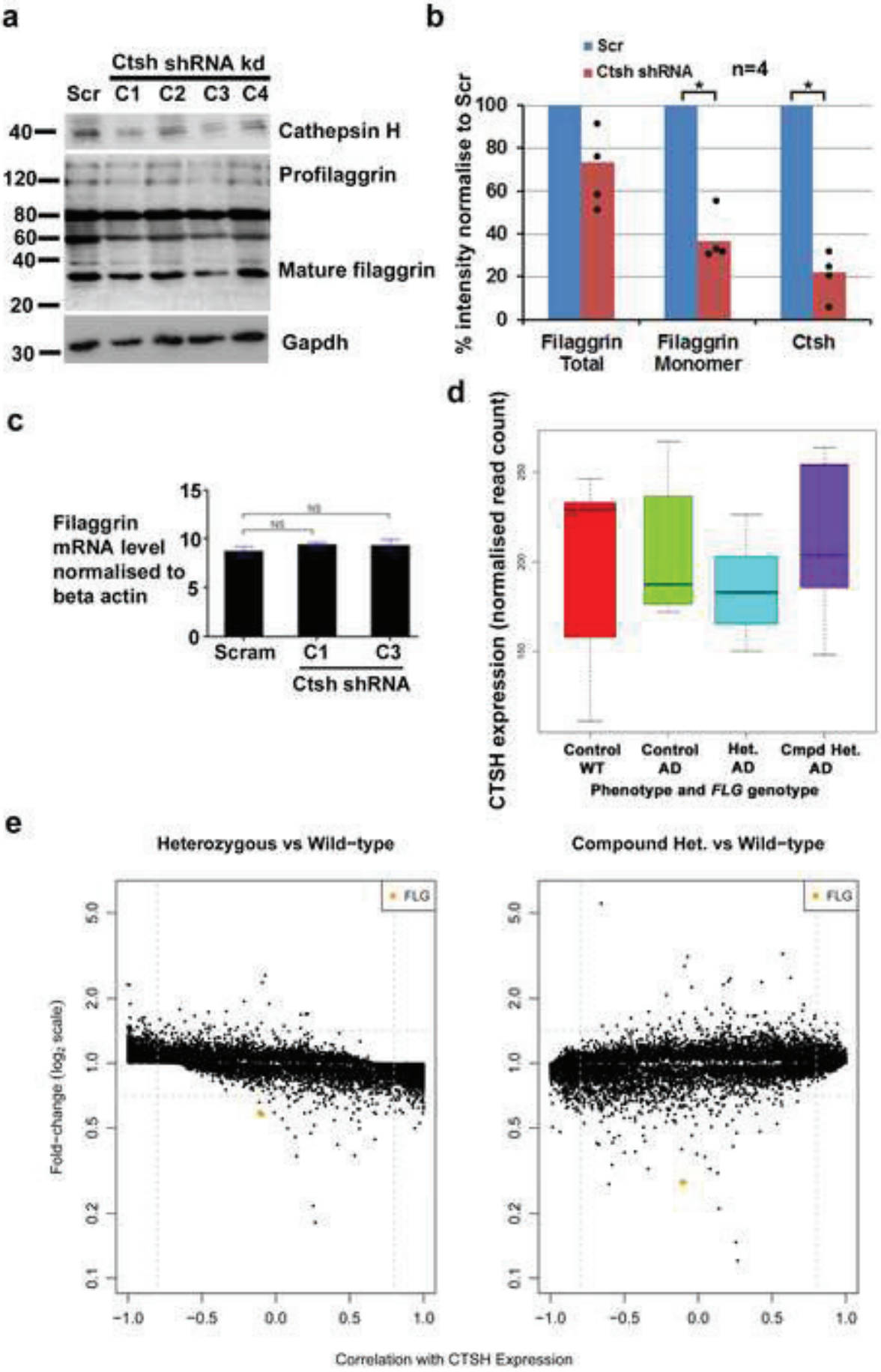

Repository E Figure 6

Click here to download high resolution image

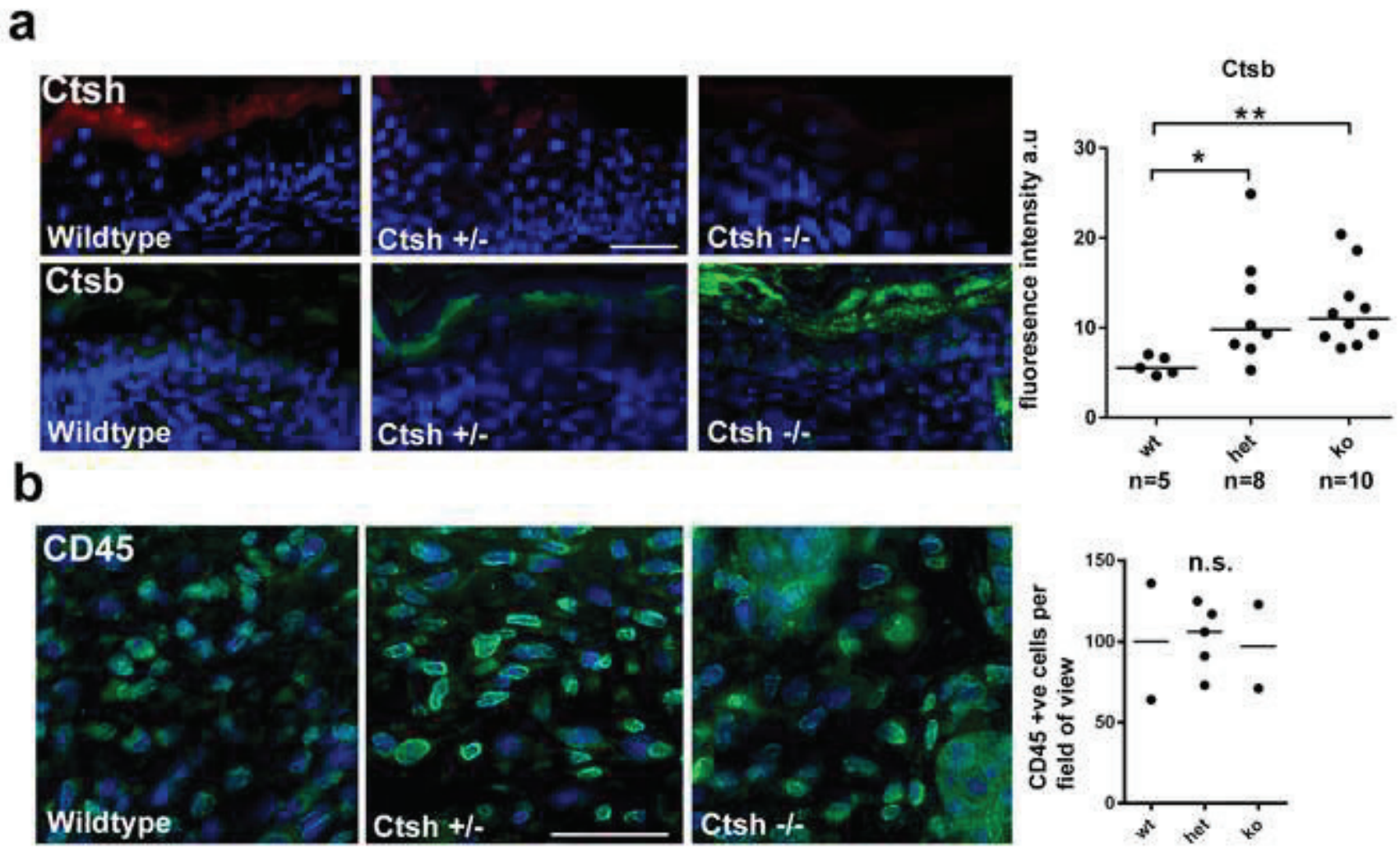

Repository E Figure 7
Click here to download high resolution image

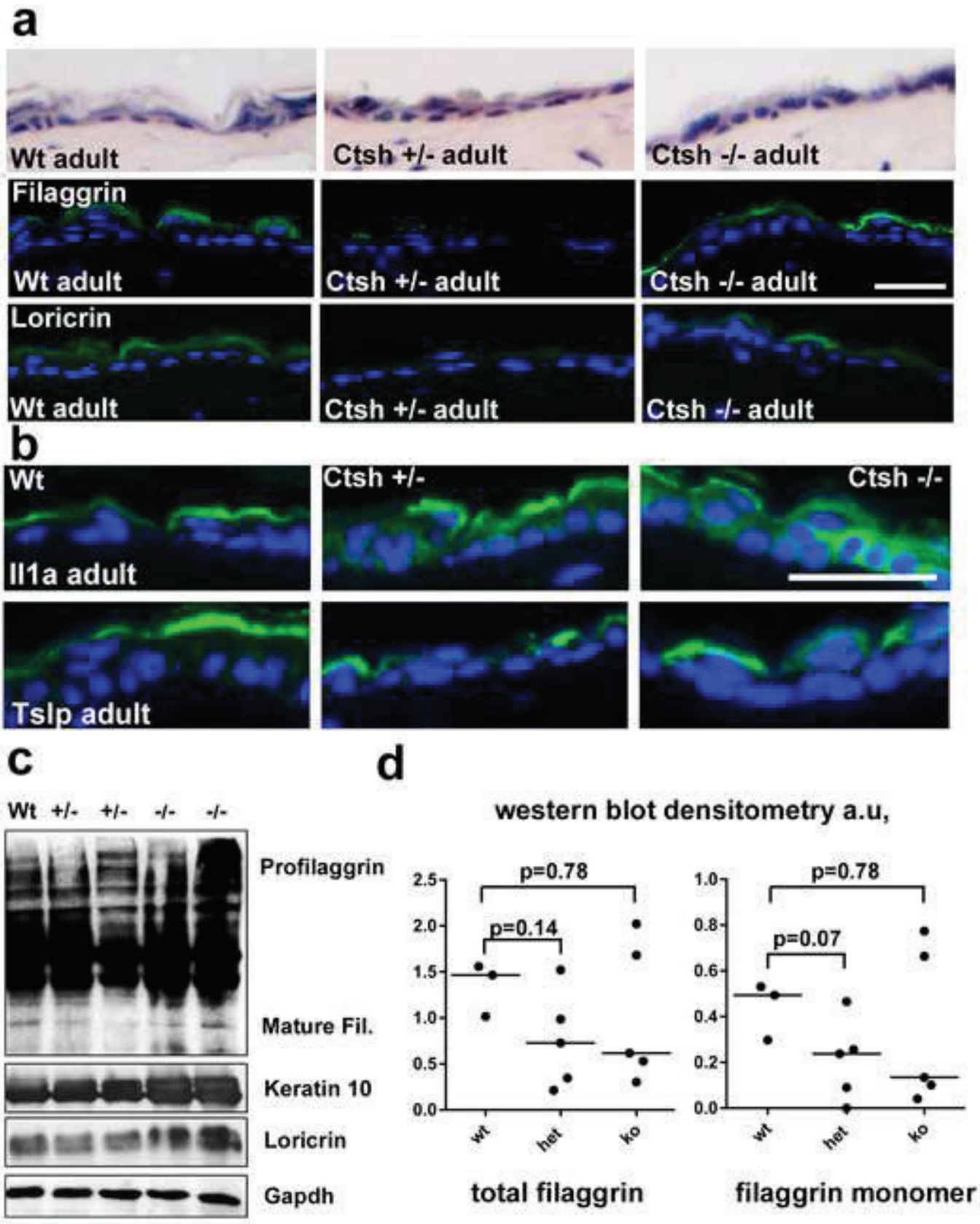

Supplementary table E1

Patient information for the 5 AD patients from Great Ormond Street Hospital. Location of biopsy for the non-lesional samples. Previous treatment, AZA, azathioprine; CSA cyclosporine

Patient	Sex	Age	Location of Biopsy	Previous Treatment
1	F	13	R Waist	oral steroid and AZA
2	M	13	L Arm	AZA
3	M	13	L Thigh	AZA
4	F	12	R Upper leg	AZA and CSA
5	M	11	Lower Back	No systemic treatment

Patient information for the Cole et al, cohort[14]: biopsies were taken from the non-lesional skin (the upper buttock with no clinical signs of active inflammation) of children aged 6 to 16 years who had early onset, persistent and severe atopic eczema. The 10 controls were non-atopic individuals ie no eczema, asthma or hay fever. Severity measurement is by physician global assessment

	severity at time of biopsy				
	mild	moderate	severe	not recorded	total
FLG wt	1	4	2	0	7
FLG het	3	4	4	1	12
FLG compound het	1	2	3	1	7
Total	5	10	9	2	26

Supplementary table E2: List of the 84 genes strongly correlated or anti-correlated with RAPTOR expression levels in unaffected compound heterozygote AD patient skin that are significantly differentially expressed in Cole et al 2014[14], GeneName, official HUGO nomenclature, WT, Het and Cmpd, are mean normalised expression levels of WT, Heterozygote and Compound Heterozygote respectively, s.d are the standard deviations of each cohort. Cor, Pearson correlation coefficient. FC fold change, pval is the p value after correction for multiple testing

Gene	Description	WT	Het	Cmpd	WT.sd	Het.sd	Cmpd.sd	cor	FC	logFC	pval
PTPRC	protein tyrosine phosphatase, receptor type, C	6.6	11	16	3	14	21	1	2.5	1.3	0.0079
IRF1	interferon regulatory factor 1	18	30	43	6.9	44	73	1	2.4	1.3	0.012
ISG15	ISG15 ubiquitin-like modifier	12	19	27	5.1	35	45	1	2.3	1.2	0.023
HAPLN3	hyaluronan and proteoglycan link protein 3	7.2	11	14	2	12	19	1	1.9	0.91	0.023
TIMM22	translocase of inner mitochondrial membrane 22 homolog (yeast)	9.6	13	17	3.6	6.5	11	1	1.8	0.84	0.0074
CKAP2	cytoskeleton associated protein 2	15	20	26	2.9	7.3	6.5	1	1.7	0.78	0.0013
CARD10	caspase recruitment domain family, member 10	12	16	21	5.6	5.6	8.1	1	1.7	0.78	0.014
TAP2	transporter 2, ATP-binding cassette, sub-family B (MDR/TAP)	38	47	62	7.9	33	61	1	1.7	0.73	0.031
TRIM22	tripartite motif containing 22	28	39	47	4.7	52	63	0.99	1.7	0.76	0.049
DBF4	DBF4 zinc finger	8	10	13	3.3	2.7	2.4	1	1.6	0.7	0.0071

UBE2L6	ubiquitin-conjugating enzyme E2L 6	25	32	38	8.6	24	37	1	1.5	0.59	0.0085
SNX11	sorting nexin 11	8.3	10	12	1.5	2.5	2.9	1	1.5	0.55	0.009
GXYLT1	glucoside xylosyltransferase 1	7.2	8.6	10	2	2.2	3.2	1	1.5	0.54	0.0096
IFI27	interferon, alpha-inducible protein 27	190	230	280	140	340	450	1	1.5	0.54	0.011
PSMB10	proteasome (prosome, macropain) subunit, beta type, 10	13	16	19	4.2	12	17	1	1.5	0.57	0.015
LCP2	lymphocyte cytosolic protein 2 (SH2 domain containing leukocyte protein of 76kDa)	8.2	9.8	12	2.1	8.1	8.3	1	1.5	0.56	0.023
PARP9	poly (ADP-ribose) polymerase family, member 9	31	40	48	12	46	54	1	1.5	0.62	0.024
NUAK2	NUAK family, SNF1-like kinase, 2	18	23	27	11	12	13	1	1.5	0.55	0.026
KCNK1	potassium channel, two pore domain subfamily K, member 1	30	37	44	7	9.2	6.7	0.99	1.5	0.55	0.035
HLA-DOA	major histocompatibility complex, class II, DO alpha	13	15	18	3.4	6.9	13	1	1.4	0.51	0.012
PRAF2	PRA1 domain family, member 2	19	16	14	4.3	3.4	4.4	-1	0.71	-0.5	0.025
NOV	nephroblastoma overexpressed	53	46	37	16	14	8.9	-1	0.7	-0.51	0.0049
ZBTB14	zinc finger and BTB domain containing 14	13	11	9	3.6	2.8	2.2	-1	0.7	-0.52	0.017
ENTPD4	ectonucleoside triphosphate diphosphohydrolase 4	18	15	12	3.6	3	2.9	-1	0.7	-0.52	0.022
SLC9B2	solute carrier family 9, subfamily B (NHA2,	17	15	12	5.2	3.7	3.1	-1	0.7	-0.51	0.026

	cation proton antiporter 2), member 2										
TPM2	tropomyosin 2 (beta)	110	90	75	66	40	21	-1	0.7	-0.52	0.028
LAMA3	laminin, alpha 3	19	16	13	9.2	3.8	5.1	-1	0.7	-0.52	0.041
RHOU	ras homolog family member U	17	14	12	7.4	5.8	3.5	-1	0.7	-0.51	0.046
ABHD4	abhydrolase domain containing 4	11	9.8	7.9	1.7	2.3	1.7	-1	0.69	-0.54	0.0028
MXRA8	matrix-remodelling associated 8	21	18	15	8.3	5.4	4.7	-1	0.69	-0.54	0.01
CD1A	CD1a molecule	31	26	21	12	8.7	9.5	-1	0.69	-0.53	0.021
RNF152	ring finger protein 152	43	36	30	7.6	8.9	6.8	-1	0.69	-0.53	0.024
CLDN10	claudin 10	13	11	8.7	9.5	5.7	5.5	-1	0.68	-0.56	0.032
GPR137	G protein-coupled receptor 137	11	8.9	7.4	3.6	2.3	3	-1	0.68	-0.55	0.04
ZDHHC11	zinc finger, DHHC-type containing 11	29	24	20	16	12	12	-1	0.68	-0.56	0.041
RP11-613D13.4	none	28	25	19	17	8	6.6	-1	0.68	-0.56	0.045
LPCAT1	lysophosphatidylcholine acyltransferase 1	15	12	10	4.2	3.8	3.2	-1	0.68	-0.56	0.046
DCLK1	doublecortin-like kinase 1	18	16	12	9.7	7.1	7	-1	0.68	-0.55	0.049
MT-ND1	mitochondrially encoded NADH dehydrogenase 1	360	310	240	92	91	40	-1	0.67	-0.57	0.0023
NCALD	neurocalcin delta	38	33	25	16	12	10	-1	0.67	-0.58	0.017
NNMT	nicotinamide N-methyltransferase	30	26	20	13	14	6.6	-1	0.67	-0.57	0.017
WNK2	WNK lysine deficient protein kinase 2	12	11	8.4	3.8	4	4	-1	0.67	-0.57	0.019
PIGV	phosphatidylinositol glycan anchor biosynthesis, class V	11	9.6	7.4	1.7	3.5	2.9	-1	0.67	-0.58	0.022

CCNG2	cyclin G2	27	24	18	11	8.1	11	-1	0.67	-0.58	0.036
PRELP	proline/arginine-rich end leucine-rich repeat protein	60	49	40	23	8.1	11	-1	0.67	-0.57	0.041
C11orf96	chromosome 11 open reading frame 96	28	25	19	17	8	6	-1	0.67	-0.58	0.049
FLNC	filamin C, gamma	13	11	8.3	5.9	3.8	4	-1	0.66	-0.59	0.0016
SNED1	sushi, nidogen and EGF-like domains 1	11	9.8	7.6	5.5	4.2	3.9	-1	0.66	-0.59	0.0072
FMOD	fibromodulin	32	28	21	13	9.1	6.7	-1	0.66	-0.6	0.028
MT-ND5	mitochondrially encoded NADH dehydrogenase 5	630	550	410	300	240	180	-1	0.66	-0.61	0.035
TLE2	transducin-like enhancer of split 2	13	12	8.6	4.3	3	3.5	-1	0.66	-0.6	0.049
UTY	ubiquitously transcribed tetratricopeptide repeat containing, Y-linked	13	11	8.6	5.2	6.9	5.4	-1	0.65	-0.62	0.015
CYBA	cytochrome b-245, alpha polypeptide	11	9.3	7.3	3.3	4.8	7.1	-1	0.65	-0.63	0.021
KLF9	Kruppel-like factor 9	60	49	39	36	18	12	-1	0.64	-0.65	0.023
ZDHHC11B	zinc finger, DHHC-type containing 11B	26	23	17	17	12	8.3	-1	0.64	-0.64	0.032
THBS1	thrombospondin 1	32	25	20	19	9	6.6	-1	0.64	-0.65	0.039
CRELD1	cysteine-rich with EGF-like domains 1	22	17	14	6.7	3	4.7	-1	0.64	-0.65	0.046
RAI2	retinoic acid induced 2	15	13	9.6	3.9	4.7	4.6	-1	0.63	-0.68	0.021
NOVA1	neuro-oncological ventral antigen 1	20	17	12	5	5.6	6.2	-1	0.63	-0.67	0.046
EBF1	early B-cell factor 1	19	16	12	8.8	6	3.3	-1	0.62	-0.68	0.014
FAM13A	family with sequence similarity 13, member A	39	31	24	33	11	5.1	-1	0.62	-0.7	0.014
HNMT	histamine N-	19	15	12	4.3	5	5.2	-1	0.62	-0.68	0.036

	methyltransferase										
ZG16B	zymogen granule protein 16B	49	38	30	32	15	12	-1	0.62	-0.69	0.043
IGF2	insulin-like growth factor 2	21	17	13	12	6.7	3.8	-1	0.61	-0.7	0.0099
MT-CO1	mitochondrially encoded cytochrome c oxidase I	460	370	280	120	140	59	-1	0.61	-0.71	0.016
HOTAIR	HOX transcript antisense RNA	13	11	7.8	7.4	3.3	5.4	-1	0.6	-0.73	0.0056
MXRA7	matrix-remodelling associated 7	15	12	9.1	5.4	3.2	2.7	-1	0.6	-0.74	0.013
INSR	insulin receptor	14	12	8.7	7.8	3.4	5.3	-1	0.6	-0.73	0.024
LIG1	ligase I, DNA, ATP-dependent	15	12	8.7	3.1	5.3	3.5	-1	0.6	-0.75	0.031
SPRN	shadow of prion protein homolog (zebrafish)	14	11	8.2	5.3	6.1	4.6	-1	0.58	-0.79	0.027
HRH1	histamine receptor H1	11	9.4	6.3	5.6	4.7	3.4	-1	0.58	-0.78	0.047
RGCC	regulator of cell cycle	74	58	42	29	25	11	-1	0.57	-0.8	0.012
PRR4	proline rich 4 (lacrimal)	54	40	30	60	69	24	-1	0.56	-0.83	0.05
S100P	S100 calcium binding protein P	62	47	34	18	17	24	-1	0.54	-0.89	0.026
IGFBP6	insulin-like growth factor binding protein 6	84	65	45	40	21	8.3	-1	0.53	-0.91	0.0075
MUCL1	mucin-like 1	460	350	240	290	190	200	-1	0.53	-0.92	0.028
KIAA1841	KIAA1841	21	17	11	8.3	4.9	3.6	-1	0.5	-1	0.017
MT-CO2	mitochondrially encoded cytochrome c oxidase II	110	89	54	36	53	19	-1	0.5	-0.99	0.043
C2orf74	chromosome 2 open reading frame 74	19	15	8.5	8.2	5.2	3.1	-1	0.46	-1.1	0.044
HSPB6	heat shock protein, alpha-crystallin-related, B6	24	19	10	14	7.6	6.8	-1	0.43	-1.2	0.04

CYP4B1	cytochrome P450, family 4, subfamily B, polypeptide 1	22	14	8.6	13	6.8	4.2	-1	0.4	-1.3	0.042
CILP	cartilage intermediate layer protein, nucleotide pyrophosphohydrolase	33	25	11	18	19	7.9	-1	0.32	-1.6	0.032
FLG	filaggrin	3300	1900	920	680	460	270	-1	0.28	-1.8	0.044
SCGB1D2	secretoglobin, family 1D, member 2	110	61	30	63	65	17	-1	0.28	-1.8	0.049

Supplementary Table E3 Concordance of the top 22 highly expressed and differentially expressed genes strongly correlated or anti-correlated with RAPTOR expression with gene whose expression level correlated with FLG expression levels[14] in unaffected compound heterozygote AD patient skin that are significantly differentially expressed, Gray denote either positive or negative correlation in both analyses. GeneName, official HUGO nomenclature, WT, Het and Cmpd, are mean normalised expression levels of WT, Heterozygote and Compound Heterozygote respectively, s.d are the standard deviations of each cohort. Cor, pearson correlation coefficient. FC fold change, pval is the p value after correction for multiple testing

Gene	Description	WT	Cmpd	FC	logFC	pval
TAP2	**transporter 2, ATP-binding cassette, sub-family B (MDR/TAP)**	38	62	1.7	0.73	**0.031**
TRIM22	**tripartite motif containing 22**	28	47	1.7	0.76	**0.049**
IFI27	**interferon, alpha-inducible protein 27**	190	280	1.5	0.54	**0.011**
KCNK1	**potassium channel, two pore domain subfamily K, member 1**	30	44	1.5	0.55	**0.035**
PARP9	**poly (ADP-ribose) polymerase family, member 9**	31	48	1.5	0.62	**0.024**
NOV	**nephroblastoma overexpressed**	53	37	0.7	-0.51	**0.005**
TPM2	**tropomyosin 2 (beta)**	110	75	0.7	-0.52	**0.028**
RNF152	**ring finger protein 152**	43	30	0.7	-0.53	**0.024**
MT-ND1	**mitochondrially encoded NADH dehydrogenase 1**	360	240	0.7	-0.57	**0.002**
PRELP	**proline/arginine-rich end leucine-rich repeat protein**	60	40	0.7	-0.57	**0.041**
MT-ND5	**mitochondrially encoded NADH dehydrogenase 5**	630	410	0.7	-0.61	**0.035**
KLF9	**Kruppel-like factor 9**	60	39	0.6	-0.65	**0.023**
ZG16B	**zymogen granule protein 16B**	49	30	0.6	-0.69	**0.043**
MT-CO1	**mitochondrially encoded cytochrome c oxidase I**	460	280	0.6	-0.71	**0.016**
RGCC	**regulator of cell cycle**	74	42	0.6	-0.8	**0.012**
PRR4	**proline rich 4 (lacrimal)**	54	30	0.6	-0.83	**0.05**
S100P	**S100 calcium binding protein P**	62	34	0.5	-0.89	**0.026**
IGFBP6	**insulin-like growth factor binding protein 6**	84	45	0.5	-0.91	**0.008**
MUCL1	**mucin-like 1**	460	240	0.5	-0.92	**0.028**
MT-CO2	**mitochondrially encoded cytochrome c oxidase II**	110	54	0.5	-0.99	**0.043**
FLG	**filaggrin**	3300	920	0.3	-1.8	**0.044**
SCGB1D2	**secretoglobin, family 1D, member 2**	110	30	0.3	-1.8	**0.049**

Supplementary Table E4

A table showing the average fold change in expression in both Akt1 kd lines of all genes 2-fold and above differentially expressed; The 1.5 –fold or more down-regulated genes related to MTORC signalling and Proteases in the GSEA analysis are also shown in this table.

2-fold up- and down-regulated genes		
Symbol	**Entrez Gene Name**	**Fold Change**
Khdrbs3	KH domain containing, RNA binding, signal transduction associated 3	7.4
Pdlim2	PDZ and LIM domain 2	7.2
Ckmt1	creatine kinase, mitochondrial 1	5.2
Tmbim4	transmembrane BAX inhibitor motif containing 4	5.1
Bin3	bridging integrator 3	5.1
Sema3a	sema domain, immunoglobulin domain (Ig), short basic domain, secreted, (semaphorin) 3A	4.8
Ppp3cc	protein phosphatase 3, catalytic subunit, gamma isoform	4.7
Cldn3	claudin 3	3.7
Asrgl1	asparaginase like 1	3.6
Ccbl1	cysteine conjugate-beta lyase, cytoplasmic	3.6
Expi	extracellular proteinase inhibitor	3.5
Sepp1	selenoprotein P, plasma, 1	-2.1
Fads1	fatty acid desaturase 1	-2.1
Pkib	protein kinase (cAMP-dependent, catalytic) inhibitor beta	-2.1
Il33	interleukin 33	-2.1
Nt5e	5' nucleotidase, ecto	-2.4
Calml3	calmodulin-like 3	-2.7
S100g	S100 calcium binding protein G	-2.7
Slfn3	schlafen 3	-2.9
Ctsh	cathepsin H	-3.9
1.5-fold or more down-regulated genes involved in mTORC signalling		
Fads2	Fatty Acid Desaturase 2	-1.6
Cth	Cystathionine Gamma-Lyase	-1.8
Hmgcs1	3-Hydroxy-3-Methylglutaryl-CoA Synthase 1 (Soluble)	-1.9
Elovl6	ELOVL Fatty Acid Elongase 6	-1.9
Idi1	Isopentenyl-Diphosphate Delta Isomerase 1	-2.0
Fads1	Fatty Acid Desaturase 1	-2.1
1.5-fold or more down-regulated proteases		
Ace2	Angiotensin I Converting Enzyme 2	-1.6
Pcsk6	Proprotein Convertase Subtilisin/Kexin Type 6	-1.6
C1s	Complement Component 1, S Subcomponent	-1.6
Ctsh	Cathepsin H	-3.9